UNIVERSITY OF TARTU

Faculty of Science and Technology

Institute of Physics

Kristjan Müürsepp

THE FLAVOR HIERARCHY PROBLEM IN THE STANDARD MODEL AND BEYOND THE STANDARD MODEL THEORIES

Master's thesis (30 ECTS)

Supervisor:
Dr Luca Marzola
Co-supervisor:
Dr Stefan Groote

Tartu   2020

The Flavor Hierarchy Problem in the Standard Model and Beyond the Standard Model Theories

The flavour hierarchy problem, manifested in the large order of magnitude difference in the masses and mixing angles of the fundamental fermions of the Standard Model (SM) is a well known curiosity in particle physics. Although these masses and mixing angles can be included in the SM with a suitable parametrization, the SM offers no explanation for the difference of many orders of magnitude in these free parameters. In this thesis, the flavour hierarchy problem will be used as motivation for models of new physics. Within the new models, the origin of the flavour hierarchy will be theoretically explained as resulting from higher order radiative corrections, induced by the new fields in the model. Furthermore, a numerical scan will be run in order to fit the effective parameters to the experimental observations. Finally, the analytical form of the radiative amplitudes will be used in order to check the consistency of the effective parametrization approach. Further phenomenological consequences of these models will be outlined.

Lõhnaprobleem Osakestefüüsika Standardmudelis ja selle edasiarendustes

Standardmudeli (SM) lõhnaprobleem seisneb erinevate fundamentaalsete fermionite vahelises suures massi ja segunemisnurkade erinevuses. Kuigi kõik fermionite massid ja segunemisnurgad on vabade parameetrite abil võimalik SMi lisada, jääb vastavate parameetrite mitme suurusjärgune erinevus SMi kontekstis seletamata. SMi lõhnaprobleem võetakse antud lõputöös aluseks, uurimaks võimalike uue füüsika mudelid. Kasutades erinevaid SMi edasiarendusi, kirjeldatatakse lõputöös üht võimaliku SMi lõhnaprobleemi seletust kõrgemat järku kiirguslike parandite näol. Loomaks seoseid kiirguslike parandite efektiivse kirjelduse ning reaalsete eksperimenditulemuste vahel, viiakse läbi numbriline uuring efektiivse parameetriruumi ulatuses. Lisaks kontrollitakse mudelis rakendatud efektiivse parametrisatsiooni teoreetilist õigsust, kasutades kõrgemat järku amplituudide täpset analüütilist valemit. Ühtlasi kirjeldatatakse vastavate uute osakestefüüsika mudelite fenomenoloogiat.

Contents

Introduction

Throughout scientific history, laws of physics have been formulated in order to model the natural phenomena in a minimal set of fundamental rules. Currently, all observed physical processes can be explained by four fundamental forces known as the gravitational, the electromagnetic, the strong and the weak force. In order to describe physics at microscopic scales, the electromagnetic, the strong and the weak forces can be combined into one coherent theory known as the Standard Model of Particle Physics (SM). These forces are modelled as interactions between matter particles, and are mediated by a different type of particles known as the gauge bosons. The SM describes the properties and interactions of the fundamental particles that constitute matter and mediate the fundamental forces. The elementary constituents of matter belong to the group of fermions, while the mediators of the forces belong to the group of bosons. Adhering to Pauli's spin-statistics theorem, the fermions are defined as particles with spin $\frac{n}{2}$, while bosons have spin n, with $n \in \mathbb{N}$. [1] Overall, there are 12 fermions (6 quarks and 6 leptons), each of which have an antiparticle counterpart. The antifermions have identical physical properties, such as mass, but opposite quantum numbers compared to their counterparts.[1] The positively and negatively charged quarks, as well as the charged and uncharged leptons each organize into three generations. The precise particle content of fermions in the SM can be found from Table 1.

Although the SM has been remarkably successful in describing a wide range of physical phenomena, the original formulation of the SM still suffers from few shortcomings which may be used as directions for the search of a more complete description of particle physics.

---

[1]Provided that the CPT invariance holds exactly. [2]

Table 1: The fermions of the Standard Model

Generation	u-type quarks	d-type quarks	Charged leptons	Neutral leptons
1	u	d	e	ν_e
2	c	s	μ	ν_μ
3	t	b	τ	ν_τ

In this thesis, a particular issue of the SM known as the flavour hierarchy problem will be taken under inspection. In order to explain the flavour hierarchy problem, Chapters 1 and 2 will provide a review of the SM and the Higgs mechanism that is responsible for generating the masses of the bosons and fermions of the SM. Next, addressing the flavour hierarchy problem will lead to two distinct extensions of the SM, both of which can be realized by extending the gauge group of the SM and by adding new fields. The first of these approaches, known as the Froggat-Nielsen mechanism will be briefly described in Chapter 3 in order to offer a review of one of the most common solutions to the flavour hierachy problem. However, the novel work that was carried out during the completion of this thesis is centered around an alternative model, which can be described as one representative of a class of radiative models. Chapter 4 will first introduce the new features of this model, including the new fields as compared to the SM and their mass generation mechanism. After that, the radiative model will be used to explain the flavour hierarchy problem that was first introduced in Chapter 2. In regard to using the radiative model, my own independent contributions were individually working out the previously known theoretical details of the radiative model that can be found from [3] and [4], most importantly the calculations given in Appendices G and F; and also running numerical scans for the free parameters in the model in order to match the theoretical details with the experimental constraints. To that end, I contributed as a coauthor of a paper on the application of the Left-Right Symmetric radiative models for explaining the quark flavour hierarchy. [4] Finally, after explaining the usage of the radiative model in order to explain the flavour hierarchy, this new extension of the SM will be shown to have many interesting phenomenological features, which make it an interesting alternative to SM irrespective of the flavour hierarchy problem.

Chapter 1

The Standard Model of Particle Physics

1.1 Mathematical Formulation

The SM Lagrangian describes the dynamics, masses and interactions of fermions and bosons. In general, the number of terms that can be added to the Lagrangian is constrained by Lorentz invariance, local gauge invariance and renormalizability. The gauge group of the SM is a direct product of three Lie groups: $SU(3)_c \times SU(2)_L \times U(1)_Y$, where the subscripts refer to the color, weak isospin and hypercharge quantum numbers respectively. [5] Given that the Lagrangian must be invariant under a local transformation of this gauge group, the derivatives appearing in the kinetic terms of the Langrangian must be generalized to covariant derivatives. [6] The generalization to covariant derivatives can be easily carried out by using a minimal substitution as follows:

$$\partial_\mu \to D_\mu = \partial_\mu - ig'B_\mu Y - igW_\mu^a t^a - ig_s G_\mu^b t^b, \tag{1.1}$$

where g', g, g_s are the coupling constants of $U(1)_Y$ and $SU(2)_L$, $SU(3)_c$ respectively. The indices $a = 1, 2, 3$, $b = 1, .., 8$ reflect the 3- and 8-dimensional Lie algebras of the nonabelian groups $SU(2)_L$ and $SU(3)_c$ respectively. Hence, new bosonic fields of spin 1 are introduced : eight vector fields G_μ^b for $SU(3)_c$, three vector fields W_μ^a for $SU(2)_L$ and one vector field B_μ for $U(1)_Y$. These gauge fields arise from the adjoint representation of the corresponding gauge group. Overall the Lagrangian of the SM becomes [7]

$$\mathcal{L} = -\frac{1}{4}B_{\mu\nu}B^{\mu\nu} - \frac{1}{4}W_{\mu\nu}^a W^{a\mu\nu} - \frac{1}{4}G_{\mu\nu}^b G^{b\mu\nu}$$
$$+i\bar{\psi}_L \not{D}\psi_L + i\bar{\psi}_R \not{D}\psi_R + (D_\mu\phi)^\dagger D^\mu\phi + \mu^2\phi^\dagger\phi - \lambda(\phi^\dagger\phi)^2 + Y_{ij}\bar{\psi}_{L,i}\phi\psi_{R,j} + h.c., \tag{1.2}$$

where $a = 1, 2, 3$ and $b = 1, .., 8$, and i, j run over the three generations of the charged leptons and u- and d-type quarks given in Table 1. The first three terms appearing in equation (1.2) describe the kinetic terms of the vector bosons corresponding to the photon of electromagnetism, the $W^\pm$ and Z bosons of the weak interaction and the eight gluons of the strong interaction respectively. Explicitly one has

$$B_{\mu\nu} = \partial_\mu B_\nu - \partial_\nu B_\mu, \tag{1.3}$$

$$W^a_{\mu\nu} = \partial_\mu W^a_\nu - \partial_\nu W^a_\mu + g f^{abc} W^b_\mu \tag{1.4}$$

with $a, b, c = 1, 2, 3$, and

$$G^a_{\mu\nu} = \partial_\mu G^a_\nu - \partial_\nu G^a_\mu + g_s f^{abc} G^b_\mu \tag{1.5}$$

with $a, b, c = 1, ..8$. [6] The structure constants f^{abc} appearing in equations (1.4) and (1.5) arise from the Lie algebras of $SU(2)_L$ and $SU(3)_c$ respectively, by the following definition:

$$[t^a, t^b] = i f^{abc} t^c. \tag{1.6}$$

Interestingly, it follows from equations (1.2), (1.4), (1.5) and (1.6) that the gauge bosons corresponding to non-abelian Lie groups exhibit self interactions via three-and four-point vertices.

The fermions of the SM are described by spin $1/2$ spinor fields ψ.[1] More precisely, the fermion sector is chiral, comprising the left-handed fields ψ_L transforming as doublets under $SU(2)_L$ and the right-handed fields transforming as singlets under $SU(2)_L$. [8] The spinor field ψ may stand for either the lepton fields or the quark fields. The explicit form of the left-handed lepton doublets is

$$L_{eL} = \begin{pmatrix} \nu_L \\ e_{eL} \end{pmatrix} \qquad L_{\mu L} = \begin{pmatrix} \nu_{\mu L} \\ \mu_L \end{pmatrix} \qquad L_{\tau L} = \begin{pmatrix} \nu_{\tau L} \\ \tau_L \end{pmatrix}. \tag{1.7}$$

Analogously, the quark doublets are given by[2]

$$Q^c_{1L} = \begin{pmatrix} u^c_L \\ d^c_L \end{pmatrix} \qquad Q^c_{2L} = \begin{pmatrix} c^c_L \\ s^c_L \end{pmatrix} \qquad Q_{3L} = \begin{pmatrix} b^c_L \\ t^c_L \end{pmatrix}. \tag{1.8}$$

---

[1]Here the generation and color indices have been suppressed for the sake of clarity.

[2]The index $c = r, b, g$ denotes the color index associated to the fundamental representation of $SU(3)_c$. From hereon, the color index is understood appearing implicitly in all quark fields.

Table 1.1: The gauge quantum numbers of the fundamental fermion fields of the SM. The $SU(2)_L$ quantum numbers have been assigned according to the doublet description presented in equations (1.8) and (1.7), while the hypercharges Y are fixed by the requirement of matching the $SU(2)_L$ quantum numbers and the experimentally observed electric charge, by using equation (2.30).

	Q_L	u_R	d_R	L_L	e_R
$U(1)_Y$	$\frac{1}{6}$	$\frac{2}{3}$	$-\frac{1}{3}$	$-\frac{1}{2}$	-1
$SU(2)_L$	$(\frac{1}{2}, -\frac{1}{2})$	0	0	$(\frac{1}{2}, -\frac{1}{2})$	0
$SU(3)_c$	triplet	triplet	triplet	singlet	singlet

The explicit form of the right handed lepton singlets is given by

$$e_{eR} = e_R \quad e_{\mu R} = \mu_R \quad e_{\tau R} = \tau_R. \tag{1.9}$$

Similarly, the quark right-handed singlets are given by

$$q^U_{uR} = u_R \quad q^U_{cR} = c_R \quad q^U_{tR} = t_R \tag{1.10}$$

$$q^D_{dR} = d_R \quad q^D_{sR} = s_R \quad q^D_{bR} = b_R. \tag{1.11}$$

Moreover, the relevant quantum numbers can be found from Table 1.1.

The first term on the second line of equation (1.2) describes the kinetic terms of the fermion fields, where the partial derivative has been replaced by the covariant derivative and $\slashed{D} = D_\mu \gamma^\mu$. Due to the covariant derivative, interaction terms between the fermions and the gauge bosons will appear in the Lagrangian in addition to the kinetic terms of the fermion fields. These interactions are governed by the gauge coupling constants g, g', g_S. Although g and g' grow with increasing energy, g_s on the other hand increases when the energy is lowered. Consequently, at very low energies the particles with nonzero color charge are very strongly bound together. As a result, quarks and gluons are confined at low energies, meaning that they cannot be observed as free particles. [9, 10, 11]

In addition, a scalar field ϕ of spin 0 can also be included in the SM Lagrangian. As will be shown in Chapter 2, this field is necessary for carrying out the spontaneous breaking of the $SU(2)_L \times U(1)_Y$ symmetry. It should be noted that since ϕ is associated with the $SU(2)_L \times U(1)_Y$ the last term of equation (1.1) does not appear in $(D_\mu \phi)^\dagger D^\mu \phi$. Consequently, the covariant derivative acting on ϕ does not result in the interaction of ϕ with the massless gluons. The interactions of ϕ with the other gauge bosons are discussed

in Chapter 2. The quadratic and quartic operators in ϕ appearing in equation (1.2) describe the so-called Higgs potential, which sources the spontaneous symmetry breaking (SSB) in the electroweak (EW) sector, as will be shown in Chapter 2. Finally, the last term of the SM Lagrangian in equation (1.2) collects the Yukawa terms responsible for generating the fermion masses after spontaneous breaking of the EW symmetry, discussed in Section 2.3. These terms do not follow from any symmetry consideration and must be solely added to the Lagrangian to match experimental observations. Crucially, the vector boson and the spinor fields have no explicit mass terms in equation (1.2) since the inclusion of mass terms is constrained by local gauge invariance. Further details about the mass generation mechanism for the fields of the SM are given in Chapter 2.

1.2 The Electroweak Sector of the Standard Model

The Lagrangian of the EW sector of the SM without the mass terms for the gauge bosons and the charged fermions is symmetric under local $SU(2)_L \times U(1)_Y$ gauge transformation.[3] [8] It consists of the kinetic terms for the spinor field and for the gauge fields. The mass terms, as will be shown, are forbidden by the requirement of local gauge invariance. The interactions between the gauge bosons and the fermions are encoded in the covariant derivative, which again must be added to the Lagrangian in order to maintain invariance under local $SU(2)_L \times U(1)_Y$ transformations.[4]

The SM Lagrangian can be made invariant under the local gauge transformations of the fermion fields:[5]

$$U(1)_Y : \ \psi \rightarrow \ e^{i\lambda_Y(x)Y}\psi \tag{1.12}$$

and,

$$SU(2)_L : \ \psi \rightarrow e^{i\lambda_L^a(x)T^a}\psi, \tag{1.13}$$

by simultaneously transforming the gauge fields:

$$U(1)_Y : \ B_\mu \rightarrow \ B_\mu + \frac{1}{g'}\partial_\mu\lambda_Y(x) \tag{1.14}$$

---

[3]Here the terms associated with $SU(3)_c$ are omitted as this symmetry remains unbroken during the spontaneous breaking of the EW symmetry.

[4]In this short section, the discussion of gauge fixing and ghost terms has been omitted as it is not relevant for the introduction of the flavour hierarchy problem. However, the discussion of gauge fixing for a $U(1)$ local gauge symmetry is briefly discussed in the Appendix, where the propagator for the gauge field associated to a new $U(1)_F$ symmetry is explicitly calculated.

[5]The transformation properties of the scalar field ϕ can be chosen in such a way that the terms containing ϕ also remain invariant under simultaneously transforming ϕ, the gauge fields and the fermion fields. The transformation laws of ϕ are more carefully considered in Chapter 2.

and,

$$SU(2)_L : W_\mu^a \rightarrow W_\mu^a + \frac{1}{g}\partial_\mu \lambda_L^a(x) + \epsilon^{abc}W_\mu^b \lambda_L^c. \tag{1.15}$$

In order to obtain the states with definite chirality from a general spinor ψ, the projection operators P_L and P_R can be used, so that

$$P_R = \frac{1}{2}(1 + \gamma_5) \quad \text{and} \quad P_R\psi = \psi_R \tag{1.16}$$

and,

$$P_L = \frac{1}{2}(1 - \gamma_5) \quad \text{and} \quad P_L\psi = \psi_L. \tag{1.17}$$

Using the anticommutation relations between γ^5 and γ^0 and the hermiticity of γ^0, it is also easy to calculate:

$$\bar{\psi}P_R = \bar{\psi}_L \quad \text{and} \quad \bar{\psi}P_L = \bar{\psi}_R. \tag{1.18}$$

Then from $P_L + P_R = 1$, it follows that

$$\bar{\psi}\gamma^\mu D_\mu \psi = \bar{\psi}\gamma^\mu D_\mu P_L \psi + \bar{\psi}\gamma^\mu D_\mu P_R \psi = \bar{\psi}P_R\gamma^\mu D_\mu P_L \psi + \bar{\psi}P_L\gamma^\mu D_\mu P_R \psi. \tag{1.19}$$

Thus,

$$\bar{\psi}\gamma^\mu D_\mu \psi = \bar{\psi}_L\gamma^\mu D_\mu \psi_L + \bar{\psi}_R\gamma^\mu D_\mu \psi_R. \tag{1.20}$$

As for the mass terms of the gauge bosons, it is clear that due to equations (1.14) and (1.15), it is not possible to write down a gauge invariant mass term for B_μ and W_μ^a. Instead, the Higgs mechanism needs to be employed. This is demonstrated in Chapter 2. Analogously, gauge invariance along with requiring Lorentz invariance also forbids the mass term for the spinor fields. Although the term $m\psi\psi^\dagger$ is not Lorentz invariant, a Lorentz invariant mass term can still be written by using $\bar{\psi} = \psi^\dagger\gamma^0$ as can be seen below.[6]

$$\begin{aligned}
\bar{\psi}(x)\psi(x) = \psi^\dagger(x)\gamma^0\psi(x) &\rightarrow \psi^\dagger\left(\Lambda^{-1}x\right)S[\Lambda]^\dagger \gamma^0 S[\Lambda]\psi\left(\Lambda^{-1}x\right) \\
&= \psi^\dagger\left(\Lambda^{-1}x\right)\gamma^0 S[\Lambda]^{-1}S[\Lambda]\psi\left(\Lambda^{-1}x\right) \\
&= \psi^\dagger\left(\Lambda^{-1}x\right)\gamma^0\psi\left(\Lambda^{-1}x\right) \\
&= \bar{\psi}\left(\Lambda^{-1}x\right)\psi\left(\Lambda^{-1}x\right).
\end{aligned} \tag{1.21}$$

However, by writing this term as

$$m\bar{\psi}\psi = m\bar{\psi}P_L^2\psi + m\bar{\psi}P_R^2\psi = m\bar{\psi}_R\psi_L + m\bar{\psi}_L\psi_R, \tag{1.22}$$

---

[6]Here the transformation laws $\psi(x) \rightarrow S[\Lambda]\psi\left(\Lambda^{-1}x\right)$ and $\psi^\dagger(x) \rightarrow \psi^\dagger\left(\Lambda^{-1}x\right)S[\Lambda]^\dagger$ for the Dirac spinor and its adjoint, along with the identity $S[\Lambda]^\dagger = \gamma^0 S[\Lambda]^{-1}\gamma^0$ are used. [12]

it is clear that since the right-handed fields transform as singlets, while the left-handed fields transform as doublets under $SU(2)_L$, the mass term for the fermions cannot be written in the form displayed in equation (1.22). This problem will also be solved by the Higgs mechanism in Chapter 2.

1.3   Parameters of the Standard Model

The SM can be described by 19 parameters. [13] The 5 flavour universal parameters are the 3 gauge couplings g_s, g and g', associated to the $SU(3)_c$, $SU(2)_L$ and $U(1)_Y$ groups respectively; the Higgs quartic coupling λ and the mass squared μ^2 of the Higgs field. Observing a non-universality of any of the coupling constants across different flavours would signal a deviation from the SM, and thus is an active research topic. [14, 15] The mass squared parameter of the Higgs field was independently determined with the measurement of the Higgs boson mass by the CMS and ATLAS collaborations at CERN in 2012 [16, 17]. The quartic coupling could be inferred from the di-boson scattering experiments that will take place within the High Luminosity LHC experiments or from lepton colliders such as the Circular Electron Positron Collider (CEPC) or the Future Circular (Lepton) Collider (FCC-e). [18]. The rest of the parameters are the six quark masses, three charged lepton masses, four quark mixing parameters, including one charge-parity (CP) violating phase and three mixing angles, and one strong CP-violating parameter. The latter does not appear in the flavour hierarchy problem, so it is for the most part unimportant for the purpose of this thesis.[7] The neutrinos remain massless in the original formulation of the SM, which is the approach taken in this thesis, although it is well known from the observation of neutrino oscillations, that neutrinos indeed do have a mass, small in value in comparison to the masses of the charged leptons. [19] Extending the SM to contain massive neutrinos would mean including either 9 or 7 additional parameters to the SM, depending on whether the neutrinos are considered to be Majorana or Dirac fermions.

The electron mass has been very precisely measured using Penning traps. [20] The value cited by the Particle Data Group (PDG) is given by

$$m_e = 0.5109989461 \pm 0.0000000031 \text{ MeV}. \tag{1.23}$$

---

[7]As a minor exception, the question of the strong CP violation is briefly tackled in Section 4.5 where the novel phenomenological implications of the radiative left-right symmetric theories explaining the flavour hierarchy problem are considered.

The mass of the muon is determined by measuring the Zeeman transition frequencies in the muonium atoms. The value of the muon mass is [19]

$$m_\mu = 105.6583715 \pm 0.0000035 \text{ MeV}. \tag{1.24}$$

For the tau mass, the PDG quotes the average of several measurements over the tau decay channels as well as the mass inferred from electron-positron collisions. [19] The mass is given by

$$m_\tau = 1776.86 \pm 0.12 \text{ MeV}. \tag{1.25}$$

Determining the quark masses is much more difficult due to quark confinement, mentioned in Section 1.1. Hence, the quark masses must be inferred from the properties of hadrons. The light quark masses can be obtained by lattice-QCD calculations,[8] by fine-tuning the constituent quark masses to reproduce the masses of the observed pions, kaons and eta-mesons. [21] The values quoted by the Flavour Lattice Averaging Group (FLAG) collaboration are [21, 22]

$$\overline{m_u} = 2.50(17) \text{ MeV} \quad \overline{m_d} = 4.88(20) \text{ MeV} \quad \overline{m_s} = 92.9(0.7) \text{ MeV}. \tag{1.26}$$

The mass of the charm quark depends strongly on the momentum scale due to the running of the mass. Estimations can be obtained from correlation functions by using D-, D_s- and charmonium mesons' data. [21] The FLAG collaboration quotes the charm quark mass at the renormalization scale $p = \overline{m_c}$ [21]

$$\overline{m_c}(\overline{m_c}) = 1.280(13) \text{ GeV}. \tag{1.27}$$

Detailed description of the estimation of the bottom quark mass is outside the scope of this thesis. In short, the PDG collaboration quotes the bottom quark mass as [19]

$$\overline{m_b}(\overline{m_b}) = 4.198(12) \text{ GeV}. \tag{1.28}$$

The top quark is special, as it is the only quark that can decay semi-leptonically, by the emission of an on-shell W-boson. [19] For this reason, the top quark decays before hadronization, and hence its mass can be inferred directly from scattering experiments. Currently, the most precise measurement has been performed by the CMS collaboration: [23]

$$\overline{m_t} = 172.22 \pm 0.73 \text{ GeV}. \tag{1.29}$$

---

[8]In this section all of the quark masses are quoted within the modified minimal subtraction scheme ($\overline{MS}$).

All of the above mass values can be included in the SM via the Higgs mechanism, which will be introduced in the next section. However, by solely using the SM one cannot explain the large difference in masses between quarks and leptons of different generations. Moreover, the quark mixing parameters also follow a noticeable spread in values as will be shown in Section 2.4. These issues will eventually lead to the extensions of the SM.

Chapter 2

Spontaneous Breaking of the Electroweak Symmetry

2.1 Introducing the Higgs Boson

As was mentioned in the previous chapter, the requirement of gauge invariance forbids the mass terms for the fermions and gauge bosons of the SM. Hence, in order to have a theory with massive fields, it is necessary to introduce a gauge-invariance breaking mechanism. This is realized in this chapter by the introduction of a scalar field ϕ, which spontaneously breaks the $SU(2)_L \times U(1)_Y$ symmetry.[1] [24, 25, 26] The scalar field ϕ can be written as follows:

$$\phi = \frac{1}{\sqrt{2}} \begin{pmatrix} \phi_1 + i\phi_2 \\ \phi_3 + i\phi_4 \end{pmatrix}. \tag{2.1}$$

It is a color singlet, a $SU(2)_L$ doublet with hypercharge $Y = 1/2$ and it appears in the Lagrangian of the SM through the following terms[2]

$$\mathcal{L}_\phi = \left(D_\mu \phi \right)^\dagger \left(D^\mu \phi \right) - V(\phi) + \mathcal{L}_{Yuk}. \tag{2.2}$$

The first term in $\mathcal{L}_\phi$ contains the kinetic terms and the interaction of ϕ with the SM gauge fields. Secondly, the $V(\phi)$ term represents the most general gauge invariant potential involving ϕ:

$$V(\phi) = -\mu^2 \phi^\dagger \phi + \lambda \left(\phi^\dagger \phi \right)^2. \tag{2.3}$$

---

[1]This $SU(2)_L \times U(1)_Y$ symmetry breaking mechanism is usually referred to as the Higgs mechanism.
[2]Here, the conventions and charge assignments of [27] are used.

Higher powers of ϕ are omitted on the grounds of renormalizability. To investigate equation (2.3) further, it is customary to explore the behaviour of the minima of the potential for different values of μ and λ. The field configurations giving rise to the minima of the potential in equation (2.3) define the vacuum of the theory and the corresponding field values $\langle\phi\rangle$ which are known as the vacuum expectation values (vev).

1. If $\lambda < 0$, then the potential is not bounded from below and there is no stable vacuum state.

2. When $\lambda > 0$ and $-\mu^2 > 0$, then the minimum energy state is defined by $\phi = 0$. In that case, the vacuum state given by $\phi = 0$ is unchanged under a gauge transformation, and hence the $SU(2)_L \times U(1)_Y$ symmetry remains unbroken.

3. Finally, if $\lambda > 0$ and $-\mu^2 < 0$, then it can be easily seen that the minimum energy configuration is given by

$$\langle\phi\phi^\dagger\rangle = \frac{\mu^2}{2\lambda}. \tag{2.4}$$

In that case the $SU(2)_L \times U(1)_Y$ gauge symmetry has been spontaneously broken and ϕ obtains a expectation value, given by equation (2.4).

With the normalization given by equation (2.1), the potential in equation (2.3) can be written as follows:

$$V(\phi) = -\frac{\mu^2}{2}\left(\phi_1^2 + \phi_2^2 + \phi_3^2 + \phi_4^2\right) + \frac{\lambda}{4}\left(\phi_1^2 + \phi_2^2 + \phi_3^2 + \phi_4^2\right)^2 \tag{2.5}$$

Clearly, using equation (2.1) equation (2.4) can also be rewritten as[3]

$$\frac{1}{2}\left(\phi_1^2 + \phi_2^2 + \phi_3^2 + \phi_4^2\right) = \frac{\mu^2}{2\lambda} = \frac{v^2}{2}. \tag{2.6}$$

In the unitary gauge, ϕ can be written as[4]

$$\phi = \frac{1}{\sqrt{2}}\begin{pmatrix} 0 \\ \phi_3 \end{pmatrix}. \tag{2.7}$$

Furthermore, ϕ_3 can be decomposed as

$$\phi_3 = h + v \quad \text{with} \quad \langle h\rangle = 0. \tag{2.8}$$

---

[3]In this chapter, from now the symbol v will be used in the sense of equation (2.6) and called the vacuum expectation value (vev).

[4]The benefit of using the unitary gauge is that the $SU(2)_L \times U(1)_Y$ symmetry can be broken without breaking the $U(1)_{EM}$ symmetry associated with electromagnetism. Thus the symmetry breaking scheme is $SU(2)_L \times U(1)_Y \rightarrow U(1)_{EM}$.

The fact that ϕ_3 is a real scalar field means that ϕ_3 describes a neutral boson of spin 0. This guarantees that the vaccuum does not become electrically charged after the SSB of the $SU(2)_L \times U(1)_Y$ symmetry. With this modification, equation (2.5) becomes

$$V(\phi) = \frac{-\mu^2}{2} \left(\phi_1^2 + \phi_2^2 + (h+v)^2 + \phi_4^2 \right) + \frac{\lambda}{4} \left(\phi_1^2 + \phi_2^2 + (h+v)^2 + \phi_4^2 \right)^2. \tag{2.9}$$

Since the fields ϕ_1, ϕ_2, h, ϕ_4 are treated as small excitations of the vaccuum, the Higgs potential appearing in (2.9) can be expanded about the field values, omitting higher order terms. Rewriting equation (2.9) in the unitary gauge and eliminating $\mu^2 = \lambda v^2$ gives

$$V(\phi) = const + 0\phi_1^2 + 0\phi_2^2 + \lambda v^2 h^2 + 0\phi_4^2 + O\left(\phi^3\right), \tag{2.10}$$

where $O\left(\phi^3\right)$ denote the third order terms in either h or ϕ_i, for $i = 1, 2, 4$. Clearly, the only field with quadratic terms is h. Hence, only the scalar field h will obtain a mass. Adhering to the convention of writing the mass term of a real scalar field as $\frac{1}{2}m^2\phi^2$, [27] it follows that the mass of h is given by

$$m_h = \sqrt{2\lambda v^2}. \tag{2.11}$$

The 3 massless Goldstone boson fields ϕ_1, ϕ_2, ϕ_4 are therefore absorbed into the gauge transformation and the associated degrees of freedom re-appear as longitudinal polarization modes of the massive vector bosons W^+, W^-, Z. More details can be found in Appendix A.

2.2   Masses of the Gauge Bosons

In the unitary gauge, the kinetic term appearing in equation (2.2) takes the following form [27]

$$\left(D_\mu \phi\right)\left(D^\mu \phi\right)^\dagger = \frac{1}{2}\left(\partial_\mu h\right)\left(\partial^\mu h\right) + \frac{1}{8}g^2(v+h)^2\left(W_\mu^1 - iW_\mu^2\right)\left(W^{1\mu} + iW^{2\mu}\right)$$
$$+ \frac{1}{8}(v+h)^2\left(-g'B_\mu + gW_\mu^3\right)^2. \tag{2.12}$$

The first term appearing in equation (2.12) is the kinetic term for the Higgs field. To interpret the second term of equation (2.12), it is useful to consider the covariant derivative terms for the left-handed quark fields.[5]

$$\bar{\psi}_L \gamma^\mu D_\mu \psi_L = \begin{pmatrix} \bar{u} & \bar{d} \end{pmatrix} \gamma^\mu \left(\partial_\mu - i\frac{g'}{2}B_\mu - i\frac{g}{2}W_\mu^a \sigma^a \right) \begin{pmatrix} u \\ d \end{pmatrix}. \tag{2.13}$$

---

[5]In Chapter 1 it was shown that the left and right handed fermion fields decouple for the case of kinetic terms.

For the W_μ^1 and W_μ^2 terms one can write

$$W_\mu^1 \sigma^1 + W_\mu^2 \sigma^2 = \frac{1}{2} \left(W_\mu^1 - i W_\mu^2 \right) \left(\sigma^1 + i \sigma^2 \right) + \frac{1}{2} \left(W_\mu^1 + i W_\mu^2 \right) \left(\sigma^1 - i \sigma^2 \right). \tag{2.14}$$

Thus, by defining $2\sigma^+ \equiv \sigma_1 + i\sigma_2$ and $2\sigma^- \equiv \sigma_1 - i\sigma_2$, it is possible to write the W_μ^1 and W_μ^2 terms of equation (2.13) as

$$
\begin{aligned}
\begin{pmatrix} \bar{u} & \bar{d} \end{pmatrix} \gamma^\mu \left(-i\frac{g}{2} W_\mu^1 \sigma^1 - i\frac{g}{2} W_\mu^2 \sigma^2 \right) P_L \begin{pmatrix} u \\ d \end{pmatrix} &= -g\sqrt{2} \frac{W_\mu^1 - i W_\mu^2}{\sqrt{2}} \begin{pmatrix} \bar{u} & \bar{d} \end{pmatrix} \gamma^\mu \sigma^+ P_L \begin{pmatrix} u \\ d \end{pmatrix} \\
&\quad - g\sqrt{2} \frac{W_\mu^1 + i W_\mu^2}{\sqrt{2}} \begin{pmatrix} \bar{u} & \bar{d} \end{pmatrix} \gamma^\mu \sigma^- P_L \begin{pmatrix} u \\ d \end{pmatrix}.
\end{aligned}
\tag{2.15}
$$

After using the explicit matrix representation of σ^+ and σ^-, equation (2.15) takes the form:

$$- g \frac{W_\mu^1 - i W_\mu^2}{\sqrt{2}} \bar{u}\gamma^\mu P_L d - g \frac{W_\mu^1 + i W_\mu^2}{\sqrt{2}} \bar{d}\gamma^\mu P_L u. \tag{2.16}$$

Since the Higgs mechanism leaves the $U(1)_{EM}$ symmetry invariant, it follows that the terms of the Lagrangian must be charge neutral, otherwise the $U(1)$ symmetry of electromagnetism would be broken. Thus, the following charged bosonic fields may be defined:

$$W^\pm = \frac{W^1 \mp i W^2}{\sqrt{2}}, \tag{2.17}$$

where the $\pm$ refers to the electric charge. Then, using equation (2.17) for the vector mediators, the second term in equation (2.12) can be written as

$$
\begin{aligned}
\frac{1}{8} g^2 (v+h)^2 \left(W_\mu^1 - i W_\mu^2 \right) \left(W^{1\mu} + i W^{2\mu} \right) &= \\
\frac{g^2 v^2}{4} W_\mu^+ W^{-\mu} + \frac{g^2 v}{2} h W_\mu^+ W^{-\mu} &+ \frac{g^2}{4} hh W_\mu^+ W^{-\mu}.
\end{aligned}
\tag{2.18}
$$

From equation (2.18) it is easy to identify the W-boson mass:

$$m_W^2 = \frac{g^2 v^2}{4}, \tag{2.19}$$

the coupling factor for the Higgs-W three-point vertex:

$$g_{hWW} = \frac{g^2 v}{2} \tag{2.20}$$

and the coupling factor for the Higgs-W four-point vertex:

$$g_{hhWW} = \frac{g^2}{4}. \tag{2.21}$$

It remains to investigate the third term of equation (2.12). In order to relate this term to the physical fields, the reparametrization with the introduction of the Weinberg angle θ_W

$$\frac{g}{\sqrt{g^2 + g'^2}} \equiv \cos\theta_W \quad \text{and} \quad \frac{g'}{\sqrt{g^2 + g'^2}} \equiv \sin\theta_W, \tag{2.22}$$

can be used, to rewrite:

$$gW_\mu^3 - g'B_\mu = \sqrt{g^2 + g'^2}\left(\cos\theta_W W_\mu^3 - \sin\theta_W B_\mu\right). \tag{2.23}$$

In that case, the third term in equation (2.12) becomes

$$\begin{aligned}
\frac{1}{8}(v+h)^2\left(-g'B_\mu + gW_\mu^3\right)^2 &= \frac{\left(g^2 + g'^2\right)v^2}{8}Z^\mu Z_\mu \\
&+ \frac{\left(g^2 + g'^2\right)v}{4}Z^\mu Z_\mu h + \frac{\left(g^2 + g'^2\right)}{8}Z^\mu Z_\mu hh.
\end{aligned} \tag{2.24}$$

From equation (2.24) it is evident that the Lagrangian contains a massive physical field Z^μ with mass given by

$$M_Z^2 = \frac{\left(g^2 + g'^2\right)v^2}{4}. \tag{2.25}$$

Moreover, there is a Higgs-Z trilinear vertex, with a coupling factor of

$$g_{ZZh} = \frac{\left(g^2 + g'^2\right)v}{4}, \tag{2.26}$$

and a Higgs-Z four-point vertex, with a coupling factor of

$$g_{ZZhh} = \frac{\left(g^2 + g'^2\right)}{8}. \tag{2.27}$$

The orthogonal state to Z_μ, given by

$$A_\mu \equiv \sin\theta_W W_\mu^3 + \cos\theta_W B_\mu, \tag{2.28}$$

can be used along with the definitions of W_μ^+, W_μ^-, $Z_{-\mu}$ to rewrite the covariant derivative as [27]

$$
\begin{aligned}
D_\mu = \partial_\mu &- i\frac{g}{\sqrt{2}}\left(W_\mu^+ T^+ + W_\mu^- T^-\right) \\
&- iZ_\mu\left(g\cos\theta_W T^3 - g'\sin\theta_W Y\right) \\
&- iA_\mu\left(g\sin\theta_W T^3 + g'\cos\theta_W Y\right).
\end{aligned}
\tag{2.29}
$$

Moreover, it is evident that the field A_μ as defined by equation (2.28) does not have a mass term in any of the summands appearing in equation (2.12). Hence, A_μ can be identified with the only massless field in the EW sector - the photon. In fact, the photon coupling in equation (2.29) can be further simplified, by invoking the Gell-Mann-Nishijima relation[6] [28]

$$
Q = T^3 + Y.
\tag{2.30}
$$

Then from equations (2.22) and (2.30) it follows that[7]

$$
g\sin\theta_W T^3 + g'\cos\theta_W Y = \frac{gg'}{\sqrt{g^2 + g'^2}}\left(T^3 + Y\right) \equiv eQ.
\tag{2.31}
$$

Thus, the coupling constants of the $SU(2)_Y$ and $U(1)_Y$ groups and the electric charge are not independent, but related via

$$
e = \frac{gg'}{\sqrt{g^2 + g'^2}} = g\sin\theta_W = g'\cos\theta_W.
\tag{2.32}
$$

2.3 Masses of Fermions

As shown in equation (1.22), the fermion mass term cannot be written in terms of spinor fields only. Instead, the fermion masses are generated by the SSB mechanism, by coupling the fermion fields to the scalar $SU(2)_L$ doublet ϕ, analogous to the generation of the gauge boson masses in Section 2.2. [29, 30] Since the mass dimension of the fermion fields is $\frac{3}{2}$ and the mass dimension of a scalar field is 1, the only renormalizable mass term that can be generated via SSB, must be of the form $y\bar{\psi}\phi\psi$. The dimensionless constant y is called the Yukawa coupling. After SSB, it will play a crucial role in determining the masses of fermions, as is shown below.

---

[6] Again, the conventions of [27] are used.

[7] The inclusion of the electric charge e follows from the assumption that the A_μ-term in the covariant derivative takes the form $-ieA_\mu Q$.

2.3.1 Masses of the Charged Leptons

For the charged leptons, the Yukawa terms in the Lagrangian,[8] responsible for the generation of the lepton masses are given by [5, 31]

$$\mathcal{L}^l_{Yuk} = - \sum_{i,j=e,\mu,\tau} \left(y_{ij} \bar{e}'_{iR} \phi^\dagger L'_{jL} + y^*_{ij} \bar{L}'_{jL} \phi e'_{iR} \right), \tag{2.33}$$

Using the unitary gauge, equation (2.33) becomes

$$\mathcal{L}^l_{Yuk} = - \sum_{i,j=e,\mu,\tau} \frac{1}{\sqrt{2}} \left[(v+h) \, y_{ij} \bar{e}'_{iR} e'_{jL} + (v+h) \, y^*_{ij} \bar{e}'_{jL} e'_{iR} \right]. \tag{2.34}$$

Consequently, the mass terms for the charged leptons are given by the rescaled eigenvalues of the Yukawa matrix

$$m_i = \frac{y_{ii} v}{\sqrt{2}} \quad i = e, \mu, \tau \tag{2.35}$$

and the coupling constants of the charged leptons to the Higgs field are given by

$$g_{ij} = \frac{y_{ij}}{\sqrt{2}}. \tag{2.36}$$

Evidently, by diagonalizing the Yukawa matrix via a biunitary transformation it is possible to both identify the mass eigenstates, as well as to write down the Higgs-lepton coupling in a diagonal basis.[9]

2.3.2 Masses of Quarks

Whilst considering quarks, most of the arguments used in Subsection 2.3.1 can be taken over. For the down type quarks, the Yukawa terms can be written as [27, 31]

$$\mathcal{L}^D_{Yuk} = \sum_{i=1,2,3} \sum_{j=d,s,b} Y'^D_{ij} \bar{Q}'_{iL} \phi q'^D_{jR} + Y'^{D*}_{ij} \bar{q}'^D_{jR} \phi^\dagger Q'_{iL}. \tag{2.37}$$

In order to generate the Yukawa terms for u-type quarks, one has to take care of a subtlety related to the hypercharges. Namely, the product $\bar{Q}'_{iL} q'^U_{jR}$ has hypercharge $Y = \frac{1}{2}$. Hence, in order to couple this bilinear to the Higgs, the scalar field needs to have a hypercharge

---

[8]The prime symbols on top of the lepton fields denote the gauge eigenstates, i.e. terms that have only diagonal interactions with the gauge fields.

[9]The mathematical details are given in Appendix B.

$Y = -\frac{1}{2}$ to maintain gauge invariance. To that end, one might consider

$$\widetilde{\phi} \equiv i\sigma_2 \phi. \tag{2.38}$$

The transformation law of $\widetilde{\phi}$ is given by

$$\widetilde{\phi} \rightarrow i\sigma_2 \left(e^{-i\lambda_Y(x)Y - i\lambda_L^a(x)\sigma^{a*}} \sigma_2 \right) i\sigma_2 \phi^* = e^{-i\lambda_Y(x)Y + i\lambda_L^a(x)\sigma^a} i\sigma_2 \phi^*$$
$$= e^{-i\lambda_Y(x)Y + i\lambda_L^a(x)\sigma^a} \widetilde{\phi}, \tag{2.39}$$

where the equalities $\sigma_2\sigma_2 = I$ and $\sigma_2\sigma^{\mu*}\sigma_2 = -\sigma^\mu$ were used. As can be seen from equation (2.39), $\widetilde{\phi}$ transforms like ϕ under $SU(2)_L$ and has hypercharge $Y = -\frac{1}{2}$, allowing to write the Yukawa terms for the u-type quarks

$$\mathcal{L}_{Yuk}^U = -\sum_{i=1,2,3} \sum_{j=u,c,t} Y_{ij}^{\prime U} \bar{Q}^\prime_{iL} \widetilde{\phi} q_{jR}^{\prime U} + Y_{ij}^{\prime U*} \bar{q}^{\prime U}_{jR} \widetilde{\phi}^\dagger Q^\prime_{iL}. \tag{2.40}$$

As in the previous subsection, in order to find the quark mass eigenstates, we need to diagonalize the Yukawa matrices $Y^{\prime D}$ and $Y^{\prime U}$ by biunitary transformations. Explicitly

$$V_L^{D\dagger} Y^{\prime D} V_R^D = Y^D \quad Y_{ij}^D = y_i^D \delta_{ij}, \quad i, j = d, s, b, \tag{2.41}$$

$$V_L^{U\dagger} Y^{\prime U} V_R^U = Y^U \quad Y_{ij}^U = y_i^U \delta_{ij}, \quad i, j = u, c, t. \tag{2.42}$$

The matrices used to perform the biunitary transformations in equations (2.41) and (2.42) can also be used to define the mass eigenstates of quarks as follows:

$$q_L^D = V_L^{D\dagger} \begin{pmatrix} d_L^\prime \\ s_L^\prime \\ b_L^\prime \end{pmatrix} = \begin{pmatrix} d_L \\ s_L \\ b_L \end{pmatrix} \quad q_R^D = V_R^{D\dagger} \begin{pmatrix} d_R^\prime \\ s_R^\prime \\ b_R^\prime \end{pmatrix} = \begin{pmatrix} d_R \\ s_R \\ b_R \end{pmatrix} \tag{2.43}$$

$$q_L^U = V_L^{U\dagger} \begin{pmatrix} u_L^\prime \\ c_L^\prime \\ t_L^\prime \end{pmatrix} = \begin{pmatrix} u_L \\ c_L \\ t_L \end{pmatrix} \quad q_R^U = V_R^{U\dagger} \begin{pmatrix} u_R^\prime \\ c_R^\prime \\ t_R^\prime \end{pmatrix} = \begin{pmatrix} u_R \\ c_R \\ t_R \end{pmatrix}. \tag{2.44}$$

After diagonalization, the quark masses are simply given by rescaled eigenvalues of the Yukawa matrix

$$m_i = \frac{y_{ii}^D v}{\sqrt{2}} \quad i = d, s, b, \tag{2.45}$$

$$m_i = \frac{y_{ii}^U v}{\sqrt{2}} \quad i = u, c, t. \tag{2.46}$$

The eigenvalues of the Yukawa matrices are unknown parameters of the SM which have to be obtained from experiment.[10]

2.4 The Weark Charged Current and the CKM Matrix

2.4.1 The CKM Matrix

In the SM two types of interactions between the fermions and bosons mediating the weak force can be distinguished. As the currents participating in these interactions are coupled to charged ($W^\pm$) and neutral (Z) bosons, they are called weak charged currents (WCC) and weak neutral currents (WNC) respectively. In this section, the focus is on WCC, while the WNC will be considered in the next section. In agreement with the experiment, the WCC arising from the covariant derivative of the lepton and quark fields is given by [31]

$$j_W^\mu = j_{W,L}^\mu + j_{W,Q}^\mu. \tag{2.47}$$

In terms of the gauge eigenstates the leptonic WCC is given by

$$j_{W,L}^\mu = \sum_{i=e,\mu,\tau} \left[\bar{\nu}'_{iL} \gamma^\mu e'_{iL} + \bar{e}'_{iL} \gamma^\mu \nu'_{iL} \right]. \tag{2.48}$$

Since the neutrinos in the SM are assumed massless, one can rewrite equation (2.48) as[11]

$$j_{W,L}^\mu = \overline{\nu'_\mathbf{L}} \gamma^\mu \mathbf{e}'_\mathbf{L} + \overline{\mathbf{e}'_\mathbf{L}} \gamma^\mu \nu'_\mathbf{L} = \overline{\nu_\mathbf{L}} V_L^{L\dagger} \gamma^\mu V_L^L \mathbf{e_L} + \overline{\mathbf{e}'_\mathbf{L}} V_L^{L\dagger} \gamma^\mu V_L^L \nu'_\mathbf{L}, \tag{2.49}$$

where

$$\nu'_\mathbf{L} = \begin{pmatrix} \nu'_{eL} \\ \nu'_{\mu L} \\ \nu'_{\tau L} \end{pmatrix} \qquad \mathbf{e}'_\mathbf{L} = \begin{pmatrix} e'_L \\ \mu'_L \\ \tau'_L \end{pmatrix} \tag{2.50}$$

and,

$$\nu_\mathbf{L} = V_L^L \nu'_\mathbf{L} \qquad \mathbf{e_L} = V_L^L \mathbf{e}'_\mathbf{L}. \tag{2.51}$$

---

[10]The current experimental and theoretical progress on determining the quark masses is very briefly mentioned in Section 1.3. More details can be found from [19] and references therein.

[11]The massless neutrino fields will remain massless after transformation by any unitary matrix. Hence the neutrino fields can be rotated by the same matrix V_L that diagonalizes the Yukawa matrix of the charged leptons.

Then, from the unitarity of V_L^L it follows that

$$j_{W,L}^\mu = \overline{\nu_\mathbf{L}}\gamma^\mu\mathbf{e_L} + \overline{\mathbf{e_L}}\gamma^\mu\nu_\mathbf{L}. \tag{2.52}$$

From equation (2.52), it is clear that in the charged current interactions, the three lepton numbers L_e, L_μ and L_τ are conserved. This is related to the global symmetry of the Lagrangian under rephasing the neutrino fields (cf. Appendix C.2).

As was shown in the previous section, all quark fields in the SM are massive. This is different from the case of leptons, where the neutrino fields were assumed massless within the context of the SM and has important consequences on the quark mixing. [32, 33] The hadronic WCC is given by

$$j_{W,Q}^\mu = \sum_{i=1,2,3}\left[\overline{d'_{L,i}}\gamma^\mu u'_{L,i} + \overline{u'_{L,i}}\gamma^\mu d'_{L,i}\right]. \tag{2.53}$$

By using equations (2.44) and (2.43), equation (2.53) can be written as

$$j_{W,Q}^\mu = \overline{\mathbf{d'_L}}\gamma^\mu\mathbf{u'_L} + \overline{\mathbf{u'_L}}\gamma^\mu\mathbf{d'_L} = \overline{\mathbf{d_L}}V_L^{D\dagger}\gamma^\mu V_L^U\mathbf{u_L} + \overline{\mathbf{u_L}}V_L^{U\dagger}\gamma^\mu V_L^D\mathbf{d_L}. \tag{2.54}$$

Defining the Cabbibo-Kobayashi-Maskawa (CKM) matrix

$$V_q \equiv V_L^{U\dagger}V_L^D, \tag{2.55}$$

equation (2.54) can be written as

$$j_{W,Q}^\mu = \overline{\mathbf{d_L}}V_q^\dagger\gamma^\mu\mathbf{u_L} + \overline{\mathbf{u_L}}V_q\gamma^\mu\mathbf{d_L}. \tag{2.56}$$

Equation (2.56) displays the explicit mixing between quarks of different flavour caused by the WCC.

2.4.2 Parametrization of the CKM matrix

In general a complex $N \times N$ matrix can be parametrized by $2N^2$ values. Since V_q is unitary,[12] there are N^2 constraints on the matrix elements of V_q. Hence, V_q can be described by N^2 parameters. These can be divided into $\frac{N(N-1)}{2}$ mixing angles and $\frac{N(N+1)}{2}$ phases. [31] However, not all of these phases are observable. This idea will be illustrated for both $N = 2$ and $N = 3$.

---

[12]This simply follows from the definition of V_q in equation (2.55): $V_q V_q^\dagger = V_L^{U\dagger}V_L^D V_L^{D\dagger}V_L^U = I$.

Many low energy physical processes can be described by considering only two generations of quarks. In that case one can define

$$q_L^U = \begin{pmatrix} u_L \\ c_L \end{pmatrix} \quad q_L^D = \begin{pmatrix} d_L \\ s_L \end{pmatrix}. \tag{2.57}$$

As described above, for $N = 2$ there is 1 phase and 1 mixing angle. The CKM matrix can then be parametrized as

$$V_q = \begin{pmatrix} \cos\theta_C e^{i\omega_1} & \sin\theta_C e^{i(\omega_2+\eta)} \\ -\sin\theta_C e^{i(\omega_1-\eta)} & \cos\theta_C e^{i\omega_2} \end{pmatrix} \tag{2.58}$$

Then, by rephasing the quark fields:

$$u_L \to e^{i(\omega_1+\eta)} u_L \quad c_L \to e^{i\omega_2} c_L \quad d_L \to e^{i\eta} d_L, \tag{2.59}$$

the quark mixing matrix for two generations can be written as

$$V = \begin{pmatrix} \cos\theta_C & \sin\theta_C \\ -\sin\theta_C & \cos\theta_C \end{pmatrix}. \tag{2.60}$$

The angle θ_C is known as the Cabibbo angle. [32] Its experimental value is commonly inferred from hyperon decays and is given by [19]

$$\sin\theta_C = 0.2243 \pm 0.005. \tag{2.61}$$

For 3 generations, there are 3 mixing angles and 6 phases. The quark fields can be rephased as follows

$$q_{iL}^U \to e^{i\phi_i} q_{iL}^U \quad q_{jL}^D \to e^{i\phi_j} q_{jL}^D. \tag{2.62}$$

Factoring out a single phase, equation (2.53) becomes

$$\begin{aligned} j_{W,Q}^\mu = & e^{-(i\psi_s - i\psi_c)} \sum_{i=d,s,b} \sum_{j=u,c,t} \bar{q}_{iL}^D e^{i\psi_s - i\psi_i} \left(V_q\right)_{ij} \gamma^\mu q_{jL}^U e^{i\psi_j - i\psi_c} \\ & + e^{-i(\psi_c - \psi_s)} \sum_{i=u,c,t} \sum_{j=d,s,b} \bar{q}_{iL}^U e^{i\psi_c - i\psi_i} \left(V_q\right)_{ij} \gamma^\mu q_{jL}^D e^{i\psi_j - i\psi_s} \end{aligned} \tag{2.63}$$

It is clear from equation (2.63) that 5 out of 6 phases in the case of $N = 3$ can be removed by rephasing the quark fields. The last phase cannot be removed, because rephasing all of the quark fields leaves the Lagrangian invariant. This is related to the conservation

of baryon number.[13] In conclusion, the CKM matrix for 3 generations of quarks has 4 parameters : 3 rotation angles and 1 phase. The elements of the CKM matrix are often denoted as

$$V_q = \begin{pmatrix} V_{ud} & V_{us} & V_{ub} \\ V_{cd} & V_{cs} & V_{cb} \\ V_{td} & V_{ts} & V_{tb} \end{pmatrix}. \tag{2.64}$$

The standard parametrization is given by [34]

$$
\begin{aligned}
V_q &= \begin{pmatrix} 1 & 0 & 0 \\ 0 & c_{23} & s_{23} \\ 0 & -s_{23} & c_{23} \end{pmatrix} \begin{pmatrix} c_{13} & 0 & s_{13}e^{-i\delta} \\ 0 & 1 & 0 \\ -s_{13}e^{i\delta} & 0 & c_{13} \end{pmatrix} \begin{pmatrix} c_{12} & s_{12} & 0 \\ -s_{12} & c_{12} & 0 \\ 0 & 0 & 1 \end{pmatrix} \\
&= \begin{pmatrix} c_{12}c_{13} & s_{12}c_{13} & s_{13}e^{-i\delta} \\ -s_{12}c_{23} - c_{12}s_{23}s_{13}e^{-i\delta} & c_{12}c_{23} - s_{12}s_{23}s_{13}e^{i\delta} & s_{23}c_{13} \\ s_{12}s_{23} - c_{12}c_{23}s_{13}e^{i\delta} & -c_{12}s_{23} - s_{12}c_{23}s_{13}e^{i\delta} & c_{23}c_{13} \end{pmatrix},
\end{aligned}
\tag{2.65}
$$

where $s_{ij} = \sin\theta_{ij}$, $c_{ij} = \cos\theta_{ij}$ and δ is the phase responsible for the CP-violating phenomena in the flavour changing processes of the SM. All the angles θ_{ij} can be chosen within the first quadrant, so that $s_{ij} > 0$ and $c_{ij} > 0$. [19] Experimentally, the quark mixing angles exhibit a strong hierarchy

$$s_{13} << s_{23} << s_{12} << 1. \tag{2.66}$$

Thus, it is often easy to use the Wolfenstein parametrization [35]

$$s_{12} = \lambda = \frac{|V_{us}|}{\sqrt{|V_{ud}|^2 + |V_{us}|^2}} \quad s_{23} = A\lambda^2 = \lambda\frac{|V_{cb}|}{|V_{us}|} \quad s_{13}e^{i\delta} = V_{ub}^* = A\lambda^3\left(\rho + i\eta\right). \tag{2.67}$$

For instance up to $O(\lambda^4)$, the CKM matrix is then given by [35]

$$V_q = \begin{pmatrix} 1 - \frac{\lambda^2}{2} & \lambda & A\lambda^3\left(\rho - i\eta\right) \\ -\lambda & 1 - \frac{\lambda^2}{2} & A\lambda^2 \\ A\lambda^3\left(1 - \rho - i\eta\right) & -A\lambda^2 & 1 \end{pmatrix}. \tag{2.68}$$

The experimental values of the elements of V_q are briefly reported in Subsection 2.4.5. More detailed information can be found from [19].

---

[13]The invariance of Lagrangian under a continuous symmetry transformation is always related to a conserved quantity, as outlined in Appendix C. The specific calculation of the conserved baryon number operator closely resembles that of the lepton number, performed in Appendix C.2.

2.4.3 The Phase of the CKM Matrix and CP-Violation

As mentioned in the previous section, the physical phase δ is responsible for the CP-violation in the SM processes.[14] CP-violating processes are often used as tests of beyond the SM physics, and for this reason, the connection between the phase of the CKM matrix and the CP-violation will be taken under closer consideration. First, the charged boson field that is coupled to the WCC transforms under CP in the following way [5]

$$
W^{\mu}(x) \xrightarrow{CP} \eta_W^* W_{\mu}^{\dagger}(x') \, . \tag{2.69}
$$

Then, by choosing $\eta_W = -1$, the W-bosons transform as

$$
W^{\pm\mu} \xrightarrow{CP} -W_{\mu}^{\mp}, \tag{2.70}
$$

where the lowering of the Lorentz index follows from the $\eta_{\mu\nu} = diag(1, -1, -1, -1)$ convention for the Lorentz metric, implying also that x transforms under parity as,

$$
x = (t, \mathbf{x}) \xrightarrow{P} x' = (t, -\mathbf{x}) \, . \tag{2.71}
$$

The WCC responsible for the quark flavour mixing (cf. equation (2.56)) transforms under CP in the following way:

$$
\begin{aligned}
&- \sum_{i,j=1,2,3} \left(\bar{d}_{iL} \gamma^{\mu} (V_q)_{ij}^{\dagger} u_{jL} + \bar{u}_{iL} \gamma^{\mu} (V_q)_{ij} d_{jL} \right) \\
&\xrightarrow{CP} \sum_{i,j=1,2,3} \left(\bar{u}_{jL} \gamma^{\mu} (V_q)_{ij}^{\dagger} d_{iL} + \bar{d}_{jL} \gamma^{\mu} (V_q)_{ij} u_{iL} \right) \\
&= \sum_{i,j=1,2,3} \left(\bar{u}_{jL} \gamma^{\mu} (V_q)_{ji}^{*} d_{iL} + \bar{d}_{jL} \gamma^{\mu} (V_q)_{ji}^{*\dagger} u_{iL} \right)
\end{aligned} \tag{2.72}
$$

Thus, the Lagrangian is transformed as follows:

$$
\begin{aligned}
\mathcal{L}_{W,Q}(t, \mathbf{x}) &= -\frac{g}{\sqrt{2}} \left[\bar{\mathbf{q}}_{\mathbf{L}}^{\mathbf{D}} \gamma^{\mu} V_q^{\dagger} \mathbf{q}_{\mathbf{L}}^{\mathbf{U}} W_{\mu}^{-} + \bar{\mathbf{q}}_{\mathbf{L}}^{\mathbf{U}} \gamma^{\mu} V_q \mathbf{q}_{\mathbf{L}}^{\mathbf{D}} W_{\mu}^{+\dagger} \right] \\
&\xrightarrow{CP} -\frac{g}{\sqrt{2}} \left[\bar{\mathbf{q}}_{\mathbf{L}}^{\mathbf{U}} \gamma^{\mu} V_q^{*} \mathbf{q}_{\mathbf{L}}^{\mathbf{D}} W_{\mu}^{+\dagger} + \bar{\mathbf{q}}_{\mathbf{L}}^{\mathbf{D}} \gamma^{\mu} V_q^{\dagger*} \mathbf{q}_{\mathbf{L}}^{\mathbf{U}} W_{\mu}^{-} \right] \, .
\end{aligned} \tag{2.73}
$$

It is evident from equation (2.73) that if $V_q = V_q^*$, then the Lagrangian of the SM is invariant under the CP transformation. However, if this equality does not hold, meaning that the CKM matrix has a nonzero phase $\delta \neq 0$, then the processes involving WCC can

---

[14]The CP-violation was first observed in the SM by [36].

exhibit CP-violation. For the case of two generations of quarks, the CKM matrix was parametrized by a single real parameter θ_C. Hence from the discussion above, it follows that there can be no CP-violation if only 2 generation of quarks are considered. In fact it was shown by Kobayashi and Maskawa, that CP-violation manifests in the mixing of all three generation of quarks. [33] This also explains the smallness of the observed CP-violation; it is suppressed by the small mixing angles between different generation of quarks. [33]

2.4.4 The Unitarity Triangle

As was already mentioned in the preceding sections, the CKM matrix is unitary. This imposes some constraints on the values of the matrix elements. Namely,

$$\sum_i V_{ij}V_{ik}^* = \delta_{jk} \qquad \sum_j V_{ij}^*V_{kj} = \delta_{ik}. \tag{2.74}$$

The importance of equation (2.74) is that the violation of the unitarity relations signals new physics effects. The vanishing contributions to equation (2.74) can be considered as triangles on the complex plane. [37] Most commonly the triangle is defined by rescaling the sum

$$V_{ud}V_{ub}^* + V_{cd}V_{cb}^* + V_{td}V_{tb}^* = 0, \tag{2.75}$$

by the most well-known value - $V_{cd}V_{cb}^*$. [19] All of the different triangles that can be constructed by the vanishing of the relations in equation (2.74) have a common area, given by half of the Jarlskog invariant J. [38] In general, J is defined by

$$Im\left[V_{ij}V_{kl}V_{il}^*V_{kj}^*\right] = J\sum_{m,n}\epsilon_{ikm}\epsilon_{jln}. \tag{2.76}$$

The importance of J is that under the rescaling of the CKM matrix by a diagonal matrix, the value of J does not change. Moreover, if $J = 0$, there can be no CP-violation within the SM. Hence J is a phase-convention independent measure of CP-violation. [38]

2.4.5 The Experimental values of the CKM Matrix Elements

As mentioned in previous sections, the CKM matrix can be parametrized by 3 rotational angles and one phase. The relation between the elements of the CKM matrix and these

parameters, whilst following the convention of equation (2.65) is as follows:

$$s_{12} = \lambda = \frac{|V_{us}|}{\sqrt{|V_{ud}|^2 + |V_{us}|^2}} \qquad s_{23} = \lambda \left| \frac{V_{cb}}{V_{us}} \right| \qquad s_{13}e^{i\phi} = V_{ub}^*. \qquad (2.77)$$

In this section, the current experimental values for the CKM matrix elements are outlined.

$|V_{ud}|$

The precise determination of $|V_{ud}|$ is inferred from the superallowed $0^+ \rightarrow 0^+$ decays. Its current value as reported by [19] is

$$|V_{ud}| = 0.97420 \pm 0.00021. \qquad (2.78)$$

$|V_{us}|$

The magnitude of the $|V_{us}|$ is reported by the Particle Data Group (PDG) by combining various different Kaon and Pion decay measurements as[15]

$$|V_{us}| = 0.2243 \pm 0.0005. \qquad (2.79)$$

$|V_{cd}|$

The value of $|V_{cd}|$ is inferred by the PDG by averaging over the measurements of leptonic and semileptonic D-meson decays together with neutrino scattering data. [19] The resulting value is given by

$$|V_{cd}| = 0.218 \pm 0.004. \qquad (2.80)$$

$|V_{cs}|$

$|V_{cs}|$ is similarly found from the analysis of the semileptonic and leptonic D-meson decay data. [19] It is given by

$$|V_{cs}| = 0.997 \pm 0.0017. \qquad (2.81)$$

$|V_{cb}|$

$|V_{cb}|$ is determined by investigating the B-meson decay into D and D^*. Its value given by PDG is [19]

$$|V_{cb}| = (42.2 \pm 0.8) \times 10^{-3}. \qquad (2.82)$$

---

[15]Further information can be found from [19] and from references therein.

$|V_{ub}|$

The value of $|V_{ub}|$ is also inferred from B-decay data. [19]. Its current value is reported by PDG as

$$|V_{ub}| = (3.94 \pm 0.36) \times 10^{-3}. \tag{2.83}$$

$|V_{td}|$, $|V_{ts}|$

The measurements of $|V_{td}|$ and $|V_{ts}|$ are unlikely to be made at tree-level, and so $B - \bar{B}$ oscillations involving box diagrams with top quarks or loop mediated rare decays of K- or B-mesons must be used. [19] The values following from these considerations as reported by [19] are

$$|V_{td}| = (8.1 \pm 0.5) \times 10^{-3} \quad |V_{ts}| = (39.4 \pm 2.3) \times 10^{-3}. \tag{2.84}$$

$|V_{tb}|$

The value for $|V_{tb}|$ can be determined by averaging over different measurements of the cross sections of a single top-quark production. [19] The PDG reports this value as

$$|V_{tb}| = 1.019 \pm 0.025. \tag{2.85}$$

2.5 The Weak Neutral Current and the GIM Mechanism

In the EW sector, the WNC can be expressed as[16] [31]

$$j_Z^\mu = j_{Z,L}^\mu + j_{Z,Q}^\mu. \tag{2.86}$$

In terms of the gauge eigenstates, the leptonic WNC is given by

$$j_{Z,L}^\mu = 2g \sum_{i=e,\mu,\tau} \bar{\nu}'_{iL} \gamma^\mu \nu'_{iL} + 2g \sum_{i=e,\mu,\tau} \left(\bar{e}'_{iL} \gamma^\mu e'_{iL} + \bar{e}'_{iR} \gamma^\mu e'_{iR} \right), \tag{2.87}$$

and the hadronic WNC is given by

$$j_{Z,Q}^\mu = 2 \sum_{i=u,c,t} \left(g \bar{q}'^U_{iL} \gamma^\mu q'^U_{iL} + g \bar{q}'^U_{iR} \gamma^\mu q'^U_{iR} \right) + 2 \sum_{i=d,s,b} \left(g \bar{q}'^D_{iL} \gamma^\mu q'^D_{iL} + g \bar{q}'^D_{iR} \gamma^\mu q'^D_{iR} \right). \tag{2.88}$$

---

[16]Both the leptonic and hadronic WNC were discovered in 1973 at CERN by the Gargamelle bubble chamber collaboration. [39, 40]

Given that the mass eigenstates of quarks do not coincide with the gauge eigenstates, it is interesting to investigate whether transforming from one basis to the other changes the mathematical form of the WNC. To that end, the matrices V^D and V^U introduced in the previous section along with equations (2.44) and (2.43) can be used to transform the hadronic neutral currents into the mass basis

$$
\begin{aligned}
j_{Z,Q}^{\mu} = {} & 2\bar{\mathbf{q}}_{\mathbf{L}}^{\mathbf{U}} V_L^U \gamma^{\mu} V_L^{U\dagger} \mathbf{q}_{\mathbf{L}}^{\mathbf{U}} + 2g\bar{\mathbf{q}}_{\mathbf{L}}^{\mathbf{U}} V_L^U \gamma^{\mu} V_L^{U\dagger} \mathbf{q}_{\mathbf{L}}^{\mathbf{U}} + \\
& 2g\bar{\mathbf{q}}_{\mathbf{L}}^{\mathbf{D}} V_L^D \gamma^{\mu} V_L^{D\dagger} \mathbf{q}_{\mathbf{L}}^{\mathbf{D}} + 2g\bar{\mathbf{q}}_{\mathbf{R}}^{\mathbf{D}} V_R^D \gamma^{\mu} V_R^{D\dagger} \mathbf{q}_{\mathbf{R}}^{\mathbf{D}} \\
= {} & 2g\bar{\mathbf{q}}_{\mathbf{L}}^{\mathbf{U}} \gamma^{\mu} \mathbf{q}_{\mathbf{L}}^{\mathbf{U}} + 2g\bar{\mathbf{q}}_{\mathbf{R}}^{\mathbf{U}} \gamma^{\mu} \mathbf{q}_{\mathbf{R}}^{\mathbf{U}} \\
& + 2g\bar{\mathbf{q}}_{\mathbf{L}}^{\mathbf{D}} \gamma^{\mu} \mathbf{q}_{\mathbf{L}}^{\mathbf{D}} + 2g\bar{\mathbf{q}}_{\mathbf{R}}^{\mathbf{D}} \gamma^{\mu} \mathbf{q}_{\mathbf{R}}^{\mathbf{D}} .
\end{aligned}
\tag{2.89}
$$

Hence, unitarity of the transformation matrices $V_{L,R}^U$ and $V_{L,R}^D$ ensures that there are no tree-level hadronic flavour changing neutral currents (FCNC) in the SM. This is known as the GIM mechanism. [41] Due to the similarity between the quark and leptonic terms in the Lagrangian, it is easy to see that the same result also holds true for leptonic FCNC.

2.6 The Flavour Hierarchy Problem in the Standard Model

The numerical values of the fermion masses obtained from theory and experiments were overviewed in Section 1.3. Evidently, the masses exhibit a large spread in magnitude, as displayed in Figure 2.1. In the context of the SM this hierarchy is described by the hierarchy of the Yukawa couplings that are associated with the charged fermion masses after SSB. Crucially, however, the SM makes no attempt to explain the spread in the Yukawa couplings which are solely inserted into the theory as free parameters. The goal of the extensions of the SM is to theoretically explain this hierarchy as emerging from new physics which is not included within the SM. Examples are provided in Chapters 3 and 4. Analogously to the fermion masses, the CKM matrix elements also exhibit a noticeable hierarchy. This is depicted on Figure 2.2. Similarly to the fermion masses, the hierarchy of the CKM elements can be traced back to the hierarchy of the Yukawa couplings. Moreover, the mixing of quarks within WCC at tree level is closely associated with the mass difference of u-type and d-type quarks.[17] The hierarchy of the CKM elements and the fermion masses together constitute what is known as the flavor puzzle. One of the goals of a successful flavor physics theory is to explain the physical origin of this hierarchy. Due to limitations in volume, in this thesis the focus has only been put on explaining the hierarchy in the

---

[17]If the u-type and d-type quarks had the same mass, then $V_{L,R}^D = V_{L,R}^U$ so $V_q = I$ and there would be no mixing at tree level.
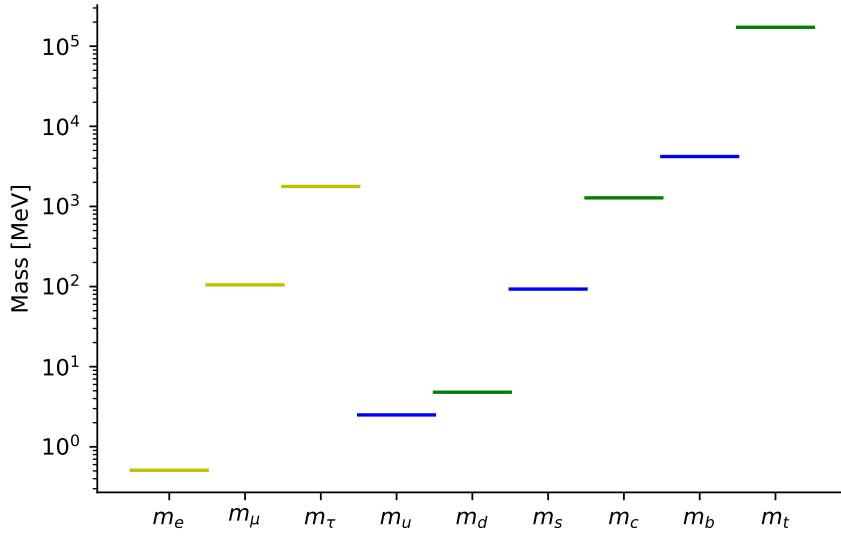
Figure 2.1: The order of magnitude hierarchy of the charged fermion masses in the SM. The yellow lines depict the masses of the charged leptons, the blue lines the masses of the u-type quarks and the green lines the masses of the d-type quarks. The nonzero neutrino masses have been omitted from this plot as they are not relevant for the purpose of this thesis.

quark masses and mixing angles. Nevertheless, similar models could be constructed to explain the charged lepton mass hierarchy, for instance by extending the framework in Chapter 4 to the lepton sector. Extending the SM by the inclusion of the neutrino masses will not be considered in this thesis.
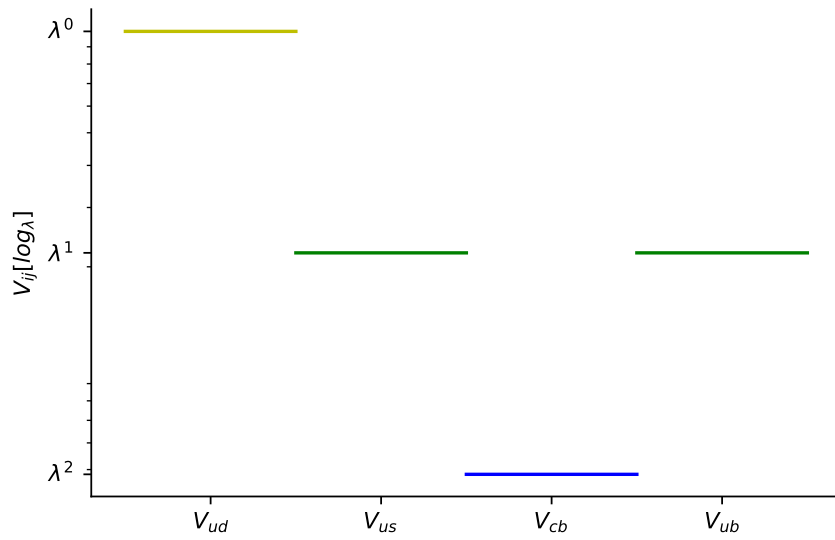
Figure 2.2: The hierarchy of the 4 independent physical parameters of the CKM matrix. The chosen matrix elemnents of V_q can be fitted as powers of the Cabibbo angle $\lambda \approx 0.22$. [42] In particular, the elements span 3 orders of magnitude.

Chapter 3

The Froggat-Nielsen Mechanism

As was discussed in Section 2.6, the SM does not explain the experimentally observed hierarchy in fermion masses and the mixing angles of the CKM matrix. In this chapter, an extension of the SM explaining the quark hierarchy and mixing, first developed by Froggat and Nielsen (FN) is presented.[1] [43] The idea of the FN mechanism is to introduce a new symmetry of the Lagrangian that forbids the inclusion of the fermion masses at tree level. One of the simplest symmetry groups for such a task is given by $U(1)_F$. Since the corresponding $U(1)_F$ charges can be assigned arbitrarily, the Higgs field can be chosen to have zero charge under $U(1)_F$ while the right and left-handed fermions can be chosen to have different $U(1)_F$ charges. In that case, if the $U(1)_F$ symmetry is exact, then no fermion mass terms can be generated at tree level via SSB as described in Chapter 2. Since the mass terms cannot be generated by the Higgs mechanism of the SM, new fields must be introduced in order to source the mass generation mechanism. In the scalar sector, a new field S called the flavon is introduced. This field transforms as a singlet under $SU(3)_c \times SU(2)_L \times U(1)_Y$, with all quantum numbers associated with the SM gauge group set to zero. However, it has a non-zero $U(1)_F$ charge R, given by $R = -1$. In addition, to distinguish the FN mechanism from the usual SSB mechanism, the flavon field does not couple directly to the SM fermions.[2] Thus, one needs additional left-and right-handed fermion fields F_L and F_R to couple the flavon to the SM fermions. The new fermions have identical quantum numbers to the SM fermions except for the mass and $U(1)_F$ charge. The $U(1)_F$ charges for the F_L and F_R fields are assigned in a way such that the mediator fermions can only couple to the standard model quarks via the Higgs doublet ϕ or the flavon field. The SM quarks are also charged under $U(1)_F$, with the left-handed quark q_j

---

[1]The considerations for charged leptons are very similar and are thus omitted from this short review.

[2]In fact, the flavon and the SM fermions cannot be coupled to each other in Yukawa-like terms, if the renormalizability conditions and invariance under the SM gauge group are imposed on the Lagrangian.
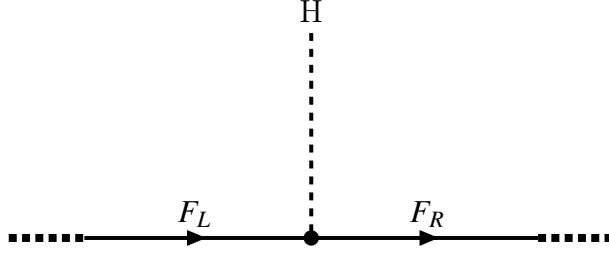
Figure 3.1: The Feynman diagram for the mass generation of the heavy mediators. The dotted lines on the sides indicate that this is an amputated diagram from a more complicated diagram.

having $R = c + b_j$ and the right-handed quark having $R = c - a_j$. Thus, the difference of the flavon charge between a left- and right-handed quark of the same generation j is given by

$$\Delta R_{L-R} = b_j + a_j. \tag{3.1}$$

By convention, $b_i \leq b_{i+1}$ and $a_j \leq a_{j+1}$, where $i = 1, 2, 3$ and $j = 1, 2, 3$ label the generations of quarks.

The fermion mediator masses can be generated analogously to the SSB mechanism introduced in Chapter 2 by giving a nonzero vev to a $R = 0$ Higgs scalar H.[3] This is depicted on Figure 3.1. The amplitude of the process in the low energy limit, $\frac{|p|}{m} \to 0$ can be approximated as

$$|\mathcal{M}| = \left| \frac{\not{p} + m}{p^2 - m^2} \right| \left| \frac{vg}{\sqrt{2}} \right| \left| \frac{\not{p} + m}{p^2 - m^2} \right| \to \frac{1}{m^2} \frac{vg}{\sqrt{2}}. \tag{3.2}$$

The masses of the SM fermions are generated by the SSB of the $R = 1$ flavon field by imposing a nonzero vev : $\langle S \rangle \neq 0$. This mechanism is described in detail on Figure 3.2.

After the $U(1)_F$ symmetry breaking, the flavon field S obtains a nonzero vev, and the symmetry breaking parameter ϵ can be introduced in order to facilitate calculations

$$\epsilon = \frac{\langle S \rangle}{m}. \tag{3.3}$$

The overall $U(1)_F$ charge conservation imposes

$$c + b_j - N = c - a_j, \tag{3.4}$$

where N denotes the number of the intermediate flavon fields. Equation (3.4) in turn

---

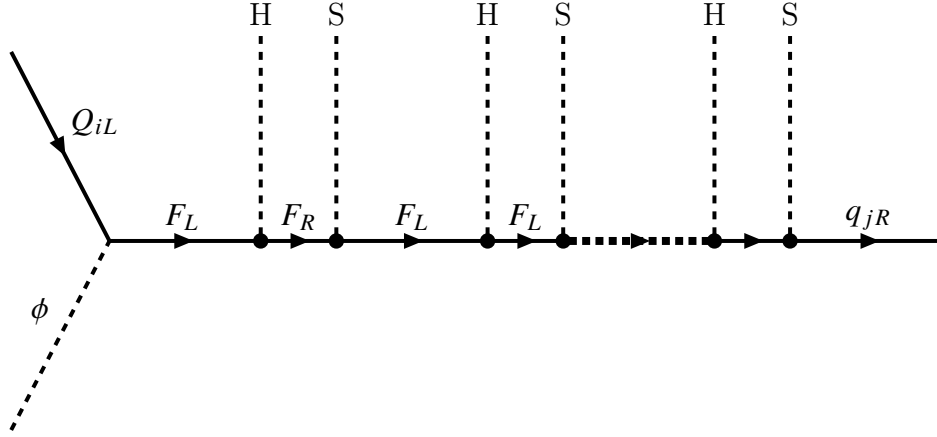[3]Not to be confused with the Higgs doublet of the SM, here denoted by ϕ.

Figure 3.2: The effective mass generation diagram for the SM fermions.

implies that

$$b_j + a_j = N. \tag{3.5}$$

Thus, the difference in the flavon charges of the left- and right-handed quarks fixes the number of intermediate flavons needed to generate the fermion masses. The amplitude for the process depicted on Figure 3.2 is given, in the low energy limit, by[4]

$$\mathcal{M}_{ij} \to \epsilon^{b_i+a_j} \bar{Q}_{iL} Y_{ij} \phi q_{jR}^a, \tag{3.6}$$

where $a = U, D$ for u- and d-type quarks, and Y_{ij} is a matrix consisting of the product of all the coupling constants relevant to Figure 3.2. Hence, the amplitude in equation (3.6) sources an effective Lagrangian for the down type quarks,

$$\mathcal{L}_{eff}^D = -\sum_{i,j} \epsilon^{b_i+a_j} \bar{Q}_{iL} Y_{ij} \phi q_{jR}^d \tag{3.7}$$

and similarly, for up quarks,

$$\mathcal{L}_{eff}^U = -\sum_{i,j} \epsilon^{b_i+a_j} \bar{Q}_{iL} Y_{ij} \tilde{\phi} q_{jR}^u. \tag{3.8}$$

By absorbing the vev of the Higgs field inside a redefined Yukawa matrix $\tilde{Y}_{ij}$, the mass matrix for the charged fermions after SSB of $SU(2)_L \times U(1)_Y$ symmetry can be written as

$$M_{ij} = \tilde{Y}_{ij} \epsilon^{b_i+a_j}. \tag{3.9}$$

The mass eigenvalues of M_{ij} corresponding to the physical quark masses can be found

---

[4]The Higgs field of the SM, ϕ is assumed to satisfy $R = 0$.

after diagonalizing the mass matrix appearing in equation (3.9) as shown in [43]. After diagonalization, the following relation is obtained

$$\frac{m_i}{m_j} \approx \epsilon^{a_i - a_j + b_j - b_i}. \tag{3.10}$$

By finding the corresponding eigenvectors one can construct the CKM matrix similarly to the procedure outlined in Section 2.4. The resulting CKM matrix is given by [43]

$$V_{q,ij} = a_{ij} e^{|b_i - b_j|} \tag{3.11}$$

where the constants a_{ij} are functions of the coupling constants contributing to the process on Figure 3.2. Equations (3.10) and (3.11) illustrate the main idea behind the Froggat-Nielsen mechanism: the hierarchy in the quark masses and the mixing angles can be generated by a suitable choice of the $U(1)_F$ charges for the quarks of the SM.

Chapter 4

Radiative Generation of the Quark Masses and Mixing

4.1 Yukawa Couplings from Radiative Generation Models

Although the Froggat-Nielsen mechanism provides an explanation for the hierarchy in the Yukawa couplings, it also exhibits certain shortcomings. Currently, there is no underlying physical justification for invoking this mechanism while the large number of scalar fields involved in operating the flavon symmetry breaking mechanism also casts a doubt on testability of such a model. [44] In light of these circumstances, it is imperative to also consider alternative models explaining the flavour hierarchy problem. For example the flavour hierarchy can readily be explained by invoking the so called radiative mass generation mechanisms. [45, 46, 47, 3, 48] In these scenarios, the Yukawa couplings are forbidden at tree level by a new symmetry imposed on the Lagrangian of the model at hand. Although the simplest symmetry that one could insist on is Z_2, [47] in this thesis the left-right (LR) symmetric model is considered instead. The advantage of the LR model is the rich phenomenology that it possesses such as providing an explanation for the strong CP problem and allowing to identify $U(1)_{B-L}$ global symmetry with the local $U(1)_Y$ symmetry. [3]

4.2 The Chiral Symmetry Breaking in the Dark Sector

If the Yukawa terms are forbidden at tree-level, then the usual Higgs SSB mechanism cannot be used to explain the generation of the fermion masses. Instead, the mass generation

mechanism could originate from higher order interactions. As an example, one can consider extending the SM with a dark sector that consists of new fermionic fields. The so-called dark fermions can then for instance acquire non-zero masses by explicitly breaking the chiral symmetry. The chiral symmetry breaking mechanism is then transmitted to the SM fields via loop diagrams associated with the interaction of the SM fields and dark fermions with a set of new fields - collectively known as the messenger sector. After integrating out the heavy fields at low energies, one recovers the hierarchy of the Yukawa couplings observed in the SM. Thus, by making use of the radiative mechanism, the hierarchy in the Yukawa couplings of the SM can be solely attributed to the properties present in the dark sector. Here, this idea is illustrated following the construction outlined in [3, 49]. In detail, the dark fermion quark sector consists of the fields Q^{Ui} and Q^{Di} associated to the three generations (i=1,2,3) of up and down-type quarks respectively, charged under a new $U(1)_F$ symmetry. Naturally, the $U(1)_F$ symmetry includes a gauge boson $\bar{A}^\mu$, named the dark photon. The covariant derivative associated to $U(1)_F$ gauge is given by

$$D_\mu = \partial_\mu + ig\hat{Q}\bar{A}^\mu, \tag{4.1}$$

where $\hat{Q}$ denotes the $U(1)_F$ charge operator. Remembering that $U(1)_F$ is an abelian group, the field strength tensor can also be defined in the usual way

$$F_{\mu\nu} = \partial_\mu \bar{A}_\nu - \partial_\nu \bar{A}_\mu. \tag{4.2}$$

With these modfications the Lagrangian for the dark sector can be written as[1]

$$\mathcal{L}_{DS} = i \sum_i \left(\bar{Q}^{Ui} D_\mu \gamma^\mu Q^{Ui} + \bar{Q}^{Di} D_\mu \gamma^\mu Q^{Di} \right) - \frac{1}{4} F_{\mu\nu} F^{\mu\nu} + \frac{1}{2\Lambda^2} \partial^\mu F_{\mu\alpha} \partial_\nu F^{\nu\alpha}. \tag{4.3}$$

The higher derivative term can be related to the emergence of massive Lee-Wick ghost fields appearing in the scattering amplitudes that cancel the quadratic divergences. [49] As shown in [50], the mass scale Λ will turn out to be proportional to the mass of the ghost fields, thereby defining a scale of new physics. Although the Lagrangian contains no explicit chiral symmetry breaking terms, the new physics scale Λ can nevertheless be used to source a dynamical chiral symmetry breaking (ChSB) mechanism, resulting in the generation of masses at low energies such that $m < \Lambda$. The dynamical ChSB proposed in [49] closely follows the approach originally proposed in [51, 52]. In particular, the masses of the dark fermions result from the 1-loop corrections to the fermion propagators depicted on

---

[1]This form of the Lagrangian does not include the interaction terms between dark fermions and the messenger fields, which are contained in $\mathcal{L}_{MS}$.
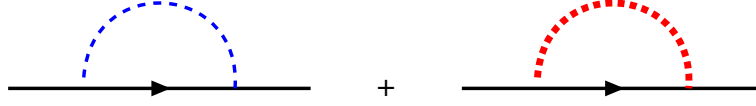
Figure 4.1: The 1-loop self-energy corrections giving rise to the dark fermion dynamical mass generation mechanism. The black line denotes the dark fermion propagator, the blue line denotes the usual gauge boson propagator, arising from the $k^2 = 0$ pole of the gauge propagator in equation (4.4), while the red line denotes the new massive ghost propagator associated to the $k^2 = \Lambda^2$ pole of equation (4.4).

Figure 4.1.[2] By using the covariant gauge fixing term, $-\frac{(\partial_\mu A^\mu)^2}{2\xi}$, the propagator becomes

$$D_{\mu\nu} = -\frac{i\Lambda^2}{k^2(\Lambda^2 - k^2)}\left(\eta_{\mu\nu} - (1 - \xi)\frac{k_\mu k_\nu}{k^2} - \xi\frac{k_\mu k_\nu}{\Lambda^2}\right), \tag{4.4}$$

justifying the two dark fermion self-energy graphs depicted on Figure 4.1. [3] Using equation (4.4), the self-energy correction becomes[4]

$$\Sigma(\slashed{p}, m) = \frac{\alpha}{2\pi}\left(\int_0^1 dx(2m - x\slashed{p})\ln\left(\frac{x\Lambda^2 + (m^2 - p^2 x)(1 - x)}{(m^2 - p^2 x)(1 - x)}\right)\right), \tag{4.5}$$

By resumming the 1-loop corrections at all orders, the well known result for the fermion propagator is then obtained[5]

$$S(p) = \frac{i}{\slashed{p} - \Sigma(\slashed{p}, m)}. \tag{4.6}$$

The self-consistency relation, known as the mass gap equation, [51, 52]

$$m = \Sigma(\slashed{p}, m)\big|_{\slashed{p}=m} \tag{4.7}$$

can then be used to determine the physical pole mass of the dark fermions. Using equations (4.5) and (4.7), one obtains the following consistency condition at low energies $m^2 \ll \Lambda^2$

$$1 = -\frac{\alpha}{2\pi}\int_0^1 dx(2 - x)\ln\left(\frac{m^2(1 - x)^2}{x\Lambda^2}\right) + O\left(\frac{m^2}{\Lambda^2}\right). \tag{4.8}$$

---

[2]More details can be found from [49, 50, 53].

[3]The formula for the self-energy correction and the formula for the propagator were taken from [49]. In order to shed some light on the emergence of these formulae, both of them have been explicitly derived in the Appendix.

[4]Here a purely gauge-dependent term $I(\xi)$ has been omitted with the understanding that the fermion self-energy when computed on-shell $\slashed{p} = m$ is a gauge-independent quantity. [49]

[5]The bare mass m_0 does not appear in the denominator of the fermion propagator since there is no bare mass in equation (4.3).

Solving equation (4.8) for the pole mass

$$m = \Lambda \exp\left[-\frac{2\pi}{3\alpha} + \frac{1}{4}\right]. \tag{4.9}$$

Finally, extending the calculation to N_f fermions all with a common charge q_f and incorporating the running of α, equation (4.9) becomes

$$m_f = \Lambda exp\left[-\frac{2\pi}{3\alpha(m_f)} + \frac{1}{4}\right]. \tag{4.10}$$

The above discussion was focused on the dynamic mass generation mechanism at low energies. However, the dynamic ChSB can also be realised at high energies in the strong coupling regime. To that end, a new Lagrangian for the dark sector, with unbroken chiral symmetry can be written down: [3]

$$\mathcal{L}_{DS} = i\bar{\psi}D_\mu\gamma^\mu\psi - \frac{1}{4}F_{\mu\nu}F^{\mu\nu}. \tag{4.11}$$

This is analogous to the Lagrangian of the massless QED. Then in the strong coupling regime

$$\alpha > \alpha_c = \frac{\pi}{3} \tag{4.12}$$

the mass gap equation has a nontrivial solution, given by [54, 55]

$$m = 4\Lambda_C e^{-\frac{\pi\alpha_c}{\sqrt{\alpha - \alpha_c}}}. \tag{4.13}$$

Contrary to the low-energy regime, the scale Λ_c now emerges spontaneously from the theory. The appearance of the mass scale Λ_c can be related to the energy scale at which the strong coupling regime dominates. Thus, the dynamical mass generation model for the dark fermions can be applied both at low energies and high energies provided that the $U(1)_F$ charges have been chosen accordingly in order to be compatible with the dark fermion hierarchy required for describing the SM flavour hierarchy.

4.3   Quark Masses in the Left-Right Symmetric Model

As was mentioned above, several different symmetry schemes can be applied in order to forbid the appearance of the Yukawa couplings at tree level. However, in this thesis only a concrete LR symmetric model is considered due to its simplicity and desirable phenomenological features. The analysis is based on [4], to which I have also given my own contribution to as described in Subsection 4.4.1; and on [3] on which [4] was built upon.

4.3.1 The Higgs Mechanism

In this section the Higgs mechanism responsible for the spontaneous $SU(2)_R \times SU(2)_L$ symmetry breaking is elucidated. The analysis is based on [3]. The Lagrangian of the Higgs sector is given by

$$\mathcal{L}_{\mathcal{H}} = D_\mu H_L \left(D^\mu H_L\right)^\dagger + D_\mu H_R \left(D^\mu H_R\right)^\dagger - V\left(H_L, H_R\right), \tag{4.14}$$

where H_L and H_R denote the left-and right-handed scalar doublets of $SU(2)_L$ and $SU(2)_R$ respectively.[6] The potential can be chosen as a general, renormalizable scalar potential symmetric under $O(2) \times O(2)$ transformations, as follows:

$$\begin{aligned}
V\left(H_L, H_R\right) = {} & \lambda_L \left(H_L H_L^\dagger\right)^2 + \lambda_R \left(H_R H_R^\dagger\right)^2 + \lambda_{LR} \left(H_R H_R^\dagger\right)\left(H_L H_L^\dagger\right) \\
& - \mu_L^2 \left(H_L H_L^\dagger\right) - \mu_R^2 \left(H_R H_R^\dagger\right).
\end{aligned} \tag{4.15}$$

After the SSB of both $SU(2)_L$ and $SU(2)_R$, the scalar doublets can be written in resemblance to the unitary gauge of the SM:

$$H_L = \frac{1}{\sqrt{2}} \begin{pmatrix} 0 \\ v_L + h_L \end{pmatrix} \qquad H_R = \frac{1}{\sqrt{2}} \begin{pmatrix} 0 \\ v_R + h_R \end{pmatrix}. \tag{4.16}$$

Consequently, the Lagrangian of the Higgs sector acquires the following form

$$\begin{aligned}
\mathcal{L}_{\mathcal{H}} = {} & \frac{1}{2}\partial_\mu h_L \left(\partial^\mu h_L\right)^\dagger + \frac{1}{2}\partial_\mu h_R \left(\partial^\mu h_R\right)^\dagger - \frac{1}{4}\lambda_L \left(h_L + v_L\right)^4 - \frac{1}{4}\lambda_R \left(h_R + v_R\right)^4 \\
& - \frac{1}{4}\lambda_{LR} \left(h_R + v_R\right)^2 \left(h_L + v_L\right)^2 + \frac{1}{2}\mu_L^2 \left(h_L + v_L\right)^2 + \frac{1}{2}\mu_R^2 \left(h_R + v_R\right)^2.
\end{aligned} \tag{4.17}$$

In order to consider the minimal amount of free parameters, the tree level mass term for the left-handed (LH) Higgs field has been set to zero, $\mu_L^2 = 0$ while the negative tree level mass term for the right-handed (RH) Higgs field $-\mu_R^2 < 0$ is retained in the model. The LH Higgs field obtains its mass via the negative portal coupling λ_{LR}. Determining the vev-s associated with the SSB of $SU(2)_L$ and $SU(2)_R$ proceeds through the minimalization of the potential appearing in equation (4.15), where the dynamical Higgs fields h_L and h_R have been set to zero, corresponding to the lowest energy state.

$$\nabla V\left(h_L, h_R\right)\Big|_{h_L = h_R = 0} = 0. \tag{4.18}$$

---

[6]Naturally, H_L transforms as singlet under $SU(2)_R$ and H_R transforms as singlet under $SU(2)_L$.

This gives the following equations

$$\frac{\partial V}{\partial h_L}\bigg|_{h_L=h_R=0} = \lambda_L v_L^2 + \frac{1}{2}\lambda_{LR} v_R^2 = 0. \tag{4.19}$$

$$\frac{\partial V}{\partial h_R}\bigg|_{h_L=h_R=0} = \lambda_R v_R^2 + \frac{1}{2}\lambda_{LR} v_L^2 - \mu_R^2 = 0. \tag{4.20}$$

Solving equation (4.19) for v_L^2 yields

$$v_L^2 = -\frac{\lambda_{LR}}{2\lambda_L} v_R^2. \tag{4.21}$$

Thus, in order to have a real vev, $v_L \in \mathbb{R}$, the portal coupling must be negative: $\lambda_{LR} < 0$. Moreover, substituting (4.21) into (4.20) gives an equation for v_R^2:

$$v_R^2 = \frac{\mu_R^2}{\left(\lambda_R - \frac{\lambda_{LR}^2}{4\lambda_L}\right)}. \tag{4.22}$$

In that case, the consistency condition $v_R \in \mathbb{R}$ demands that

$$2\sqrt{\lambda_L \lambda_R} > \lambda_{LR} > -2\sqrt{\lambda_L \lambda_R}. \tag{4.23}$$

Combining the two conditions given above, results in the overall consistency conditions

$$-2\sqrt{\lambda_L \lambda_R} < \lambda_{LR} < 0 \tag{4.24}$$

$$\lambda_{L,R} \geq 0. \tag{4.25}$$

Equation (4.25) is imposed by the requirement that the potential must be bounded from below. In addition, equation (4.24) can be translated into a hierarchy condition for the vev-s:

$$\frac{v_L^2}{v_R^2} < \sqrt{\frac{\lambda_R}{\lambda_L}}. \tag{4.26}$$

As discussed in Appendix A, the mass matrix for the two Higgs fields can be found by computing the Hessian matrix of the potential as a function of h_L and h_R.[7]

$$M^2 = \begin{pmatrix} \frac{\partial^2 V}{\partial h_L^2} & \frac{\partial^2 V}{\partial h_L \partial h_R} \\ \frac{\partial^2 V}{\partial h_R \partial h_L} & \frac{\partial^2 V}{\partial h_R^2} \end{pmatrix} \tag{4.27}$$

---

[7]The Hessian matrix is understood to have been evaluated at $h_L = 0$ and $h_R = 0$.

By using the relations

$$\lambda_{LR} = -2\lambda_L \left(\frac{v_L}{v_R}\right)^2 \qquad \mu_R^2 = \frac{\lambda_R v_R^4 - \lambda_L v_L^4}{v_R^2},$$

(4.28)

that follow from (4.21) and (4.22), the mass matrix becomes[8]

$$M^2 = 2v_R^2 \begin{pmatrix} \lambda_L \epsilon^2 & -\lambda_L \epsilon^3 \\ -\lambda_L \epsilon^3 & \lambda_R \end{pmatrix},$$

(4.29)

where the parameter $\epsilon = \frac{v_L}{v_R}$ satisfies $\epsilon \ll 1$.[9] The smallness of ϵ allows to approximate the eigenvalues of M^2 by the diagonal entries of M^2. In that case, the eigenvalues of the mass matrix are given by

$$m_1^2 = 2v_R^2 \lambda_L \epsilon^2 \qquad m_2^2 = 2v_R^2 \lambda_R.$$

(4.30)

Furthermore, the hierarchy of the masses of the two Higgs fields can be encoded in the following inequality

$$m_1^2 < \sqrt{\frac{\lambda_L}{\lambda_R}} m_2^2.$$

(4.31)

In order to achieve more precision, higher order terms in ϵ can also be included, resulting in the determination of the transformation matrix U, allowing to relate the mass eigenstates h_1, h_2 to the gauge eigenstates h_L and h_R. More details can be found from [3] and the Appendix.

4.3.2 The Gauge Sector

The main idea of the LR symmetric model is to extend the gauge group of the EW sector of the SM to $SU(2)_L \times SU(2)_R \times U(1)_Y$. [3] Consequently, the right-handed fermion fields then transform as doublets of $SU(2)_R$, while they remain singlets under $SU(2)_L$. On the contrary, the left-handed fermion fields are still doublets under $SU(2)_L$, while they become singlets under $SU(2)_R$. Analogously to Chapter 2, due to the introduction of a new $SU(2)_R$ symmetry, three new gauge fields Z_R^μ, $W_R^{+\mu}$, $W_R^{-\mu}$ arise. The gauge fields associated with the $SU(2)_L$ of the SM are now be denoted by Z_L^μ, $W_L^{+\mu}$, $W_L^{-\mu}$. The hypercharges of the RH and the LH doublets are set to reproduce the observed electric charges and to impose the LR symmetry, the coupling constants associated with $SU(2)_L$ and $SU(2)_R$ have been

---

[8]Although M^2 is referred to as the mass matrix, its eigenvalues actually describe the squared masses of the two Higgs fields.

[9]The fact that ϵ lies in the perturbative regime is a condition of the hierarchy of the vev-s, $v_L \ll v_R$. Since collider experiments' data imposes $m_{W_R} \geq 1$ TeV, $\frac{v_L^2}{v_R^2} = \frac{m_{W_L}^2}{m_{W_R}^2} \leq 0.08$.

chosen to satisfy

$$g_L = g_R. \tag{4.32}$$

After the SSB of both $SU(2)_L$ and $SU(2)_R$, the LH and RH doublets will acquire the nonzero expectation values:

$$\langle H_{L,R} \rangle = \begin{pmatrix} 0 \\ \frac{v_{L,R}}{\sqrt{2}} \end{pmatrix}. \tag{4.33}$$

Then similar to the mechanism presented in Section 2.2, by using a redefinition akin to equation (2.17)

$$W_{L,R}^{\pm\mu} = \frac{W_{L,R}^{1\mu} \mp i W_{L,R}^{2\mu}}{\sqrt{2}}, \tag{4.34}$$

the Lagrangian terms contributing to the masses of the gauge bosons can be rewritten as

$$\mathcal{L} \supset \frac{g^2}{4} \left(v_R^2 W_R^{\pm\dagger} W_R^{\pm} + v_L^2 W_L^{\pm\dagger} W_L^{\pm} \right) + \frac{v_R^2}{8} \left(g W_R^3 - g' B \right)^2 + \frac{v_L^2}{8} \left(g W_L^3 - g' B \right)^2, \tag{4.35}$$

where the contraction of the Lorentz indices of the vector fields has been left implicit and the LR symmetry condition $g = g_L = g_R$ has been used. From equation (4.35) the squared masses of $W_{L,R}^{\pm}$ can be easily identified:

$$M_{W_{L,R}}^2 = \frac{g^2 v_{L,R}^2}{4}, \tag{4.36}$$

where $W_{L,R}$ in the subscript stands both for $W_{L,R}^-$ and $W_{L,R}^+$. The remaining 3 neutral gauge fields are not mass eigenstates as exhibited by the nondiagonal squared mass matrix M^2, given by

$$M^2 \begin{pmatrix} B \\ W_L^3 \\ W_R^3 \end{pmatrix} = \begin{pmatrix} \left(v_L^2 + v_R^2 \right) g'^2 & -v_L^2 g g' & -v_R^2 g g' \\ -v_L^2 g g' & v_L^2 g^2 & 0 \\ -v_R^2 g g' & 0 & -v_R^2 g^2 \end{pmatrix} \begin{pmatrix} B \\ W_L^3 \\ W_R^3 \end{pmatrix}. \tag{4.37}$$

Instead, the squared masses can be found by diagonalizing M^2, and they are given up to order $O\left(\left(\frac{v_L}{v_R} \right)^2 \right)$ by, [10]

$$M_A = 0, \tag{4.38}$$

$$M_{Z_L}^2 = \frac{\left(g^4 + 2 g'^2 g^2 \right) v_L^2}{4 \left(g'^2 + g^2 \right)}, \tag{4.39}$$

---

[10]Importantly, the hierarchy $v_R >> v_L$ allows to omit higher order terms. The calculation is very similar to calculation of the mass eigenstates of Higgs' and thus the details are omitted for considerations of brevity. More details can be found from [3].

$$M_{Z_R}^2 = \frac{\left(v_L^2 + v_R^2\right) g'^4 + 2g'^2 g^2 v_R^2 + g^4 v_R^2}{4\left(g'^2 + g^2\right)}. \tag{4.40}$$

The mass eigenstates are given by

$$A_\mu = g B_\mu + g' \left(W_{L\mu}^3 + W_{R\mu}^3\right) \tag{4.41}$$

$$Z_{L\mu} = \frac{g'^2 \left(W_{L\mu}^3 - W_{R\mu}^3\right) - g g' B_\mu + g^2 W_{L\mu}^3}{\sqrt{2g'^4 + 3g^2 g'^2 + g^4}} \tag{4.42}$$

$$Z_{R\mu} = \frac{g W_{R\mu} - g' B_\mu}{\sqrt{g'^2 + g^2}}. \tag{4.43}$$

These equations can be inverted for the fields $W_{\mu L}^3$, $W_{\mu R}^3$ and B_μ (this is explicitly carried out in [3]) and inserted into the Lagrangian. Then, the covariant derivative terms for the fermion fields can be written as

$$\mathcal{L} \supset \bar{\psi}_L \slashed{D} \psi_L + \bar{\psi}_R \slashed{D} \psi_R$$

$$= i\bar{\psi}_L \left[\frac{g'g}{\sqrt{2g'^2 + g^2}} \left(I_L^3 + Y\right) \slashed{A} + \slashed{Z}_L \frac{g\left[g'^2\left(I_L^3 - Y\right) + g^2 I_L^3\right]}{\sqrt{\left(g'^2 + g^2\right)\left(2g'^2 + g^2\right)}} - \frac{g'^2}{\sqrt{g'^2 + g^2}} Y \slashed{Z}_R \right] \psi_L$$

$$+ i\bar{\psi}_L \left[\frac{g'g}{\sqrt{2g'^2 + g^2}} \left(I_R^3 + Y\right) \slashed{A} - \slashed{Z}_L \frac{g g'^2 \left(I_R^3 + Y\right)}{\sqrt{\left(g'^2 + g^2\right)\left(2g'^2 + g^2\right)}} + \frac{g^2 I_R^3 - g'^2 Y}{\sqrt{g'^2 + g^2}} \slashed{Z}_R \right] \psi_L. \tag{4.44}$$

Then, analogously to Section 2.2, the photon coupling terms allow to identify the LH and RH charge operators:

$$Q_{L/R} = I_3^{L/R} + Y, \tag{4.45}$$

and the value of the electric charge in terms of the coupling constants of $SU(2)_{L/R}$ and $U(1)_Y$:

$$e = \frac{g'g}{\sqrt{2g'^2 + g^2}}. \tag{4.46}$$

The resemblance of the above formalism to the gauge sector of the SM can be extended by defining θ via

$$e = \frac{g'g}{\sqrt{2g'^2 + g^2}} = g \sin \theta. \tag{4.47}$$

However, due to the trigonometric identity

$$\cos 2\theta = 1 - 2\sin^2 \theta, \tag{4.48}$$

Table 4.1: The gauge group quantum numbers for the LH and RH quark and lepton doublets. Each member of the fermion doublet $f_{L/R}$ transforms trivially under the isospin operator corresponding to the opposite chirality, i.e. $I_L^3(f_R) = 0$ and $I_R^3(f_L) = 0$. The hypercharges have been chosen to satisfy equation (4.45). The reported eigenvalues hold correspondingly for the fermions belonging to the heavier second and third generations.

Field	$I_{L/R}^3$	Y	Q
u_L	$+\frac{1}{2}$	$+\frac{1}{6}$	$+\frac{2}{3}$
d_L	$-\frac{1}{2}$	$+\frac{1}{6}$	$-\frac{1}{3}$
u_R	$+\frac{1}{2}$	$+\frac{1}{6}$	$+\frac{2}{3}$
d_R	$-\frac{1}{2}$	$+\frac{1}{6}$	$-\frac{1}{3}$
e_L	$-\frac{1}{2}$	$-\frac{1}{2}$	-1
ν_L	$+\frac{1}{2}$	$-\frac{1}{2}$	0
e_R	$-\frac{1}{2}$	$-\frac{1}{2}$	-1
ν_R	$+\frac{1}{2}$	$-\frac{1}{2}$	0

it follows that

$$1 - \frac{2g'^2}{2g'^2 + g^2} = \frac{g^2}{2g'^2 + g^2} = \cos^2 2\theta. \tag{4.49}$$

Hence, (4.47) can be rewritten as

$$e = \frac{g'g}{\sqrt{2g'^2 + g^2}} = g\sin\theta = g'\sqrt{\cos 2\theta}. \tag{4.50}$$

Equation (4.50) marks a clear distinction of the LR symmetric model from the prediction of the SM. However, the right-most equality of equation (4.50) can not be tested, since g' cannot be measured due to the absence of photon self-coupling.

The hypercharge must have the same value for each pair of LH and RH fermion doublets, due to equation (4.45) and the fixed eigenvalues of the weak isospin $I_3^{L/R} = \pm\frac{1}{2}$. The precise assignment of hypercharge enforced by the above considerations is highlighted in Table 4.1.

It can be seen from Table 4.1 that all quarks and all leptons have the same hypercharge. This allows to make a convenient identification between the hypercharges and $B - L$ quantum number

$$Y = \frac{B - L}{2}. \tag{4.51}$$

Equation (4.51) can be used to identify the local symmetry under $U(1)_Y$ with the global

Table 4.2: Field content of the hidden sector. The index i denotes the generation, and satisfies $i = 1, 2, 3$. The subscripts L and R identify the chiral structure, akin to the chirality structure of the SM; q_{U_i} and q_{D_i} denote the $U(1)_F$ charges of the quarks of the SM.

Fields	Spin	$SU(2)_L$	$SU(2)_R$	$U(1)_Y$	$SU(3)_c$	$U(1)_Y$
$S_L^{D_i}$	0	$\frac{1}{2}$	0	$\frac{1}{3}$	3	$-q_{D_i}$
$S_L^{U_i}$	0	$\frac{1}{2}$	0	$\frac{1}{3}$	3	$-q_{U_i}$
$S_R^{D_i}$	0	0	$\frac{1}{2}$	$\frac{1}{3}$	3	$-q_{D_i}$
$S_R^{U_i}$	0	0	$\frac{1}{2}$	$\frac{1}{3}$	3	$-q_{U_i}$
Q^{D_i}	$\frac{1}{2}$	0	0	0	0	q_{D_i}
Q^{U_i}	$\frac{1}{2}$	0	0	0	0	q_{U_i}

symmetry under $U(1)_{B-L}$ explaining the anomaly cancellation between the Noether currents associated with the invariance of the Lagrangian under $U(1)_B$ and $U(1)_L$.[11]

4.3.3 The Messenger sector

The purpose of the messenger sector is to transmit the ChSB from the dark sector to the SM via loop diagrams. [47, 3] Therefore, the messenger fields must interact both with the SM and the dark fermions. As a consequence of interacting with the SM fermions, gauge invariance requires that the messenger fields possess the same quantum numbers as the sleptons and squarks of the Supersymmetric (SUSY) theories. [3] In detail, gauge invariance prescribes the introduction of $2N$ doublets of $SU(2)_L$ and $2N$ doublets of $SU(2)_R$, where $N = 3$, in accordance with the existence of 3 families of up- and down-type quarks in the SM. [3] The complete field content of the dark sector, including both the messenger fields and the dark fermions, along with the corresponding quantum numbers is presented in Table 4.2.

The Lagrangian of the messenger sector can be written as follows:

$$\mathcal{L}_{MS} = \mathcal{L}_{MS}^0 + \mathcal{L}_{MS}^I. \tag{4.52}$$

Here, $\mathcal{L}_{MS}^0$ denotes the tree-level mass terms as well as the kinetic terms of the messenger fields, thus including the interaction with the SM gauge bosons via the covariant derivative. Secondly, $\mathcal{L}_{MS}^I$ consists of the interaction terms of the messenger fields with the SM fermions, dark fermions and the Higgs field. The interactions between the SM gauge

---

[11] Here $U(1)_L$ refers to the abelian symmetry responsible for the conservation of the lepton number.

bosons and the messenger fields have no significant role in the origin of the Yukawa couplings and thus are omitted from hereon. With this modification, $\mathcal{L}^0_{MS}$ can be written as

$$\mathcal{L}^0_{MS} = \sum_{i=1,2,3} \partial_\mu \hat{S}^{Ui} \partial^\mu \hat{S}^{\dagger Ui} + \partial_\mu \hat{S}^{Di} \partial^\mu \hat{S}^{\dagger Di} + \hat{S}^{Ui} M^{2Ui}_S \hat{S}^{\dagger Ui} + \hat{S}^{Di} M^{2Di}_S \hat{S}^{\dagger Di}, \qquad (4.53)$$

where $\hat{S} = \begin{pmatrix} \hat{S}_L & \hat{S}_R \end{pmatrix}$. Imposing the minimal flavour violation (MFV) hypothesis consequently requires equation (4.53) to be invariant under $SU(6)$.[12] [3] Hence, there can be only two mass scales appearing in equation (4.53) - $M^2_{S,L}$ common to all $\hat{S}^{Ui}_L$ and $\hat{S}^{Di}_L$ and $M^2_{S,R}$ common to all $\hat{S}^{Ui}_R$ and $\hat{S}^{Di}_R$. In fact, by choosing $m^2_L = m^2_R$ reflecting the LR symmetry, the number of masses can be reduced to one. The interaction Lagrangian, constrained by gauge invariance and renormalizability, contains the following terms

$$\mathcal{L}^I_{MS} = \hat{g}_L \left(\sum_{i=1}^3 \left[\bar{q}^i_L Q^{Ui}_R \right] \hat{S}^{Ui}_L + \sum_{i=1}^3 \left[\bar{q}^i_L Q^{Di}_R \right] \hat{S}^{Di}_L \right) +$$
$$\hat{g}_R \left(\sum_{i=1}^3 \left[\bar{q}^i_R Q^{Ui}_L \right] \hat{S}^{Ui}_R + \sum_{i=1}^3 \left[\bar{q}^i_R Q^{Di}_L \right] \hat{S}^{Di}_R \right) + \qquad (4.54)$$
$$\lambda \sum_{i=1}^3 \left(\tilde{H}^\dagger_L \hat{S}^{Ui}_L \hat{S}^{Ui\dagger}_R \tilde{H}_R + H^\dagger_L \hat{S}^{Di}_L \hat{S}^{Di\dagger}_R H_R \right) + h.c.$$

In equation (4.54), the contraction of $SU(3)_c$ and $SU(2)_{L,R}$ indices has been left understood. The $q^i_{L,R}$ are defined analogously to the SM, i.e. $q^i_{L,R} = \begin{pmatrix} u^i_{L,R} & d^i_{L,R} \end{pmatrix}$; H_L denotes the left-handed Higgs doublet of the SM, and H_R the corresponding analogue associated to $SU(2)_R$; the conjugate Higgs field is defined by $\tilde{H}_{L,R} = i\sigma_2 H^*_{L,R}$. The coupling constants remain in the perturbative regime, $\hat{g}_{L,R} < 1$ and the LR symmetry dictates that $\hat{g}_L = \hat{g}_R = \hat{g}$.

4.3.4 Origin of the Diagonal Yukawa Terms

After SSB of $SU(2)_R$ and $SU(2)_L$ the third line in equation (4.54) contributes to the mass terms of the scalar fields in addition to the diagonal mass terms appearing in equation (4.53). Overall, the mass matrix of the scalar fields becomes

$$M^2_S = \begin{pmatrix} m^2_L & \Delta \\ \Delta & m^2_R \end{pmatrix} \qquad (4.55)$$

---

[12]A very brief overview of MFV is given in Appendix D

wherein $\Delta = \frac{1}{2}\lambda v_R v_L$, λ denoting the coupling constant appearing in equation (4.54) and v_L, v_R denoting the vev-s of H_L and H_R respectively. [3] As discussed in the previous subsection, the minimal flavour violation, realized as the global symmetry of the Lagrangian under $SU(6)$, forces the tree-level mass terms appearing in equation (4.53) to be identical for each $S^{Di,Ui}$, where $S = \begin{pmatrix} S_L^{Di,Ui} & S_R^{Di,Ui} \end{pmatrix}$. Hence, the mass matrix described by (4.55) must be identical for each $S^{Di,Ui}$. Following equation (4.55), M_S^2 is manifestly Hermitian, meaning that it can be diagonalized by a unitary transformation. The diagonal mass matrix resulting after the diagonalization, has two distinct eigenvalues:

$$ m_\pm = \frac{1}{2}\left(m_L^2 + m_R^2 \pm \sqrt{(m_L^2 - m_R^2)^2 + 4\Delta^2} \right). \tag{4.56} $$

A restriction to a fully LR symmetric scenario, $\bar{m}^2 = m_L^2 = m_R^2$ allows to simplify equation (4.55) further

$$ m_\pm^2 = \bar{m}^2 \left(1 \pm \xi \right), \tag{4.57} $$

with the mixing parameter ξ defined by

$$ \xi = \frac{\lambda v_R v_L}{2\bar{m}^2}. \tag{4.58} $$

The diagonal Yukawa couplings responsible for the appearance of fermion masses in the SM can be generated by considering one-loop diagrams transmitting the hierarchy encoded in the dark fermion masses to the fermion fields of the SM. The required diagrams are shown on Figures 4.2 and 4.3. [3]

Since the masses of the messenger fields and the dark fermions appearing in these diagrams are above the TeV scale, the results of the effective field theory can be used. Consequently, the following effective Lagrangian is generated at one loop

$$ \mathcal{L}_{eff} = \frac{1}{\Lambda_{eff}^f} \left(\bar{\psi}_L^f H_L \right) \left(H_R^\dagger \psi_R^f \right) + h.c., \tag{4.59} $$

where $\bar{\psi}_L^f$ and ψ_R^f are generic left and right handed fermions of flavour f respectively, Λ_{eff}^f denotes the effective flavour dependent scale, which has to be determined by matching the effective theory to the analytical calculation of the 1-loop diagrams. Clearly after SSB of $SU(2)_R$, the Yukawa couplings of the SM can be obtained, depending on the flavour through the effective scale Λ_{eff}^f. Similarly, the Yukawa couplings to the right handed Higgs field H_R can be obtained after the SSB of $SU(2)_L$. It follows that the Yukawa couplings to H_R are given in terms of the Yukawa couplings of the SM up to a rescaling by $\frac{v_L}{v_R}$.[13] The

_____

[13]The lower bound of v_R lies in the TeV scale, as discussed in [3]. Thus the Yukawa couplings to H_R
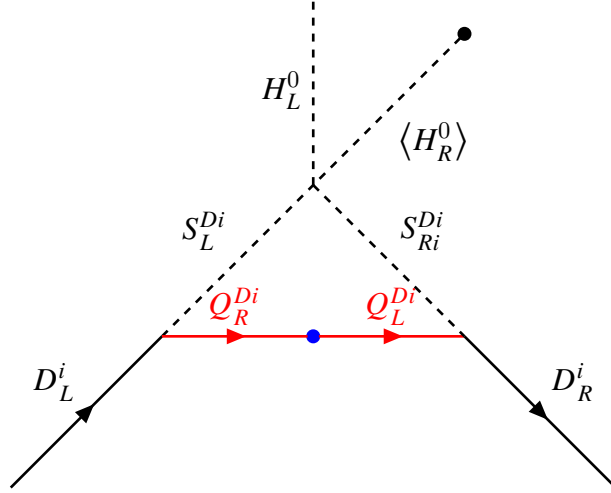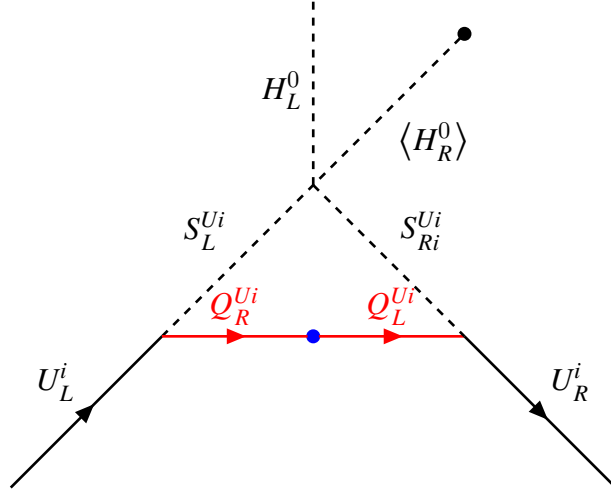
Figure 4.2: The 1-loop diagram responsible for the generation of the d-type quark masses of the SM. The solid black lines denote the propagators of the d-type quarks of the SM. The solid red lines denote the propagators of the associated dark fermions. The black dot indicates that the H_R fields has been set to its vev, after SSB of $SU(2)_R$. The blue dot denotes the mass insertion between Q_R^{Di} and Q_L^{Di}

exact expression for the Yukawa couplings of the SM after the SSB of $SU(2)_R$ is given by [56]

$$Y_f = \left(\frac{g_{LR}^2}{16\pi^2} \right) \left(\frac{\xi M_{Qf} \sqrt{2}}{v_L} \right) f_1(x_f, \xi) \tag{4.60}$$

where M_{Qf} is the mass of the dark fermion associated with the SM quark of flavour f, $x_f = \frac{M_{Qf}^2}{\bar{m}^2}$ and ξ is the mixing parameter introduced in equation (4.58). The loop function $f_1(x_f, \xi)$ is given by [3]

$$f_1(x_f, \xi) = \frac{1}{2} \left[C_0 \left(\frac{x}{1-\xi} \right) \frac{1}{1-\xi} + C_0 \left(\frac{x}{1+\xi} \right) \frac{1}{1+\xi} \right]. \tag{4.61}$$

In turn, the scalar loop function C_0 is given by, [3]

$$C_0(x) = \frac{1 - x(1 - \log x)}{(1-x)^2}. \tag{4.62}$$

Equation (4.60) evidently displays a partial solution to the flavour hierarchy puzzle. In detail, the mass hierarchy of the SM quarks follows directly from the mass hierarchy of the associated dark fermions due to the dependence of Y_f on M_{Qf}. Moreover, the mass hierarchy of the dark fermions can be traced back to the dynamical ChSB in the dark sector arising from a hidden $U(1)_F$ symmetry. Thus, no fine tuning of the Yukawa couplings is needed in order to recover the observed hierarchy in the quark masses.

---

are very small compared to the Yukawa couplings of the SM.

Figure 4.3: The 1-loop diagram responsible for the generation of the u-type quark masses of the SM. The solid black lines denote the propagators of the u-type quarks of the SM. The solid red lines denote the propagators of the associated dark fermions. The black dot indicates that the H_R fields has been set to its vev, after SSB of $SU(2)_R$. The blue dot denotes the mass insertion between Q_R^{Ui} and Q_L^{Ui}

4.4 The Quark Mixing in the Left-Right Symmetric Model

Previously, it was shown that the quark masses of the SM can be explained by a radiative generation mechanism in the context of LR symmetric models. However, in order to reconcile the radiative mechanism with the observed flavour hierarchy of the SM, the hierarchy of the CKM matrix must also be explained in the same framework. In fact, the evident structure of CKM matrix can be explained analogously to the mass generation mechanism, via two- and three-loop diagrams, as will be shown in this section.

In the present framework, the CKM matrix results from a Lagrangian of the form, [4]

$$\mathcal{L}_{CKM} = \hat{g}_L \bar{q}_L^i X_{ij}^L Q_R^j \hat{S}_L^j + \hat{g}_R \bar{q}_R^i X_{ij}^R Q_L^j \hat{S}_R^j, \tag{4.63}$$

where X_{ij} is a generic matrix in flavour space, and the sum over flavour indices $i, j = u, d, c, s, t, b$ has been understood. Moreover, the sum over the color and spin indices is also implicitly assumed. The CKM matrix appears in the SM due to the misalignment between mass and gauge eigenstates, (cf. Section 2.4). Here the misalignment is encoded in X_{ij}, which can be parametrized as,

$$X_{ij} = \delta_{ij} + \Delta_{ij}. \tag{4.64}$$

Without any misalignment, X_{ij} would take the form δ_{ij} resulting only in the generation of the diagonal Yukawa couplings responsible for the masses of the SM quarks, (cf. Section 4.3). Broadly speaking, the off-diagonal elements Δ_{ij} result from the misalignment between the mass matrices of the quark and the associated dark fermion fields. This mechanism has important phenomenological consequences for FCNC-studies and hadron physics. [56] Moreover, to reproduce the observed hierarchy of the CKM matrix, the off-diagonal elements must satisfy

$$\Delta_{ij} << 1. \tag{4.65}$$

Albeit in line with the MFV hypothesis, several other *ad-hoc* constraints are needed to justify equation (4.65). The inherent hierarchy between the elements of δ_{ij} and Δ_{ij} can be explained if the elements of Δ_{ij} are generated by higher-order processes. For instance, this scenario can be realized by the introduction of a new scalar field F - the dark flavon, sourcing two- and three-loop diagrams responsible for generating the elements of Δ_{ij}. In particular, F is a complex singlet of SM, transforming with charge q_D under $U(1)_F$. Furthermore, in order to generate the necessary higher order diagrams, the $U(1)_F$ charges of the dark fermions are constrained in terms of q_F

$$q_F = q_2^U - q_1^U = q_3^U - q_2^U = q_2^D - q_1^D = q_3^D - q_2^D, \tag{4.66}$$

where q_i^U, q_i^D denote the $U(1)_F$ charges of the dark fermions associated with quarks of generation i in U and D sectors respectively. Equation (4.66) imposes a simple relation between the $U(1)_F$ charges between dark fermions of different generation,

$$q_2^{U,D} = \frac{q_3^{U.D} + q_1^{U.D}}{2}. \tag{4.67}$$

Furthermore, gauge invariance of the Lagrangian introduced in Section 4.3 ensures that analogous charge assignment holds for $S_{Li}^{U,D}$ and $S_{Ri}^{U,D}$. Constrained by renormalizability and the $U(1)_F$-invariance, the Lagrangian containing the flavon field can be written as,

$$\mathcal{L}_F = \frac{1}{2}(D_\mu F)^\dagger (D^\mu F) - \frac{1}{2}m_F^2 FF^\dagger + (\eta_U \bar{Q}^{U1} Q^{U2} + \eta_U' \bar{Q}^{U2} Q^{U3})F + (\eta_D \bar{Q}^{D1} Q^{D2} + \eta_D' \bar{Q}^{D2} Q^{D3})F$$
$$+\mu_U(\hat{S}_L^{U1\dagger}\hat{S}_L^{U2} + \hat{S}_L^{U2\dagger}\hat{S}_L^{U3})F + \mu_D(\hat{S}_L^{D1\dagger}\hat{S}_L^{D2} + \hat{S}_L^{D2\dagger}\hat{S}_L^{D3})F + (L \leftrightarrow R) + h.c. \tag{4.68}$$

where $(L \leftrightarrow R)$ denotes the same expression with L and R indices swapped.

The form of the flavon Lagrangian $\mathcal{L}_F$ allows for an insertion of the flavon fields into the one loop diagrams of Section 4.3. Consequently, two- and three-loop diagrams presented on Figures 4.4, 4.5, 4.6 can be obtained. [4] For the sake of brevity only the diagrams
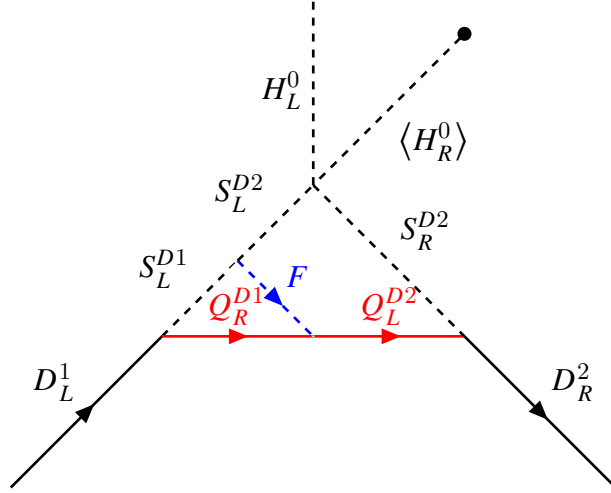
Figure 4.4: The 2-loop diagram generating the Y_{12}^D Yukawa matrix. The solid black lines denote the propagators of the d-type quarks of the SM. The solid red lines denote the propagators of the associated dark fermions. The black dot indicates that the H_R field has been set to its vev, after SSB of $SU(2)_R$. The blue dotted line denotes the scalar propagator associated to the flavon field.

generating the off-diagonal terms of the d-type quark Yukawa matrix have been shown, with the understanding that the diagrams generating the off-diagonal terms of the u-type quark Yukawa matrix follow analogously.

Crucially, the two-and three-loop diagrams result in smaller amplitudes than the one-loop diagrams presented in the previous section, hence explaining the relative smallness of the off-diagonal Yukawa couplings compared to the diagonal ones. Therefore, the two- and three-loop amplitudes can also be understood to have only negligible contribution to the masses of the SM quarks. [4] As far as CP-violation is concerned, at least two complex couplings - $\eta_{U,D}$ and $\eta'_{U,D}$ are needed to account for the CP-violation. [4]

Using effective parametrization the Yukawa matrix for the down sector generated by the diagrams on Figures 4.4, 4.5 and 4.6 can be written as [4]

$$\frac{Y^D}{y_b} = \begin{pmatrix} A_r^D \eta_D & \varepsilon_1^D & A^D \varepsilon_1^D \varepsilon_2^D \\ \varepsilon_1^{D*} & \eta_S & \varepsilon_2^D \\ A^D \varepsilon_1^{D*} \varepsilon_2^{D*} & \varepsilon_2^{D*} & 1 \end{pmatrix}, \tag{4.69}$$

where $\frac{Y^D}{y_b}$ denotes the down-type Yukawa matrix parametrized in terms of the Yukawa coupling of the bottom quark y_b. The constants η_i satisfy $\eta_i = \frac{m_i}{m_b}$, wherein $i = D, S$. The free parameters A^D and A_r^D are real coefficients of $\mathcal{O}(1-10)$ and $\mathcal{O}(0-1)$ respectively. In more detail, A^D is used to compensate the extra loop and coupling suppression yielding from
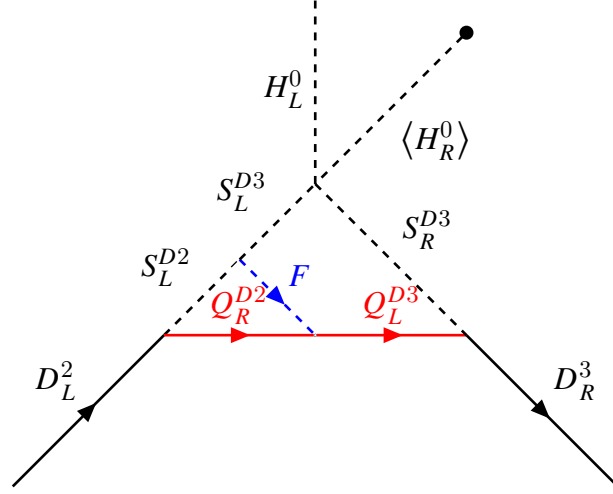
Figure 4.5: The 2-loop diagram generating the Y_{23}^D Yukawa matrix. The solid black lines denote the propagators of the d-type quarks of the SM. The solid red lines denote the propagators of the associated dark fermions. The black dot indicates that the H_R field has been set to its vev, after SSB of $SU(2)_R$. The blue dotted line denotes the scalar propagator associated to the flavon field.
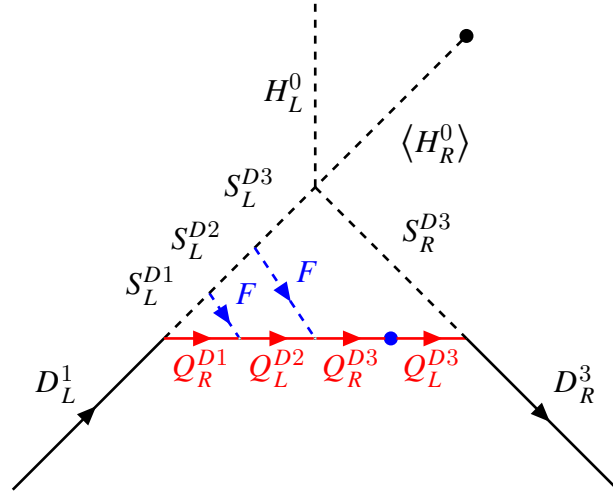

Figure 4.6: The 3-loop diagram generating the Y_{13}^D element of the Yukawa matrix. The solid black lines denote the propagators of the d-type quarks of the SM. The solid red lines denote the propagators of the associated dark fermions. The black dot indicates that the H_R field has been set to its vev, after SSB of $SU(2)_R$. The blue dotted lines denote the scalar propagators associated to the flavon field. The blue dot denotes the mass insertion between Q_R^{D3} and Q_L^{D3}.

modelling a three-loop process as a product of two two-loop processes. [4] The constant A_r^D, in turn factors in the contribution of the quark mixing into the first generation down quark masses. [4] Contributions from loops are taken into account with the introduction of $\varepsilon_{1,2}$ that lie well in the perturbative regime $|\varepsilon_{1,2}| << 1$. Recalling that the up sector exhibits similar loop diagrams to those that were presented on Figures 4.4, 4.5 and 4.6, the Yukawa matrix parametrized in terms of the top Yukawa coupling y_t becomes

$$\frac{Y^U}{y_t} = \begin{pmatrix} A_r^U \rho_D & \varepsilon_1^U & A^D \varepsilon_1^U \varepsilon_2^U \\ \varepsilon_1^{U*} & \rho_S & \varepsilon_2^U \\ A^D \varepsilon_1^{U*} \varepsilon_2^{U*} & \varepsilon_2^{U*} & 1 \end{pmatrix}, \tag{4.70}$$

where $\rho_i = \frac{m_i}{m_t}$, with $i = U, C$. The CKM matrix can be found from the relation

$$V_{CKM} = V^U (V^D)^\dagger, \tag{4.71}$$

by finding V^U and V^D such that

$$V^U Y^U (V^U)^\dagger = Y^U_{diag} \quad V^D Y^D (V^D)^\dagger = Y^D \tag{4.72}$$

where $Y^{U,D}_{diag}$ represents a diagonalized Yukawa matrix of up- and down-sectors respectively.

4.4.1 Matching Theory with Experimental Results

In the previous section an effective parametrization of the down and up sector Yukawa matrices was proposed following [4]. Diagonalizing Y^D, Y^U the CKM matrix can be calculated for any fixed values of the free parameters appearing in the Yukawa matrices. Consequently, the computed CKM matrix can be compared against the experimentally observed results to constrain the free parameters responsible for the generation of Y^U, Y^D. For the sake of simplifying this task all the phases of the complex parameters have been omitted, amounting to a rearrangement of the relative phases. Moreover, Y^U has been chosen to be already diagonalized. [4] Although this convention introduces mixing factors in the interaction terms of the u-type quarks with the scalar mediators and dark fermions, it considerably reduces the number of parameters required for carrying out the numerical analysis. With the described modifications in mind, a preliminary scan was first conducted to determine the relevant parameter space to be further analysed. The resulting bounds on the parameter space can be found from Table 4.3.

Then, for each combination of the input parameters in the range reported in Table 4.3, the squared Y_D was diagonalized and thus the predictions for the quark masses could

Table 4.3: The ranges of the input parameters.

Input parameter	Lower bound	Upper bound	Number of points
A_r^D	10^{-5}	10	200
ϵ_1^D	$10^{-2.5}$	10^{-2}	200
ϵ_2^D	$10^{-1.5}$	10^{-1}	200
A^D	5	45	200

be calculated by multiplying the square root of the eigenvalues of Y_D by m_b. Having determined the eigenvalues of the Y_D, the matrix V^D appearing in equation (4.72) could be determined, thus allowing to calculate the CKM by using equation (4.71) [14]

$$V_{CKM} = (V^D)^\dagger. \tag{4.73}$$

Having obtained V_{CKM} the mixing angles could be calculated from,[15]

$$\begin{aligned} \sin\theta_{12} &= \frac{V_{12}}{\sqrt{V_{23}^2 + V_{33}^2}} \\ \sin\theta_{23} &= \frac{V_{23}}{\sqrt{V_{23}^2 + V_{33}^2}} \\ \sin\theta_{13} &= V_{13}. \end{aligned} \tag{4.74}$$

For each combination of input parameters, the resulting quark masses as well as the sines of the mixing angles were then compared against the experimental bounds highlighted in Table 4.4.

In particular, for lighter quarks, more conservative ranges were used to account for the running of their masses. For the bottom quark mass and the mixing angles the 3σ range from [57] were used. The comparison of the calculated masses and mixing angles against the observed values allowed to constrain the effective phase space of the input parameters appearing in Table 4.3 as well as to study the effect on the predictions of the model for each choice of input parameters. During the course of this work, 45 correlation plots were produced encompassing a correlation plot between all possible combinations of input and output parameters. The six panels constraining the effective phase space of the input

---

[14]Since Y^U was chosen as a diagonal matrix, V^U turns out to be proportional to the identity matrix and hence can be omitted from the definition of the CKM matrix, since the proportionality factor can be absorbed into the elements of V_D.

[15]In the following formula, the matrix elements of V_{CKM} are written in the form V_{ij} for the sake of compactness.

Table 4.4: The experimental constraints on the masses and the mixing angles of the d-type quarks in the SM.

Parameter	Lower bound	Upper bound
$m_d(GeV)$	10^{-3}	10^{-2}
$m_s(GeV)$	5×10^{-2}	1.5×10^{-1}
$m_b(GeV)$	4.06	4.3
$sin\theta_{12}$	0.2195	0.2291
$sin\theta_{23}$	0.0368	0.0458
$sin\theta_{13}$	0.0022	0.0052

parameters are presented on Figure 4.7.

The first three panels on Figure 4.7 depict the dependence of A_r^D on different loop factors. On closer inspection, two distinct regions can be identified on all three panels. The first region, where $A_r^D < 1$, encloses the area of allowed phase space where the mass of the down quark is mostly accounted for by the quark mixing effects. Conversely, for the other region where $A_r^D > 1$, the mass of the d-quark mostly results from the (diagonal) element Y_{11}^D of the Yukawa matrix. Importantly, for both cases the allowed range for the loop parameters are relatively similar. The three remaining panels describe the magnitude of the two loop radiative corrections ϵ_1^D and ϵ_2^D appearing on Figures 4.4 and 4.5 as well as the magnitude of the compensation factor resulting from the three loop diagram on Figure 4.6.

The correlation plots of the effective input parameters and the resulting d-type quark masses and mixing angles are shown on Figure 4.8. The first panel on 4.8 depicts the dependence of the d-quark mass on A_r^D. Again, two regions for the values of A_r^D can be distinguished depending on the dominant contribution to m_d. Interestingly, if the mass of the down quark exceeds 5 MeV, then necessarily $A_r^D > 1$. This means that above 5 MeV the mass of the d-quark must be predominantly sourced by the Y_{11}^D element of the Yukawa matrix. Naturally, the effect of the quark mixing on m_d must then be smaller. In fact, as the top right panel of Figure 4.8 shows, the parameter ε_1^D regulating Y_{12}^D indeed decreases with the increase of m_d after m_d exceeds 5 MeV. On the two bottom panels, the dependence of the mixing angles on the effective input parameters responsible for the corresponding loop corrections are shown. In both cases a clear positive correlation between those parameters can be seen, meaning that enhancing higher-order loop effects increases the mixing of d-quarks.
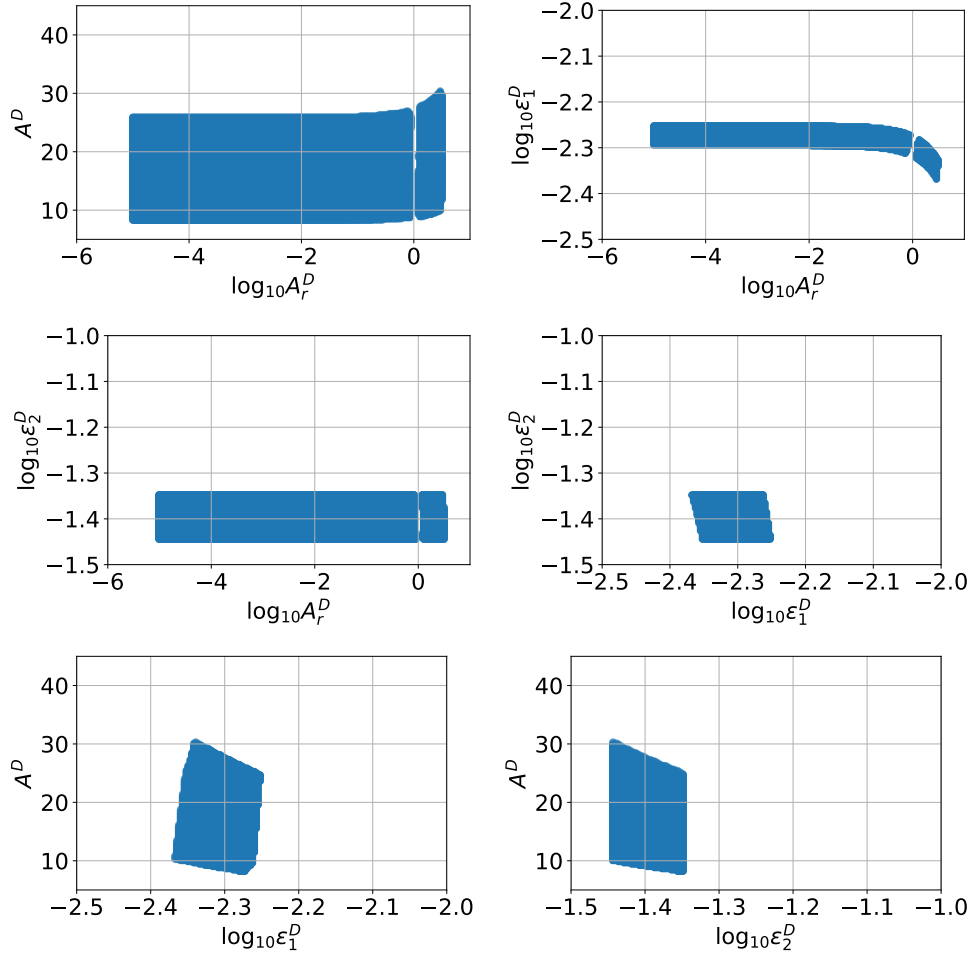
Figure 4.7: The correlation plots between effective input parameters given in Table 4.3

4.4.2 Matching the Effective Parametrization with Fundamental Theory

Previously, an effective field theory approach was used in order to constrain the parameters responsible for the generation of the Yukawa couplings at the low energy regime. In this section, analytical expressions for the two- and three-loop amplitudes will be employed to constrain the parameters associated to the dark sector.[16] The relevant amplitudes for this task are given in Appendix E. The exact details of the calculation of these amplitudes can be found from [4] and so in this section only the information important for this thesis have been outlined. In order to understand the expansion of the 2-loop amplitudes given in Appendix E, it is crucial to remember that these amplitudes mark a hierarchy of three different mass scales that enable an expansion in powers of the different scales. In more detail, one can distinguish between the mass scales of the dark fermion (m_Q),

---

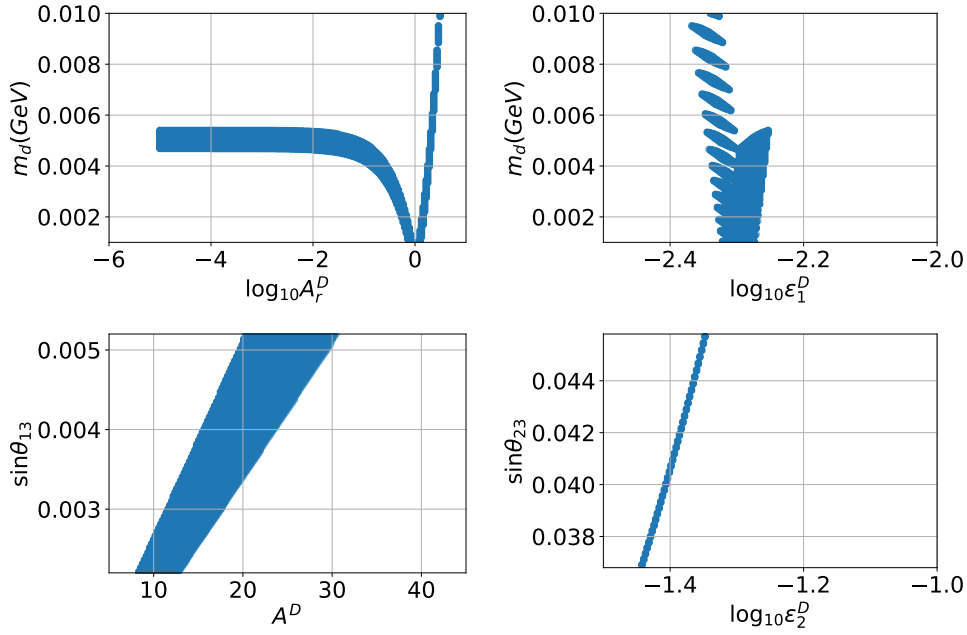[16]This section is entirely based on the work presented in [4].

Figure 4.8: Selected correlation amongst the down-quark masses, the CKM parameters and the effective input parameters.

the messenger sector (m_S) and the dark flavon (m_F).[17] The requirement for a stable dark matter candidate from the dark sector enforces $m_Q < m_S$, while not imposing any other restrictions on the hierarchy of the scales.[18] In fact, although the loop functions are sensitive to the relative size of m_S and m_F there is no way to *a priori* determine whether $m_F > m_S$ or $m_F < m_S$. Thus, following [4] the choice $m_F = m_S$ has been made to simplify the following discussion. Furthermore, in the following all dimensionless couplings have been parametrized by χ and the flavon trilinear coupling with the messenger fields has been parametrized by $\mu_D = \rho m_F$. In this way, the asymptotic expansion in terms of $x_Q = \frac{m_Q}{m_F}$ and the loop suppression factor $L = 16\pi^2$ can be used to investigate the size of the Yukawa couplings as a function of the effective parameter A_D and the ratio of the two mass scales m_F and m_Q. The plots needed for this analysis have been reproduced by using the code provided by the authors of [4] with their permission. The results can be found from Figure 4.9.

From Figure 4.9 and Figure 4.7 it is clear that in order to generate the effective parameters ϵ_1^D and ϵ_2^D of the observed size, the mass scales of the dark fermions and the flavon are constrained to lie rather close to each other. Moreover, it can be seen that the trilinear coupling μ_D takes a sizeable value relative to the dark flavon mass. If one wishes to further increase the strength of the rescaled Yukawa couplings $Y_{12,23}^D/y_b$ at a fixed value of

---

[17]To first order the messenger fields can be approximated as a having a universal mass scale.
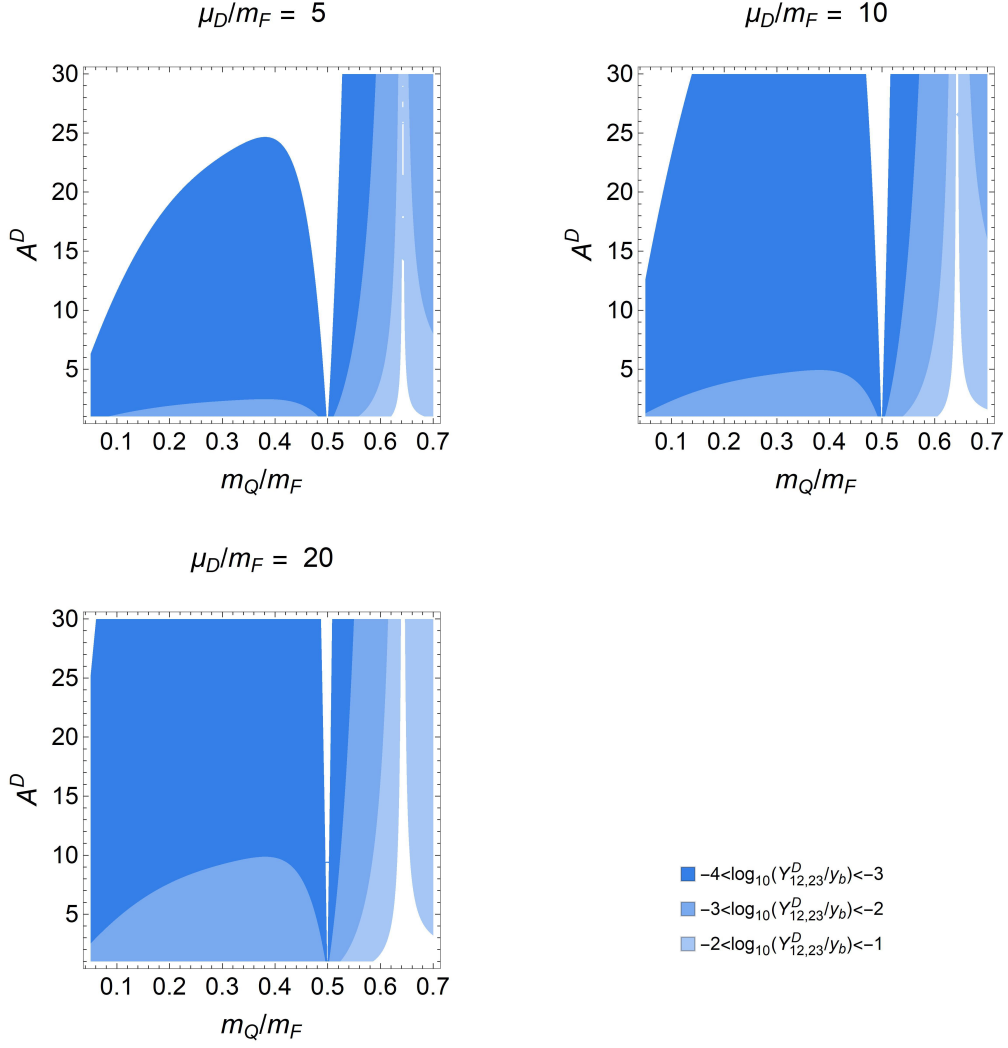
[18]More details are given in Section 4.5.

Figure 4.9: Values of the off-diagonal Yukawa couplings (rescaled by y_b to make contact with the effective parametrization from the previous section) generated by the two-loop amplitudes given in Appendix E as a function of A_D and the mass hierarchy between the messenger sector and the dark fermions. All dimensionless coupling constants are set to $1/2$, while the dark flavon trilinear coupling $\rho = \mu_D/m_F$ is set at the reported values.

A_D without affecting the relative size of the mass scale, then the trilinear coupling may further have to be increased as shown on Figure 4.9. Finally, using the formulae given in Appendix E the validity of modelling three loop amplitudes as a product of two two-loop amplitudes that was inherent in the effective parametrization may also be checked. Indeed, the requirement $Y_{13}^D \approx A^D Y_{12}^D Y_{13}^D$ can always be satisfied with a suitable choice of $\frac{m_F}{v_R}$. Given that v_R can be constrained for example by collider experiments, this observation may place further bounds on m_F.

4.5 Phenomenological Implications

In this section, the phenomenological implications of the LR symmetric model used throughout this chapter are briefly described.

Lower bound on v_R

Since the $W_R^\pm$ has not yet been experimentally observed, it is natural to expect the lower bound on v_R to lie above the TeV scale. In fact, by assuming that the lightest messenger mass m_- is greater the mass of the heaviest dark fermion M_{Qt}, it can be shown that the lower bound for v_R is given by[19] [3]

$$v_R \approx \frac{8m_t^2}{\lambda v_L} \left(\frac{16\pi^2}{g_{L,R}^2} \right) \frac{1}{\xi},$$

(4.75)

where ξ is the mixing parameter first introduced in equation (4.58). By using equation (4.60), it is clear that, if $\xi \to 0$, the Yukawa couplings also approach zero, so that for smaller mixing values ξ, large values of v_R are needed in order to generate the Yukawa couplings, as is also evident from equation (4.75).

4.5.1 The ρ-Parameter

The ρ - parameter of the EW sector is defined as

$$\rho = \frac{M_{W_L}^2}{M_{Z_L}^2 \cos^2 \theta_W}.$$

(4.76)

In the SM $\rho = 1$, and any deviation from this value for extensions of the SM may have important phenomenological implications. In fact, in [3] it has been shown, that in the LR symmetric extension of the SM presented in this chapter, $\rho = 1$, up to corrections of order $O\left(\left(\frac{v_L}{v_R} \right)^2 \right)$. Since $\left(\frac{v_L}{v_R} \right)^2 \approx 10^{-8}$, these contributions are negligible.

The Strong CP Problem

The strong CP problem involves a delicate fine-tuning issue between a parameter of Quantum Chromodynamics (QCD) and a parameter of the flavour sector. In detail, the

---

[19]In particular, this result holds if $\xi << 1$.

physical CP-violating parameter contributing to the electric dipole moment of the neutron is given by [58]

$$\bar{\theta} = \theta + \arg(\det M), \tag{4.77}$$

where θ and M refer to the QCD phase resulting from non-trivial vacuum configurations, and to the mass matrix of quarks of all generations respectively, both resulting from the Lagrangian of the form [59]

$$\mathcal{L}_{QCD} = \frac{\theta g_s^2}{32\pi^2} G^{a\mu\nu}\tilde{G}_{a\mu\nu} + q_L M q_R. \tag{4.78}$$

In the above equation, q_L and q_R denote a vector composed of quarks of all generations, and

$$\tilde{G}_{a\mu\nu} = \varepsilon_{\alpha\beta\mu\nu} G^{a\alpha\beta}, \tag{4.79}$$

where $a = 1, .., 8$. On the other hand the phase of the determinant $\theta_q = \arg(\det M)$ is related to the global $U(1)$ symmetry resulting from the decomposition of the overall global symmetry of the Lagrangian $U(3) = SU(3) \times U(1)$ for vanishing quark masses. As shown in [58], by using (4.77), these two parameters can be combined into a single effective Lagrangian:

$$\mathcal{L}_{StrongCp} = \bar{\theta}\frac{\alpha_s}{8\pi} G_{a\mu\nu}\tilde{G}^{a\mu\nu} \tag{4.80}$$

Since the effective neutron dipole moment resulting from this Lagrangian is given by [58, 60]

$$d_n \approx \frac{e\bar{\theta}m_q}{M_N^2}, \tag{4.81}$$

the experimental observations constrain $\bar{\theta} \le 10^{-9}$. [58] Thus, the measurements of the neutron dipole moment seemingly require a delicate fine tuning between two unrelated parameters of the SM. Commonly, this problem is solved by introducing a new anomalous symmetry $U(1)_{PQ}$ known of as the Peccei-Quinn symmetry. [61] The new symmetry solves the strong CP problem by rotating away the CP-violating parameter $\tilde{\theta}$ at a price of introducing a new field - the axion - which appears as the pseudo Nambu-Goldstone boson after the breaking of $U(1)_{PQ}$. [58] Alternatively, the strong CP problem can also be solved within the formalism of the LR symmetric theories. [62, 63] In this thesis, only a sketch of the solution to the strong CP problem provided by LR symmetric theories is given. More details are outlined in [4]. In order to illustrate the idea without unnecessary technicalities only the first generation of quarks is considered. The mass terms of the first generation quarks in the Lagrangian are given by [4]

$$\mathcal{L}_{mass} = e^{i\theta_q} m_q \bar{q}_L q_R + e^{-i\theta_q} m_q \bar{q}_R q_L, \tag{4.82}$$

where the possible complex phase of the mass is explicitly written out. Clearly if one invokes the requirement of LR symmetry, one has $\theta_Q = 0$, for otherwise the Lagrangian would not be symmetric under the interchange of left-and right-handed fields. Thus, the small value of $\tilde{\theta}$ can be explained by the small value of a single parameter θ and no fine tuning between θ and θ_q is needed.

Dark Matter

As the name suggests, the dark sector contains fields that can be associated to dark matter. The integral condition in this regard is the stability of the dark matter candidates. As it turns out, the flavon field allows for the decay of the heaviest dark fermions Q^{U_3} and Q^{D_3} to lighter states. [4] The exact allowed decay channels are

$$Q^{U_3} \to Q^{U_2} + Q^{U_2} + \bar{Q}^{U_1} \tag{4.83}$$

$$Q^{D_3} \to Q^{D_2} + Q^{D_2} + \bar{Q}^{D_1} \tag{4.84}$$

and the subsequent decay:

$$Q^{U_2} \to Q^{U_1} + Q^{D_2} + \bar{Q}^{D_1}, \tag{4.85}$$

assuming that the dark fermions associated with the down-sector are lighter than the dark fermions associated with the up-sector, mimicking the hierarchy of the Yukawa couplings for the SM. From the discussion, it is clear that the dark sector consists of 3 stable dark matter candidates: Q^{D_1}, Q^{D_2} and Q^{U_1}. These considerations place the bounds of the heaviest stable dark matter particle in the $\mathcal{O}(100\,\text{GeV})$ range.

Summary

The SM is a successful physical theory of the microscopic world, describing the properties and interactions of the fundamental fermions and gauge bosons. The interactions of the fundamental fermions and the gauge bosons follow naturally from requiring local gauge invariance under the $SU(3)_c \times SU(2)_L \times U(1)_Y$ gauge group, while the experimentally observed masses of the gauge bosons and the fermions are generated by the Higgs mechanism after the SSB of the $SU(2)_L \times U(1)_Y$ symmetry. In order to introduce the Higgs mechanism, a new scalar field, known as the Higgs field, is needed. Using the Higgs field, all fermion masses can be introduced via introducing the Yukawa couplings, which are experimentally determined fixed parameters. Although the Yukawa couplings allow to recover all the experimentally observed masses of fermions, the SM offers no explanation to the large hierarchy for these couplings across the different flavours of fermions, which can be experimentally observed as the large difference between the orders of magnitude of the masses of quarks and leptons of different flavours as well as the spread in the mixing angles of quarks. This thesis focused explicitly of the flavour hierarchy in the quark sector to address potential extensions of the SM. As a first example, the Froggat-Nielsen mechanism was briefly summarized, explaining the quark flavour hierarchy as resulting from the introduction of a new $U(1)_F$ and new scalar fields. However, due to the high dimensionality of the operators that are needed to generate the Yukawa terms in the Froggat-Nielsen approach, the novel work carried out in this thesis focused on an alternative mechanism. In detail, the SM gauge group was extended to $SU(3)_c \times SU(2)_L \times SU(2)_R \times U(1)_Y \times U(1)_F$ and new scalar and fermionic fields were introduced. With these modifications, the Yukawa couplings could not anymore be included in the Lagrangian at tree level but instead had to be radiatively generated after integrating out the heavy messenger and dark fermion fields. During the preparation of this thesis, I contributed to the development of the theory mainly by determining the spectra of the quark masses and mixing angles that could be generated by this model, thus constraining the range of the free parameters responsible for the radiative mechanism. It was shown, that all observed values of the physical quark masses and mixing angles can indeed be generated with the radiative mechanism, and

that the resulting free parameters remain in the perturbative range, as is necessary for a consistent formulation of the theory. Finally, some novel phenomenological implications of the LR symmetric radiative Yukawa coupling generation mechanism were investigated.

Acknowledgements

Bibliography

[1] W.Pauli. The Connection Between Spin and Statistics. *Phys. Rev.*, 58:716, 1940.

[2] H. Murayama. CPT Tests: Kaon vs Neutrinos. *Phys. Lett. B*, 597:73, 2004.

[3] E.Gabrielli L.Marzola and M.Raidal. Radiative Yukawa Couplings in the Simplest Left-Right Symmetric Model. *Phys. Rev. D*, 95:035005, 2017.

[4] Emidio Gabrielli, Carlo Marzo, Luca Marzola, and Kristjan Müürsepp. Dark Origin of the Quark Flavor Hierarchy and Mixing. *Phys. Rev. D*, 101:075019, 2020.

[5] P. Langacker. *The Standard Model and Beyond*. CRC Press, A Taylor Francis Group, 2010.

[6] C.N.Yang and R.L.Mills. Conservation of Isotopic Spin and Isotopic Gauge Invariance. *Phys. Rev.*, 96:191, 1954.

[7] W.Buchmüller and C.Lüdeling. Field Theory and Standard Model. arXiv:hep-ph/0609174v1, 2006.

[8] S.Glashow. Partial Symmetries of The Weak Interaction. *Nuc. Phys.*, 22:579, 1961.

[9] D.J.Gross and F.Wilczek. Ultraviolet Behavior of Non-Abelian Gauge Theories. *Phys. Rev. Lett.*, 30:1343, 1973.

[10] D.J.Gross and F.Wilczek. Asymptotically Free Gauge Theories. I. *Phys. Rev. D*, 8:3633, 1973.

[11] D.J.Gross and F.Wilczek. Asymptotically Free Gauge Theories. II. *Phys. Rev. D*, 9:980, 1974.

[12] M. E Peskin and D. V. Shroeder. *An Introduction to Quantum Field Theory*. Westview Press, 1995.

[13] K.S.Babu. TASI Lectures on Flavor Physics. arXiv:0910.2948v1 [hep-ph], 2009.

[14] R. Aaij *et al.* (LHCb Collaboration). Search for Lepton Universality Violation in $B^+ \rightarrow K^+ e^+ e^-$ Decays. *Phys. Rev. Lett*, 122:191801, 2019.

[15] R. Aaij *et al.* (LHCb Collaboration). Test of Lepton Universality with $\lambda_b^0 \rightarrow p K^- l^+ l^-$ Decays. arXiv:1912.08139v1 [hep-ex], 2019.

[16] CMS Collaboration. Observation of a New Boson at a Mass of 125 GeV with the CMS Experiment at the LHC. *Phys. Lett. B*, 716:30, 2012.

[17] G. Aad *et al.* (ATLAS Collaboration). Observation of a New Particle in the Search for the Standard Model Higgs Boson with the ATLAS Detector at the LHC. *Phys. Lett. B*, 716:30–61, 2012.

[18] J. Alison *et al.* (FERMILAB CONF. 19-468-E-T). Higgs Boson Potential at Colliders: Status and Perspectives. *Edited by : B. Di Micco, M. Gouzevitch, J. Mazzitelli, C. Vernieri*, arXiv:1910.00012v3 [hep-ph], 2020.

[19] M.Tanabashi *et al.* (Particle Data Group). *Phys. Rev. D*, 98:03001, 2018 and 2019 Update.

[20] S. Sturm *et al.* Atomic Mass of the Electron. *Nature*, 506:467, 2014.

[21] S. Aoki *et al.* (Flavour Lattice Averaging Group (FLAG)). FLAG Review 2019. arXiv:1902.08191v2 [hep-lat], 2019.

[22] D. Giusti *et al.* (RM123 Collaboration). Leading Isospin - Breaking Corrections to Pion, Kaon and Charmed - Meson Masses with Twisted - Mass Fermions. *Phys. Rev. D*, 95:114504, 2017.

[23] Measurement of the Top-Quark Mass in t t-bar Events with Lepton+Jets Final States in pp Collisions at sqrt(s)=8 TeV. Technical Report CMS-PAS-TOP-14-001, CERN, Geneva, 2014.

[24] F.Englert and R.Brout. Broken Symmetry and the Mass of Gauge Vector Mesons. *Phys. Rev. Lett.*, 13:321, 1964.

[25] P.Higgs. Broken Symmetries and the Masses of Gauge Bosons. *Phys. Rev. Lett.*, 13:508, 1964.

[26] C.R.Hagen G.S.Guralnik and T.W.Kibble. Global Conservation Laws and Massless Particles. *Phys. Rev. Lett.*, 13:585, 1964.

[27] H. E. Logan. TASI 2013 Lectures on Higgs Physics Within and Beyond the SM. arXiv:1406.1786v2 [hep-ph], 2014.

[28] T. Nakano and K. Nishijima. Charge Independence for V-Particles. *Prog. of Theor. Phys.*, 10:581, 1953.

[29] S.Weinberg. A Model of Leptons. *Phys. Rev. Lett.*, 19:1264, 1967.

[30] M.K.Gaillard J. Ellis and D.V.Nanopoulus. A Historical Profile of the Higgs Boson. arXiv:1201.6045v1 [hep-ph], 2012.

[31] C. Giunti and C.W.Kim. *Fundamentals of Neutrino Physics and Astrophysics*. Oxford University Press, 2007.

[32] N. Cabibbo. Unitary Symmetry and Leptonic Decays. *Phys. Rev. Lett.*, 10:531, 1963.

[33] M.Kobayashi and T.Maskawa. CP Violation in the Renormalizable Theory of the Weak Interaction. *Prog. of Theor. Phys.*, 49:652, 1973.

[34] L-L Chau and W-Y Keung. Comments on the Parametrization of the Kobayashi-Maskawa Matrix. *Phys. Rev. Lett.*, 53:1802, 1984.

[35] L. Wolfenstein. Parametrization of the Kobayashi-Maskawa Matrix. *Phys. Rev. Lett.*, 51:1945, 1983.

[36] J. H. Christenson *et al.* Evidence for the 2π Decay of the K_2^0 Meson. *Phys. Rev. Lett.*, 13:138, 1964.

[37] J.D.Bjorken and I.Dunietz. Rephasing-Invariant Parametrizations of Generalized Kobayashi-Maskawa matrices. *Phys. Rev. D.*, 36:2109, 1987.

[38] C.Jarlskog. Commutator of the Quark Mass Matrices in the Standard Electroweak Model and a Measure of Maximal CP Nonconservation. *Phys. Rev. Lett*, 55:1039, 1985.

[39] F.J.Hasert *et al.* Search for Elastic Muon-Neutrino Electron Scattering. *Phys. Lett. B.*, 46:121, 1973.

[40] F.J.Hasert *et al.* Observation of Neutrino-Like Interactions Without Muon or Electron in the Gargamelle Neutrino Experiment. *Phys. Lett. B.*, 46:138, 1973.

[41] J.Iliopoulos S.L.Glashow and L.Maiani. Weak Interactions with Lepton-Hadron Symmetry. *Phys. Rev. D*, 2:1285, 1970.

[42] Ferruccio Feruglio. Pieces of the Flavour Puzzle. *The European Physical Journal C*, 75(8), 2015.

[43] C.D. Froggat and H.B.Nielsen. Hierarchy of Quark Masses, Cabibbo Angles and CP-Violation. *Nuc. Phys. B.*, 147:277, 1979.

[44] K.Schmitz. *The* B–L P*hase* T*ransition - I*mplications for Cosmology and Neutrinos. Springer International Publishing, 2014.

[45] S.Fraser and E.Ma. Anomalous Higgs Yukawa Couplings. *EPL (Europhysics Letters)*, 108:11002, 2014.

[46] K.S.Babu and E.Ma. Radiative Mechanisms for Generating Quark and Lepton Masses: Some Recent Developments. *Mod. Phys. Lett. A*, 4:1975, 1989.

[47] E.Gabrielli and M.Raidal. Exponentially Spread Dynamical Yukawa Couplings from Nonperturbative Chiral Symmetry Breaking in the Dark Sector. *Phys. Rev. D*, 89:015008, 2014.

[48] C.Marzo L.Marzola S.Fraser, E.Gabrielli and M.Raidal. Left-Right Supersymmetry as the Origin of Flavor Structure. *Phys. Rev. D*, 100:115002, 2019.

[49] E.Gabrielli. Dynamical Breaking of Chiral Symmetry: A New Mechanism. *Phys. Rev. D*, 77:055020, 2008.

[50] D.O'Connell B.Grinstein and M.B.Wise. The Lee-Wick Standard Model. *Phys. Rev. D*, 77:025012, 2008.

[51] Y.Nambu and G.Jona-Lasinio. Dynamical Model of Elementary Particles Based on an Analogy with Superconductivity. I. *Phys. Rev.*, 122:345, 1961.

[52] Y.Nambu. and G.Jona-Lasinio. Dynamical Model of Elementary Particles Based on an Analogy with Superconductivity. II. *Phys. Rev.*, 124:246, 1961.

[53] T.D. Lee and G.C. Wick. Negative Metric and the Unitarity of the S-Matrix. *Nuc. Phys. B,*, 9:209, 1969.

[54] V.P Gusynin P.I Fomin and V.A Miransky. Vacuum Instability of Massless Electrodynamics and the Gell-Mann-Low Eigenvalue Condition for the Bare Coupling Constant. *Phys. Lett. B*, 78:136, 1978.

[55] V.A Miransky. Dynamics of Spontaneous Chiral Symmetry Breaking and the Continuum Limit in Quantum Electrodynamics. *Nuov Cim A*, 90:149, 1985.

[56] M.Raidal E.Gabrielli, B.Mele and E.Venturini. FCNC Decays of Standard Model Fermions Into a Dark Photon. *Phys. Rev. D*, 94:115013, 2016.

[57] S.Eidelman et al. (Particle Data Group). Review of Particle Physics. *Phys. Lett. B*, 592:1, 2004.

[58] R. D. Peccei. QCD, Strong CP and Axions. arXiv:1711.01852 [hep-ex], 1996.

[59] A.Hook. TASI Lectures on the Strong CP Problem and Axions. arXiv:1812.02669v1 [hep-ph], 2008.

[60] R.D.Peccei. Reflections on the Strong CP Problem. *Nuc. Phys. B - Proceedings Supplements*, 72:3, 1999.

[61] R.D.Peccei and H.R.Quinn. CP Conservation in the Presence of Pseudoparticles. *Phys. Rev. Lett.*, 38:1440, 1977.

[62] Rašin R.N.Mohapatra and G.Senjanović. C,P, and Strong CP in Left-Right Supersymmetric Models. *Phys. Rev. Lett.*, 79:4744, 1997.

[63] R.N.Mohapatra and G.Senjanović. Natural Suppression of Strong P and T Non-Invariance,. *Phys. Lett. B*, 79:283, 1978.

[64] Max Dohse. Tikz-Feynhand: Basic User Guide. arXiv:1802.00689v1 [cs.OH], 2018.

[65] J.P.Ellis. Tikz-Feynman: Feynman Diagrams with Tikz. *Comp. Phys. Comm.*, 210:103, 2017.

[66] J.Goldstone. Field Theories with Superconductor Solutions. *Nuovo Cim.*, 19:154, 1961.

[67] D.N.Levin J.M.Cornwall and G.Tiktopoulos. Derivation of Gauge Invariance from High-Energy Unitarity Bounds on the S Matrix. *Phys. Rev. D.*, 10:1145, 1974.

[68] S.M.Bilenky and S.T.Petcov. Massive Neutrinos and Neutrino Oscillations. *Rev. Mod. Phys.*, 59:671, 1987.

[69] E.Noether. Invariante Variationsprobleme. *Nachr. d. Köning Gesellsh. d. Wiss. zu Göttigen, Math-Phys., Klasses*, pages 235–257, 1918.

[70] E.Noether. Invariant Variation Problems - English Translation by M.A.Tavel. *Transp. Theor. and Stat. Phys.*, 1:183, 1971.

[71] I. A. Reyes M. Banados. A Short Review on Noether's Theorems, Gauge Symmetries and Boundary Terms. arXiv:1601.03616v3 [hep-th], 2017.

[72] K. Skovpen. Search for Flavour-Changing Neutral Currents with Top Quarks. arXiv:1711.01852 [hep-ex], 2017.

[73] G.Isidori G.D'Ambrosio, G.F.Giudice and A.Strumia. Minimal Flavour Violation: An Effective Field Theory Approach. *Nuc. Phys. B*, 645:155–187, 2002.

[74] J. M. Ashfaque. Some Interesting Properties of the Riemann Zeta Function. arXiv:1812.02574v1 [math.HO], 2018.

[75] C.Vergu. Polylogarithms and Physical Applications. Notes for the Summer School "Polylogarithms as a Bridge Between Number Theory and Particle Physics", Durham, UK, 2013.

[76] L.D.Faddeev and V.N. Popov. Feynman Diagrams for the Yang-Mills Field. *Phys. Lett. B*, 25:29, 1967.

Appendix A

Spontaneous Symmetry Breaking

A.1 The Nambu-Goldstone Theorem

Spontaneous Symmetry Breaking (SSB) occurs when the ground state of a system does not respect the symmetries of the system. The easiest example of SSB is the isotropic alignment of the spins of a ferromagnet at the ground state. For the case of field theories, the Goldstone theorem states that for each spontaneously broken continuous symmetry, there is a massless particle. [66] In this section of the Appendix, the Goldstone theorem will be proved, following the method of Peskin and Schroeder. [12]

A generic Lagrangian containing n scalar fields ϕ^a with $a = 1, .., n$ can be written as[1]

$$\mathcal{L} = \text{Kinetic Terms} - V(\phi). \tag{A.1}$$

The vev-s of the fields ϕ^a are given by

$$\frac{\partial}{\partial \phi^a} V \bigg|_{\phi^a(x) = \phi_0^a} = 0 \tag{A.2}$$

Expanding the potential around the vev, it follows that

$$V(\phi) = V(\phi_0) + \frac{1}{2} (\phi - \phi_0)^a (\phi - \phi_0)^b \left(\frac{\partial^2}{\partial \phi^a \partial \phi^b} V \right)_{\phi_0} + O(3). \tag{A.3}$$

---

[1]For the case of the Higgs mechanism, n = 4.

By diagonalizing the Hessian matrix

$$\left(\frac{\partial^2}{\partial\phi^a\partial\phi^b}V\right)_{\phi_0} = m_{ab}^2, \tag{A.4}$$

the squared masses of the ϕ_a can be found. Moreover, these eigenvalues are guaranteed to be non-negative, since equation (A.2) refers to the minimum of the potential $V(\phi)$. Thus, in order to prove Goldstone's theorem within a classical field theory setting, it is enough to show that every broken continuous symmetry of equation (A.1) gives rise to a zero eigenvalue of the Hessian in equation (A.4). In general, an infinitesimal continuous symmetry transformation can be written as

$$\phi^a \to \phi^a + \alpha\Delta^a(\phi). \tag{A.5}$$

The SSB occurs, when the ground state of the system does not respect the original symmetry of the Lagrangian. Since the ground state configuration is given by constant fields, as defined in (A.2), the invariance condition can be set as

$$V(\phi^a) = V(\phi^a + \alpha\Delta^a(\phi)). \tag{A.6}$$

To a first order in α

$$V(\phi^a + \alpha\Delta^a(\phi)) = \phi^a + \alpha\Delta^a\frac{\partial}{\partial\phi^a}V(\phi) + O(\alpha^a). \tag{A.7}$$

Therefore, combining equations (A.7) and (A.6)

$$\Delta^a(\phi)\frac{\partial}{\partial\phi^a}V(\phi) = 0. \tag{A.8}$$

Finally, differentiating with respect to ϕ^b and setting $\phi = \phi_0$ yields

$$0 = \left(\frac{\partial\Delta^a}{\partial\phi^b}\right)_{\phi_0}\left(\frac{\partial V}{\partial\phi^a}\right)_{\phi_0} + \Delta^a(\phi_0)\left(\frac{\partial^2}{\partial\phi^a\partial\phi^b}V\right)_{\phi_0}. \tag{A.9}$$

The first term in (A.9) vanishes due to equation (A.2). This means that the second term must also be equal to zero. If the symmetry is unbroken, then ϕ_0 is unchanged, and $\Delta(\phi_0) = 0$. If, on the other hand, the symmetry is broken by the ground state, then $\Delta^a(\phi) \neq 0$ and the corresponding eigenvalue of the Hessian matrix in equation (A.4) is zero, proving Goldstone's theorem.

For a specific example, it is useful to consider the Higgs mechanism.[2] Using the Hermitian basis, the potential can be written as

$$V(\phi) = -\frac{\mu^2}{2}\left(\phi_1^2 + \phi_2^2 + \phi_3^2 + \phi_4^2\right) + \frac{\lambda}{4}\left(\phi_1^2 + \phi_2^2 + \phi_3^2 + \phi_4^2\right)^2. \tag{A.10}$$

The unitary gauge is defined by the following ground state configurations

$$\langle\phi_1\rangle = 0 \qquad \langle\phi_2\rangle = 0 \qquad \langle\phi_3\rangle = v \qquad \langle\phi_4\rangle = 0. \tag{A.11}$$

Thus, using the relation $\mu^2 = \lambda v^2$, it follows that the only nonvanishing mass matrix eigenvalue is given by

$$m_{33}^2 = \sqrt{2\lambda}v, \tag{A.12}$$

representing the mass of the Higgs boson. The rest of three fields ϕ_1, ϕ_2 and ϕ_4 are the massless Goldstone bosons, that can be reinterpreted as longitudinal modes of the gauge bosons. The connection between the longitudinal modes of the gauge bosons and the Goldstone boson is further emphasized by the Goldstone's boson equivalence theorem, which states that at high energy the amplitude for an emission or absorption of a longitudinally polarized gauge boson becomes equal to the amplitude of the emission or absorption of the Goldstone boson that was interpreted as the longitudinal mode of the gauge boson. This theorem was first proved in [67].

---

[2]Chapter 2 deals with the Higgs mechanism in detail.

Appendix B

Diagonalizing a General Complex Matrix

B.1   Biunitary Transformations

Every nondegenerate complex matrix can be diagonalized via a biunitary transformation. This is proved in this section following [68]. Consider a complex nondegenerate matrix M.[1] Clearly,

$$\left(MM^\dagger\right)^\dagger = MM^\dagger. \tag{B.1}$$

Since $MM^\dagger$ is Hermitian, it has real eigenvalues m^2 and it can be diagonalized by a unitary matrix V. Thus,

$$MM^\dagger = Vm^2V^\dagger \quad \text{with} \quad m_{ij}^2 = m_i^2 \delta_{ij}. \tag{B.2}$$

Then, M can be diagonalized by the following transformation

$$V^\dagger MU = V^\dagger MM^\dagger Vm^{-1} = m^2m^{-1} = m, \tag{B.3}$$

where U and $U^\dagger$ are the matrices that diagonalize $M^\dagger M$. It remains to show that $U \equiv M^\dagger Vm^{-1}$ is unitary. Indeed,

$$U^\dagger U = m^{-1}V^\dagger MM^\dagger Vm^{-1} = 1. \tag{B.4}$$

Hence, the biunitary transformation can be performed by using the two matrices U and V. In flavour physics applications, these are sometimes denoted as V^D and V^U.

---

[1]Meaning $det(M) \neq 0$.

Appendix C

Symmetries and Conserved Quantum Numbers

C.1 Noether's Theorem for Global Symmetries of the Lagrangian

It is a well-known fact, first proven by E.Noether, that to each continuous symmetry transformation of the Lagrangian there is a conserved current.[1] For the simplest case of $U(1)$ symmetry, if the Lagrangian is invariant under the following rephasing of the fields

$$\psi(x) \rightarrow e^{i\theta}\psi(x) \tag{C.1}$$

which can be infinitesimally written as[2]

$$\delta\psi_r = i\psi_r\delta\theta \quad \delta\psi_r^* = -i\psi_r^*\delta\theta, \tag{C.2}$$

then the conserved current is given by

$$j^\mu = i \sum_r \left(\frac{\partial \mathcal{L}}{\partial \left(\partial_\mu \psi_r\right)}\psi_r - \psi_r^* \frac{\partial \mathcal{L}}{\partial \left(\partial_\mu \psi_r^*\right)} \right). \tag{C.3}$$

---

[1]More details about the topics covered in this section are covered in [69], [70] and [71].
[2]The space-time coordinates have been left implicit.

Using the current conservation condition $\partial_\mu j^\mu = 0$ and the Gauss' Theorem, it follows immediately that

$$Q \equiv \int d^3x\, j^0(x) = i \int d^3x \left(\sum_r \frac{\partial \mathcal{L}}{\partial\left(\partial_0 \psi_r\right)} \psi_r - \psi_r^* \frac{\partial \mathcal{L}}{\partial\left(\partial_0 \psi_r^*\right)} \right) \qquad (C.4)$$

defines a conserved charge. Equation (C.4) will be used in the next two sections to infer the conservation of lepton and baryon numbers.

C.2 The Conservation of Lepton Numbers

From the form of equation (C.3), it is clear that the only term of the Lagrangian contributing to the Noether current in the leptonic sector is given by,

$$\mathcal{L}_{Lep}^{Noether} = \sum_{i=e,\mu,\tau} \left(\bar{L}_{iL} \gamma^\mu \partial_\mu L_{iL} + \bar{e}_{iR} \gamma^\mu \partial_\mu e_{iR} \right). \qquad (C.5)$$

By rephasing all the lepton fields belonging to the same generation in the same way, i.e.,

$$\nu_{aL} \to e^{i\varphi_a} \nu_{aL} \qquad e_{aL} \to e^{i\varphi_a} e_{aL} \qquad e_{aR} \to e^{i\varphi_a} e_{aR}, \qquad (C.6)$$

it follows from equation (C.3) that the conserved current is given by

$$j_a^\mu = \bar{\nu}_{aL} \gamma^\mu \nu_{aL} + \bar{e}_{aL} \gamma^\mu e_{aL} + \bar{e}_{aR} \gamma^\mu e_{aR} = \bar{\nu}_{aL} \gamma^\mu \nu_{aL} + \bar{e}_a \gamma^\mu e_a. \qquad (C.7)$$

Thus, the conserved lepton numbers can be defined by [3]

$$L_a = \frac{1}{3} i \int d^3x \left(\bar{\nu}_{aL}(x)\, \gamma^\mu \nu_{aL}(x) + \bar{e}_a(x)\, \gamma^\mu e_a(x) \right). \qquad (C.8)$$

By using mutually orthogonal spinors, u^h and v^h with $h = \pm 1$ the Fourier expansions of the massive Dirac field, [31]

$$e_a(x) = \int \frac{d^3p}{(2\pi)^3\, 2E} \sum_{h=\pm 1} a^h(p)\, u^h(p)\, e^{-ipx} + b^{h\dagger}(p)\, v^h(p)\, e^{ipx} \qquad (C.9)$$

and the massless Dirac field, [31]

$$\nu_L(x) = \int \frac{d^3p}{(2\pi)^3\, 2E} \left[a^-(p)\, u^-\, e^{-ipx} + b^{+\dagger}(p)\, v^+(p)\, e^{ipx} \right] \qquad (C.10)$$

---

[3] With normalization chosen such that $\sum_{a=e,\mu,\tau} L_a = 1$.

one can find the normally ordered number operator $: N_a :$ for each flavour. In detail, since $\gamma^0 \gamma^0 = I$,

$$: L_a : \; = \frac{i}{3} \int d^3x \left(v_{aL}^\dagger v_{aL} + e_a^\dagger e_a \right). \tag{C.11}$$

Then, from the mutual orthogonality of u^h and v^h,

$$
\begin{aligned}
: L_a : \; = &\frac{i}{3} \int \frac{d^3p}{(2\pi)^3 \, 2E} \frac{d^3p'}{(2\pi)^3 \, 2E'} \int d^3x \Big[a^{-\dagger}(p) \, u^- e^{ipx} a^-(p) \, u^- e^{-ipx} \\
&\qquad\qquad\qquad\qquad + b^+(p) \, v^+ e^{-ipx} b^{+\dagger} v^+ e^{ipx} \Big] \\
+ &\frac{i}{3} \int \frac{d^3p}{(2\pi)^3 \, 2E} \frac{d^3p'}{(2\pi)^3 \, 2E'} \int d^3x \Big[a^{h\dagger}(p) \, u^h e^{ipx} a^h(p) \, u^h e^{-ipx} \\
&\qquad\qquad\qquad\qquad + b^h(p) \, v^h e^{-ipx} b^{h\dagger} v^h e^{ipx} \Big]
\end{aligned}
\tag{C.12}
$$

Using the properties of the delta function, the above equation can be rewritten as

$$
\begin{aligned}
: L_a : \; = &\frac{i}{3} \int \frac{d^3p}{(2\pi)^3 \, 2E} d^4p' \delta\left(\mathbf{p} - \mathbf{p}'\right) \delta\left(p_0'^2 - E'^2\right) e^{i(p_0 - p_0')} \\
&\qquad\qquad \left[a^{-\dagger}(p) \, u^- a^-(p) \, u^- + b^+(p) \, v^+ b^{+\dagger} v^+ \right] \\
+ &\frac{i}{3} \int \frac{d^3p}{(2\pi)^3 \, 2E} d^4p' \delta\left(\mathbf{p} - \mathbf{p}'\right) \delta\left(p_0'^2 - E'^2\right) e^{i(p_0 - p_0')} \\
&\qquad\qquad \left[a^{h\dagger}(p) \, u^h a^h(p) \, u^h + b^h(p) \, v^h b^{h\dagger} v^h \right]
\end{aligned}
\tag{C.13}
$$

Finally, using the anticommutativity of the fermion raising and lowering operators, integrating over p' and using the orthonormality of v^h and u^h, the lepton number operator in normal order can be written as

$$
\begin{aligned}
: L_a : \; = &\frac{i}{3} \int \frac{d^3p}{(2\pi)^3 \, 2E} \left[a_{\nu_a}^{-\dagger}(p) \, a_{\nu_a}^-(p) - b_{\nu_a}^{+\dagger}(p) \, b_{\nu_a}^+(p) \right] \\
+ &\frac{i}{3} \int \frac{d^3p}{(2\pi)^3 \, 2E} \left[a_{e_a}^{h\dagger}(p) \, a_{e_a}^h(p) - b_{e_a}^{h\dagger}(p) \, b_{e_a}^h(p) \right].
\end{aligned}
\tag{C.14}
$$

Analogous result can be proved for the conservation of baryon number by following the derivation above.

Appendix D

Minimal Flavour Violation

The majority of the current experimental data indicates that the flavour changing processes only occur through the quark mixing sourced by the quark mixing matrix. [72] Thus, it is somewhat natural to hypothesize that all observed flavour- and CP-violating processes are related to the SM Yukawa structure. [73] Then, not only can the non-observation of beyond the SM phenomena in flavour changing processes be explained, but different FCNC processes can also be related to each other through the same non-diagonal structure. [73]

As an illustration of the above discussion, first the Lagrangian of the SM from equation (1.2) is considered. The invariance of the SM Lagrangian under global $U(3)^5$ transformations is only broken explicitly by the Yukawa terms. [73] Nevertheless the Lagrangian of the quark sector can be made symmetric under a smaller global subgroup $G_F = SU(3)_{Q_L} \otimes SU(3)_{u_R} \otimes SU(3)_{d_R}$, by formally promoting the Yukawa matrices to non-dynamic spurion fields which transform nontrivially under G_F. Concretely, the G_F-symmetry can be restored if the quantum numbers of Y_U and Y_D under G_F are given by $Y_D(\bar{3}, \bar{3}, 1)$ and $Y_U(\bar{3}, 1, \bar{3})$. The MFV criterion on an effective field theory then requires that the Yukawa coupling terms and all higher dimensional operators constructed from SM fields must also be formally G_F invariant. Furthermore, the manifest G_F symmetry means that the spurion fields Y_U and Y_D can be rotated under G_F such that, [73]

$$Y_D = \lambda_D \quad Y_U = V^\dagger \lambda_U, \tag{D.1}$$

where λ_D and λ_U are diagonal matrices. Since the top Yukawa coupling is much larger than the other Yukawa coupling, the only relevant non-diagonal contribution FCNC processes is, [73]

$$\lambda_{FC} = (Y_U Y_U^\dagger)_{ij} \approx \lambda_t^2 V_{3i}^* V_{3j}. \tag{D.2}$$

MFV can also be applied to Minimal Supersymmetric Models (MSSM). In this case, the MFV imposes that the soft mass term appearing in squark sector of the Lagrangian is universal. [73] Although the corresponding physical squark masses are not universal, the mass splitting is rather constrained by the MFV requirement. More importantly, however, the FCNC processes are only mediated by the CKM matrix of the SM, consistent with experimental observations. The application of MFV to MSSM turns out to be rather illuminating for applying MFV on the LR symmetric radiative models, as the scalar messengers $S_{L,R}^{U,D}$ carry the same gauge quantum numbers as squarks of MSSM, allowing for a clear motivation for applying MFV in Chapter 4.

Appendix E

The Analytical Functions for the Non-Diagonal Yukawa Couplings

In this section of the Appendix, the analytical calculations for the non-diagonal Yukawa couplings of the down-sector have been given. As the formulae are entirely adopted from [4], and because the exact details are not relevant for the purpose of the thesis, the mathematical subtleties of the calculation are not discussed in this Appendix. Following [4], the analytical formulae of the off-diagonal Yukawa couplings are expressed by asymptotic expansions in terms of a mass ratio $x_Q = \frac{m_Q}{m_F}$, an overall heavy mass scale $m_S = m_F$ and the loop suppression factor $L = 16\pi^2$. All dimensionless couplings appearing in Equations (4.54) and (4.68) have been accounted for by a single dimensionless parameter χ. In order to allow for a verification of the results of [4] that were reported in Section 4.4.2, the expansion has been given up to the eight order in x_Q.

$$
\begin{aligned}
m_F v_R L^2 \chi^4 \rho Y_{12}^D &\approx \frac{m_F}{v_R} \frac{L^2}{\chi^4} Y_{23}^D \\
&= 112(-27S_2 + \pi^2 - 6) + \frac{1}{4}(45S_2 - \pi^2 + 2)x_Q^2 \\
&\quad + x_Q^4 \left(45S_2 + \frac{11}{3}\log x_Q - \frac{\pi^2}{2} - \frac{179}{36}\right) \\
&\quad + x_Q^6 \left(99S_2 + 4\log^2(x_Q) + \frac{353}{30}\log x_Q - \frac{\pi^2}{3} - \frac{17353}{900}\right) \\
&\quad + x_Q^8 \left(\frac{693S_2}{4} + 18\log^2(x_Q) + \frac{976}{35}\log x_Q + \frac{3\pi^2}{4} - \frac{911367}{19600}\right) + \mathcal{O}\left(x_Q^{10}\right)
\end{aligned}
\tag{E.1}
$$

$$m_F v_R \frac{L^3}{\chi^5 \rho^2} Y_{13}^D = -\frac{1}{24} x_Q (459 S_2 - 112 \zeta(3) + \pi^2)$$

$$-\frac{x_Q^3}{8640} (-9120 O_\varepsilon^{S_2} + 15(196992 S_2 + 912 T_\varepsilon^1 - 45432 \zeta(3) + 7655))$$

$$-\frac{x_Q^3}{8640} (4320(-27 S_2 + \pi^2 - 6) \log x_Q + 361 \pi^4 + 30165 \pi^2)$$

$$-\frac{x_Q^5}{38880} (-98400 O_\varepsilon^{S_2} + 1080(846 S_2 + 12 \pi^2 - 203) \log x_Q$$

$$-\frac{x_Q^5}{38880} (27102114 S_2 + 147600 T_\varepsilon^1 - 4948920 \zeta(3) + 3895 \pi^2 + 228981 \pi^2 + 782769)$$

$$+\frac{x_Q^7}{24494400} (-175778400 O_\varepsilon^{S_2} + 60480 \log x_Q)(-224325 S_2 - 10260 \log x_Q + 2565 \pi^2 + 11234)$$

$$+\frac{x_Q^7}{24494400} (-1252502190 S_2 + 263667600 T_\varepsilon^1 - 3233475000 \zeta(3) + 6957895 \pi^4)$$

$$+\frac{x_Q^7}{24494400} (740318925 \pi^2 + 3458071731) + O\left(x_Q^9\right).$$

(E.2)

In the equations above, the vev of H_R is given by $\frac{v_R}{\sqrt{2}}$ and the special functions are given by

$$S_2 \equiv \frac{4}{9\sqrt{3}} Cl_2 \left(\frac{\pi}{3}\right)$$

(E.3)

$$O_\varepsilon^{S_2} = -\frac{763}{32} - \frac{9\pi\sqrt{3}\ln^2 3}{16} - \frac{35\pi^3\sqrt{3}}{48} + \frac{195}{16}\zeta(2) - \frac{15}{4}\zeta(3)$$
$$+\frac{57}{16}\zeta(4) + \frac{45\sqrt{3}}{2} Cl_2(\frac{\pi}{3}) - 27\sqrt{3} Im\left[Li_3\left(\frac{e^{-i\pi/6}}{\sqrt{3}}\right)\right]$$

(E.4)

$$T_\varepsilon^1 = -\frac{45}{2} - \frac{\pi\sqrt{3}\ln^2 3}{8} - \frac{35\pi^3\sqrt{3}}{216}$$
$$-\frac{9}{2}\zeta(2) + \zeta(3) + 6\sqrt{3} Cl_2\left(\frac{\pi}{3}\right) - 6\sqrt{3} Im\left[Li_3\left(\frac{e^{-i\pi/6}}{\sqrt{3}}\right)\right]$$

(E.5)

$$Cl_2(x) = Im[Li_2(e^{ix})]$$

(E.6)

The Riemann zeta functions and the polylogarithms are denoted by $\zeta(N)$ and $Li_N(x)$ respectively. Details about the Riemann zeta function and the polylogarithms can be found from [74, 75].

Appendix F

The Masses and mixings of the Higgs Fields in the Radiative model

In this section of the Appendix, I have reproduced the calculations made in [3], in order to illustrate the diagonalization procedure for the mixing of the two Higgs fields. Compared to [3] the calculation presented here results in a slightly different mixing matrix for the Higgs fields. To that end, the consistency of the results is thoroughly checked. The calculations were carried out, using the Mathematica programming languages. The scripts that I wrote for this task, are presented on Figures F.1 and F.2.

Due to the smallness of the $\epsilon = \frac{v_L}{v_R}$, the eigenvalues of the mass squared matrix appearing in (4.29) can be expanded as a series in ϵ. Keeping terms up to order $\mathcal{O}(8)$, the squared mass eigenvalues are given by

$$m_1^2 = 2\lambda_L \epsilon^2 v_R^2 \left(1 - \frac{\lambda_L}{\lambda_R}\epsilon^4\right) + \mathcal{O}\left(\epsilon^8\right)$$
$$m_2^2 = 2\lambda_R v_R^2 \left(1 + \frac{\lambda_L^2}{\lambda_R^2}\epsilon^6\right) + \mathcal{O}\left(\epsilon^8\right).$$

(F.1)

The orthogonal matrix U, diagonalizing the mass matrix, in equation 4.29 is given by,

$$U = \begin{pmatrix} 1 - \frac{\epsilon^6 \lambda_L^2}{2\lambda_R^2} - \frac{\epsilon^8 \lambda_L^3}{\lambda_R^3} & -\left(\epsilon^3 \frac{\lambda_L}{\lambda_R} + \epsilon^5 \frac{\lambda_L^2}{\lambda_R^2} + \epsilon^7 \frac{\lambda_L^3}{\lambda_R^3}\right) \\ \epsilon^3 \frac{\lambda_L}{\lambda_R} + \epsilon^5 \frac{\lambda_L^2}{\lambda_R^2} + \epsilon^7 \frac{\lambda_L^3}{\lambda_R^3} & 1 - \frac{\epsilon^6 \lambda_L^2}{2\lambda_R^2} - \frac{\epsilon^8 \lambda_L^3}{\lambda_R^3} \end{pmatrix}$$

(F.2)

Then, using equations (F.1) and (F.2), it can be easily checked that

$$U^T M^2 U = \text{diag}(m_1^2, m_2^2) + O\left(\epsilon^8\right) \quad U^T U = I + O\left(\epsilon^8\right). \tag{F.3}$$

The mass eigenstates h_1, h_2 are thus given in terms of the gauge eigenstates by

$$\begin{pmatrix} h_1 \\ h_2 \end{pmatrix} \approx U \begin{pmatrix} h_L \\ h_R \end{pmatrix}. \tag{F.4}$$

Masses of Higgs

`$Assumptions =`
` lambdaL ∈ Reals && lambdaR ∈ Reals && eps ∈ Reals && lambdaL > 0 && lambdaR > 0 && eps > 0;`

In[9]:=
```
(*Mass Squared Matrix of the Higgs sector*)
M2 = {{lambdaL * eps^2, -lambdaL * eps^3}, {-lambdaL * eps^3, lambdaR}};
(* Finding the Eigenvalues*)
eigenval = Eigenvalues[M2];
(*The first eigenvalue expanded in eps^2*)
m1[x_] := eigenval[[1]] /. {eps^2 → x^2};
m12 = FullSimplify[Series[m1[x], {x, 0, 6}]] /. {x → eps};
(*The second eignevalue expanded in eps^2*)
m2[y_] := eigenval[[2]] /. {eps^2 → y^2};
m22 = FullSimplify[Series[m2[y], {y, 0, 6}]] /. {y → eps};
(*Displaying the eigenvalues as a list, with higher order terms truncated*)
{Normal[m12], Normal[m22]}
```

Out[15]= $\left\{ eps^2\ lambdaL - \dfrac{eps^6\ lambdaL^2}{lambdaR}, \dfrac{eps^6\ lambdaL^2}{lambdaR} + lambdaR \right\}$

Figure F.1: The code for calculating the masses of the Higgs fields

Mixings of Higgs

```
In[34]:= (*Calculating eigenvectors *)
    eigvec = Eigenvectors[M2];
    (*Normalizing the eigenvectors and expanding the components in series *)
    eigvec1 = Normalize[eigvec[[1]]];
    eigvec11 = Series[eigvec1[[1]], {eps, 0, 8}];
    eigvec12 = Series[eigvec1[[2]], {eps, 0, 8}];
    (* The first eigenvector is v1, the second is given by an orthogonal eigenvector v2*)
    v1 = Normal[{eigvec11, eigvec12}] // Simplify;
    v2 = Cross[v1];
    (*Constructing the rotation matrix *)
    Ort = Transpose[{v1, v2}];
    OrT = Transpose[Ort];
    (*Checking orthogonality*)
    identity = OrT.Ort // Simplify // Expand;
    (*Deleting the O(8) terms from the matrix elements*)
    id11 = identity[[1, 1]] /. eps^b_ /; b ≥ 8 → 0;
    id12 = identity[[1, 2]] /. eps^b_ /; b ≥ 8 → 0;
    id21 = identity[[2, 1]] /. eps^b_ /; b ≥ 8 → 0;
    id22 = identity[[2, 2]] /. eps^b_ /; b ≥ 8 → 0;

    (* Resulting identity matrix, up to order eight in epsilon*)
    idres = {{id11, id12}, {id21, id22}} // MatrixForm
    (*Checking diagonalization*)
    mdiag = OrT.M2.Ort // Simplify // Expand;
    (* Deleting the O(8) terms from the matrix elements*)
    md11 = mdiag[[1, 1]] /. eps^b_ /; b ≥ 8 → 0;
    md12 = mdiag[[1, 2]] /. eps^b_ /; b ≥ 8 → 0
    md21 = mdiag[[2, 1]] /. eps^b_ /; b ≥ 8 → 0;
    md22 = mdiag[[2, 2]] /. eps^b_ /; b ≥ 8 → 0;
    (* The resulting matrix is indeed the diagonal matrix of eigenvalues as required *)
    DiagEig = {{md11, md12}, {md21, md22}} // MatrixForm
```

Out[45]//MatrixForm=
$$\begin{pmatrix} 1 & 0 \\ 0 & 1 \end{pmatrix}$$

Out[51]//MatrixForm=
$$\begin{pmatrix} \text{eps}^2 \text{ lambdaL} - \frac{\text{eps}^6 \text{ lambdaL}^2}{\text{lambdaR}} & 0 \\ 0 & \frac{\text{eps}^6 \text{ lambdaL}^2}{\text{lambdaR}} + \text{lambdaR} \end{pmatrix}$$

Figure F.2: The code for calculating the mixings of the Higgs fields

Appendix G

Chiral symmetry breaking via Dark Sector

In Chapter 4 the ChSB mechanism responsible for generating the dark fermion masses was introduced. The formula for the propagator contributing to the self-energy correction of the dark fermions was given by equation (4.4) as reported in [49]. In this section, I provide my own independent calculation of this result.

The action of the gauge field of $U(1)_F$ is given by

$$S = \int d^4x \left[-\frac{1}{4}F_{\mu\nu}F^{\mu\nu} + \frac{1}{2\Lambda^2}(\partial^\alpha F_{\alpha\mu})(\partial^\beta F^\mu_\beta) \right] \tag{G.1}$$

Using the definition

$$F_{\mu\nu} = \partial_\mu \bar{A}_\nu(x) - \partial_\nu \bar{A}_\mu(x), \tag{G.2}$$

and integrating by parts, the first term in the action becomes,[1]

$$S_1 = \int d^4x \frac{1}{2}[-\partial_\nu(A_\mu(x)\partial^\nu A^\mu(x)) + A_\mu(x)\partial_\nu\partial^\nu A^\mu(x)$$
$$+ \partial_\nu(A_\mu(x)\partial^\mu A^\nu(x)) - A_\mu(x)\partial_\nu\partial^\mu A^\nu(x)]. \tag{G.3}$$

---

[1]From hereon, $\bar{A}^\mu$ is written as A^μ with the understanding that in this chapter A^μ stands for the *dark photon*.

Since the fields vanish at infinity, using the 4-dimensional Stokes' theorem yields

$$
\begin{aligned}
S_1 &= \int d^4x \left[\frac{1}{2} A_\mu(x) \partial^2 A^\mu(x) - \frac{1}{2} A_\mu(x) \partial_\nu \partial^\mu A^\nu(x) \right] \\
&= \int d^4x \left[\frac{1}{2} A_\mu(x) g^{\mu\nu} \partial^2 A_\nu(x) - \frac{1}{2} A_\mu(x) \partial^\nu \partial^\mu A_\nu(x) \right].
\end{aligned} \tag{G.4}
$$

In a completely analogous way, the second term of the action can be integrated by parts twice, using again 4-dimensional Stokes' theorem and the fact that the fields must vanish at the infinity. The result is

$$
S_2 = \int d^4x \frac{1}{2\Lambda^2} \left[A_\mu(x) g^{\mu\nu} \partial^4 A_\nu(x) - A_\mu(x) \partial^2 \partial^\mu \partial^\nu A_\nu(x) \right]. \tag{G.5}
$$

Thus, the action can be written as

$$
S = \int d^4x \left[\frac{1}{2} A_\mu(x) g^{\mu\nu} \left(\partial^2 + \frac{1}{\Lambda^2} \partial^4 \right) - \partial^\nu \partial^\mu \left(1 + \frac{1}{\Lambda^2} \partial^2 \right) A_\nu(x) \right]. \tag{G.6}
$$

In order to illustrate the calculation of the propagator, the path integral approach is used. More details on the useage of the path integral formalism on the quantization of fields can be found for instance in [12]. The identity for n-dimensional vectors y, J and for a $n \times n$-dimensional matrix B

$$
\int_{-\infty}^{\infty} \left(\Pi_{i=1}^n \frac{dy_i}{\sqrt{2\pi}} \right) e^{-\frac{1}{2} y^T B y + y^T J} = \frac{e^{\frac{1}{2} J^T B^{-1} J}}{(det B)^{1/2}}, \tag{G.7}
$$

may be generalized to the case of continuum resulting in

$$
\begin{aligned}
&\int \mathcal{D}A^\mu \exp\left\{ -\int \left[d^4x \frac{1}{2} A_\mu(x) O^{\mu\nu} A_\nu(x) - J^\mu(x) A_\mu(x) \right] \right\} \\
&= \int \mathcal{D}A^\mu \frac{\exp\left\{ -\int d^4x \left[\frac{1}{2} J^\mu(x) \Delta_{\mu\nu}(x-y) J^\nu(y) \right] \right\}}{\sqrt{det O^{\mu\nu}}}.
\end{aligned} \tag{G.8}
$$

Here,

$$
O^{\mu\nu} = g^{\mu\nu} \left(\partial^2 + \frac{1}{\Lambda^2} \partial^4 \right) - \partial^\nu \partial^\mu \left(1 + \frac{1}{\Lambda^2} \partial^2 \right), \tag{G.9}
$$

and

$$
O_{\mu\nu} \Delta^{\rho\nu}(x-y) = \delta_\mu^\rho \delta(x-y). \tag{G.10}
$$

The functional determinant is defined by $J = 0$:

$$\frac{1}{\sqrt{detO^{\mu\nu}}} = \int \mathcal{D}A^\mu \exp\left\{-\frac{1}{2}\int d^4x A_\mu(x)O^{\mu\nu}A_\nu(x)\right\}. \tag{G.11}$$

Thus, the generating functional can be written as

$$Z[J] = \sqrt{detO^{\mu\nu}}\int \mathcal{D}A^\mu \exp\left\{-i\int d^4x \left[\frac{1}{2}J^\mu(x)\Delta_{\mu\nu}(x-y)J^\nu(y)\right]\right\} \tag{G.12}$$

The identification of Δ with the propagator of the dark photon field can be easily made by using (G.12) and the defintion of the propagator of the dark photon field $\Delta_F^{\mu\nu}$

$$\Delta_F^{\mu\nu} \equiv \langle 0| T\left(A^\mu(x)A^\nu(y)\right)|0\rangle = -\left.\frac{\delta^2 Z[J]}{\delta J(x)\delta J(y)}\right|_{J=0} \tag{G.13}$$

Hence, the dark photon propagator is given by

$$\left[g^{\mu\nu}\left(\partial^2 + \frac{1}{\Lambda^2}\partial^4\right) - \partial^\nu\partial^\mu\left(1 + \frac{1}{\Lambda^2}\partial^2\right)\right]\Delta^{\rho\mu}(x-y) = i\delta_\mu^\rho\delta(x-y), \tag{G.14}$$

where i on the right hand side arises from the factor of i in the generating functional in equation (G.12). Using the appropriate Fourier transforms

$$\Delta(x-y) = \int \frac{d^4k}{(2\pi)^4}\tilde{\Delta}(k)e^{ik(x-y)} \tag{G.15}$$

and

$$\delta(x-y) = \int \frac{d^4k}{(2\pi)^4}e^{ik(x-y)}, \tag{G.16}$$

equation (G.14) becomes

$$\left[g^{\mu\nu}\left(-k^2 + \frac{k^4}{\Lambda^2}\right) + k^\nu k^\mu\left(1 - \frac{k^2}{\Lambda^2}\right)\right]\tilde{\Delta}(k)^{\rho\mu} = i\delta_\mu^\rho. \tag{G.17}$$

However, this equation does not have a solution.[2] The reason that equation (G.17) has no solution is related to the gauge invariance, namely invariance under $\tilde{A}^\mu(k) \to \tilde{A}^\mu(k) + \alpha(x)k^\mu$. In particular, the action in equation (G.6), when evaluated in

---

[2]This can be easily seen by using an *Ansatz* $\Delta^{\rho\nu} = i(A(k^2,\Lambda^2)g^{\rho\nu} + B(k^2,\Lambda^2)k^\rho k^\nu)$, which leads to a contradiction $\frac{1}{k^2} = 0$. Equivalently, the operator on the left hand side acting on $\Delta^{\rho\nu}$ in equation (G.17) has a zero determinant.

Fourier space vanishes for all $\tilde{A}^\mu(k) = \alpha(k)k^\mu$. Thus the generating functional defined by

$$Z[J] = \int \mathcal{D}A^\mu \exp\left\{i \int d^4x(\mathcal{L} + J_\mu A^\mu)\right\} \tag{G.18}$$

is divergent. In order to solve this issue, a gauge must be chosen. The process of fixing the gauge in the path integral approach was proposed by Faddeev and Popov. [76] Due to constraints in space, the exact details are omitted but can be easily found from several resources, for instance from [12]. Essentially, in order to fix the gauge an additional gauge fixing term, here chosen to be $\left(\frac{\partial_\mu A^\mu}{2\xi}\right)^2$, must be added to the Lagrangian. After adding the gauge fixing term to the action and integrating by parts as before, a new equation for the propagator is obtained:

$$\left[g_{\mu\nu}\left(\partial^2 + \frac{1}{\Lambda^2}\partial^4\right) - \partial_\nu\partial_\mu\left(1 - \frac{1}{\xi} + \frac{1}{\Lambda^2}\partial^2\right)\right]\Delta^{\rho\nu}(x-y) = i\delta^\rho_\mu\delta(x-y). \tag{G.19}$$

Thus, in Fourier space, the equation becomes

$$\left[g_{\mu\nu}\left(\frac{k^4}{\Lambda^2} - k^2\right) - k_\nu k_\mu\left(1 - \frac{1}{\xi} + \frac{k^2}{\Lambda^2}\right)\right]\tilde{\Delta}(k)^{\rho\nu} = i\delta^\rho_\mu. \tag{G.20}$$

This equation can be solved by considering the most general second-rank tensor built from the metric and k^μ.

$$D^{\nu\rho} = iA(k^2, \Lambda^2, \xi)g^{\rho\nu} + iB(k^2, \Lambda^2, \xi)k^\nu k^\rho. \tag{G.21}$$

Then, the $i\delta^\rho_\mu$ term on the right hand side can only result from $g^{\rho\nu}g_{\mu\nu}$.[3] Thus,

$$ig^{\rho\nu}g_{\mu\nu}A\left(\frac{k^4}{\Lambda^2} - k^2\right) = i\delta^\rho_\mu. \tag{G.22}$$

Hence,

$$A = -\frac{\Lambda^2}{k^2(\Lambda^2 - k^2)}. \tag{G.23}$$

The rest of the terms therefore need to cancel out.

$$-\frac{i\Lambda^2}{k^2(\Lambda^2 - k^2)}k^\rho k^\nu\left(1 - \frac{1}{\xi} - \frac{k^2}{\Lambda^2}\right) + Bg_{\mu\nu}\left(\frac{k^4}{\Lambda^2} - k^2\right)k^\rho k^\nu$$

$$+k_\mu k_\nu k^\rho k^\nu B\left(1 - \frac{1}{\xi} - \frac{k^2}{\Lambda^2}\right) = 0. \tag{G.24}$$

---

[3]From hereon, the functional dependence of A and B on k^2, Λ^2, ξ is left understood.

Therefore,

$$Bk^\rho k_\mu \left(\frac{k^4}{\Lambda^2} - k^2\right) + Bk^2 k^\rho k_\mu \left(1 - \frac{1}{\xi} - \frac{k^2}{\Lambda^2}\right)$$
$$= -\frac{k^2 B}{\xi} = \frac{i\Lambda^2}{k^2(\Lambda^2 - k^2)}\left(1 - \frac{1}{\xi} - \frac{k^2}{\Lambda^2}\right), \tag{G.25}$$

leading to

$$B = \frac{-i\Lambda^2}{k^2(\Lambda^2 - k^2)}\left(-\frac{1}{k^2}(1-\xi) - \frac{\xi}{\Lambda^2}\right). \tag{G.26}$$

Thus, using equations (G.23) and (G.26) together with (G.21), equation (4.4) can be recovered. Another interesting property of the higher-derivative term in equation (G.1) is that the self-energy correction to the dark fermion propagator, induced by the gauge field of $U(1)_F$ is finite. This is a typical example of Lee-Wick theories where ghosts with negative norm cancel out the infra-red divergences. [53, 49]. To illustrate this property explicitly, and to explain the origin of (4.5), I will provide my own independent calculation of (4.5) from (4.4). As mentioned in Section (4.2), the gauge dependent terms do not contribute to the self-energy correction evaluted at the physical pole mass m of the dark fermions. Moreover as can be seen from the dark fermion Lagrangian, equation (4.3), the Feynman rules of the dark-fermion - dark photon interaction mimick those of the quantum electrodynamics of the SM.[4]

In order to simplify the calculation, the gauge independent part of the propagator of (4.4) can be divided into two parts.

$$\frac{-i\Lambda^2}{k^2(\Lambda^2 - k^2)}g_{\mu\nu} = \left(-\frac{i}{k^2} + \frac{i}{k^2 - \Lambda^2}\right)g_{\mu\nu}. \tag{G.27}$$

The first term of the above equation, depicted on the LHS of Figure 4.1, then yields the following term for the self-energy correction

$$-i\Sigma_1(\not{p}, m) = (ig)^2 \int \frac{d^4k}{(2\pi)^4}\left(-\frac{i}{(k-p)^2}\right)\gamma^\mu g_{\mu\nu}\frac{i(\not{k}+m)\gamma^\nu}{k^2 - m^2} \tag{G.28}$$

where k denotes the momentum of the virtual dark fermion, p denotes the incoming off-shell momentum of the dark fermion, and g is the coupling constant of $U(1)_F$. The Dirac structure can be easily simplified:

$$\gamma^\mu \gamma_\mu = \gamma^\mu \gamma^\nu g_{\mu\nu} = g_{\mu\nu}\left(\frac{1}{2}\gamma^{\mu\nu} + \frac{1}{2}\gamma^{\mu\nu}\right) = \frac{1}{2}2g_{\mu\nu}g^{\mu\nu} = 4. \tag{G.29}$$

---

[4]The Feynman rules of [12] are used throughout this section.

Secondly,

$$\gamma^\mu(\not{k}+m)\gamma^\nu g_{\mu\nu} = \gamma^\mu(\not{k}+m)\gamma_\mu = \gamma^\mu k_\alpha \gamma^\alpha \gamma_\mu + 4m$$
$$= k_\alpha(2g^{\mu\alpha} - \gamma^\alpha\gamma^\mu)\gamma_\mu + 4m = 2\not{k} - 4\not{k} + 4m = 4m - 2\not{k}. \tag{G.30}$$

Thus,

$$-i\Sigma_1(\not{p},m) = -g^2 \int \frac{d^4k}{(2\pi)^4} \frac{4m-2\not{k}}{(k-p)^2(k^2-m^2)}. \tag{G.31}$$

Using Feynman parametrization, the last equation can be rewritten as follows

$$-i\Sigma_1(\not{p},m) = -g^2 \int \frac{d^4k}{(2\pi)^4} \int_0^1 dx \frac{4m-2\not{k}}{((k-p)^2x+(1-x)(k^2-m^2))^2}$$
$$= -g^2 \int \frac{d^4k}{(2\pi)^4} \int_0^1 dx \frac{4m-2\not{k}}{((k-px)^2-\Delta)^2}, \tag{G.32}$$

where $\Delta = p^2x(x-1) + m^2(1-x)$. Shifting the integration variable $l = k - px$, $\Sigma_1(\not{p},m)$ becomes

$$-i\Sigma_1(\not{p},m) = -g^2 \int \frac{d^4l}{(2\pi)^4} \int_0^1 dx \frac{4m-2(\not{l}+\not{p}x)}{(l^2-\Delta)^2}. \tag{G.33}$$

The linear term in l in the numerator vanishes because it is antisymmetric under $l \to -l$, while l^2 is symmetric under this transformation. Hence, the integral becomes simply

$$-i\Sigma_1(\not{p},m) = -g^2 \int \frac{d^4l}{(2\pi)^4} \int_0^1 dx \frac{4m-2\not{p}x}{(l^2-\Delta)^2}$$
$$= -g^2 \int_0^1 dx\,(4m-2\not{p}x) \int \frac{d^4l}{(2\pi)^4} \frac{1}{(l^2-\Delta)^2} \tag{G.34}$$

After carrying out Wick rotation the integral becomes[5]

$$-i\Sigma_1(\not{p},m) = -ig^2 \int_0^1 dx\,(4m-2\not{p}x) \int \frac{d^4l_E}{(2\pi)^4} \frac{1}{(l_E^2+\Delta)^2}$$
$$= -ig^2\pi^2 \int_0^1 dx\,(4m-2\not{p}x) \int_0^\infty \frac{dl_E^2}{(2\pi)^4} \frac{l_E^2}{(l_E^2+\Delta)^2}, \tag{G.35}$$

where l_E denotes the norm of a 4-component Euclidean vector as opposed to the Minkowski 4-vector l.

---

[5]Details on Wick rotation and Feynman parametrization can be found from [12].

The integral can be easily evaluated by shifting the integration variable $l_E^2 \to l_E^2 + \Delta$:

$$-i\Sigma_1(\not p, m) = -ig^2\pi^2 \int_0^1 dx \, (4m - 2\not p x) \int_\Delta^\infty \frac{dl_E^2}{(2\pi)^4} \left(\frac{l_E^2}{l_E^4} - \frac{\Delta}{l_E^4} \right)$$
$$= -ig^2 \frac{\pi^2}{(2\pi)^4} \int_0^1 dx \, (4m - 2\not p x) \left(\lim_{l_E^2 \to \infty} \ln l_E^2 - \ln \Delta - 1 \right) \tag{G.36}$$

The second contribution to the self-energy correction depicted on the right hand side of Figure 4.5 differs only by the overall sign and the denominator of the propagator. Thus, most of the results derived above can be adopted. The correction can be written as

$$-i\Sigma_2(\not p, m) = g^2 \int \frac{d^4k}{(2\pi)^4} \frac{4m - 2\not k}{((k-p)^2 - \Lambda^2)(k^2 - m^2)}. \tag{G.37}$$

Using Feynman parametrization

$$-i\Sigma_2(\not p, m) = -g^2 \int \frac{d^4k}{(2\pi)^4} \int_0^1 dx \frac{4m - 2\not k}{(((k-p)^2 - \Lambda^2)x + (1-x)(k^2 - m^2))^2}$$
$$= -g^2 \int \frac{d^4k}{(2\pi)^4} \int_0^1 dx \frac{4m - 2\not k}{((k - px)^2 - \Delta_2)^2}, \tag{G.38}$$

where,

$$\Delta_2 = p^2 x(x-1) + \Lambda^2 x + m^2(1-x). \tag{G.39}$$

Then the integral has the same form as in equation (G.32) and by analogy the derivation is completely identical to equation (G.36) up to the negating the sign in front and identifying $\Delta \to \Delta_2$. Hence,

$$-i\Sigma_2(\not p, m) = ig^2 \frac{\pi^2}{(2\pi)^4} \int_0^1 dx \, (4m - 2\not p x) \left(\lim_{l_E^2 \to \infty} \ln l_E^2 - \ln \Delta_2 - 1 \right) \tag{G.40}$$

Thus, adding equations (G.36) and (G.40)

$$-i\Sigma(\not p, m) = -i(\Sigma_1(\not p, m) + \Sigma_2(\not p, m)) = i\frac{g^2\pi^2}{(2\pi)^4} \int_0^1 dx \, (4m - 2\not p x) \ln \frac{\Delta}{\Delta_2} \tag{G.41}$$

Defining $\alpha = \frac{g^2}{4\pi}$ and using the definitions of Δ and Δ_2 this can be written as

$$-i\Sigma(\not p, m) = i\frac{\alpha}{2\pi} \int_0^1 dx \, (2m - \not p x) \ln \frac{p^2 x(x-1) + m^2(1-x)}{p^2 x(x-1) + \Lambda^2 x + m^2(1-x)}, \tag{G.42}$$

or

$$\Sigma(\not{p}, m) = \frac{\alpha}{2\pi} \int_0^1 dx \left(2m - \not{p}x\right) \ln \frac{(m^2 - p^2 x)(1 - x) + \Lambda^2 x}{(m^2 - p^2 x)(1 - x)}. \qquad \text{(G.43)}$$

Lihtlitsents lõputöö reprodutseerimiseks ja lõputöö üldsusele kättesaadavaks tegemiseks

Mina, Kristjan Müürsepp,

1. annan Tartu Ülikoolile tasuta loa (lihtlitsentsi) enda loodud teose

   The Flavor Hierarchy Problem in the Standard Model and Beyond the Standard Model Theories,

   mille juhendajad on Dr Luca Marzola ja Dr Stefan Groote, reprodutseerimiseks eesmärgiga seda säilitada, sealhulgas lisada digitaalarhiivi DSpace kuni autoriõiguse kehtivuse lõppemiseni.

2. Annan Tartu Ülikoolile loa teha punktis 1 nimetatud teos üldsusele kättesaadavaks Tartu Ülikooli veebikeskkonna, sealhulgas digitaalarhiivi DSpace kaudu Creative Commonsi litsentsiga CC BY NC ND 3.0, mis lubab autorile viidates teost reprodutseerida, levitada ja üldsusele suunata ning keelab luua tuletatud teost ja kasutada teost ärieesmärgil, kuni autoriõiguse kehtivuse lõppemiseni.

3. olen teadlik, et punktis 1 ja 2 nimetatud õigused jäävad alles ka autorile.

4. kinnitan, et lihtlitsentsi andmisega ei rikuta teiste isikute intellektuaalomandi ega isikuandmete kaitse seadusest tulenevaid õigusi.

Kristjan Müürsepp,
Tartu, 1. juuni 2020. a.